Comet Surface Sample Return Study Report

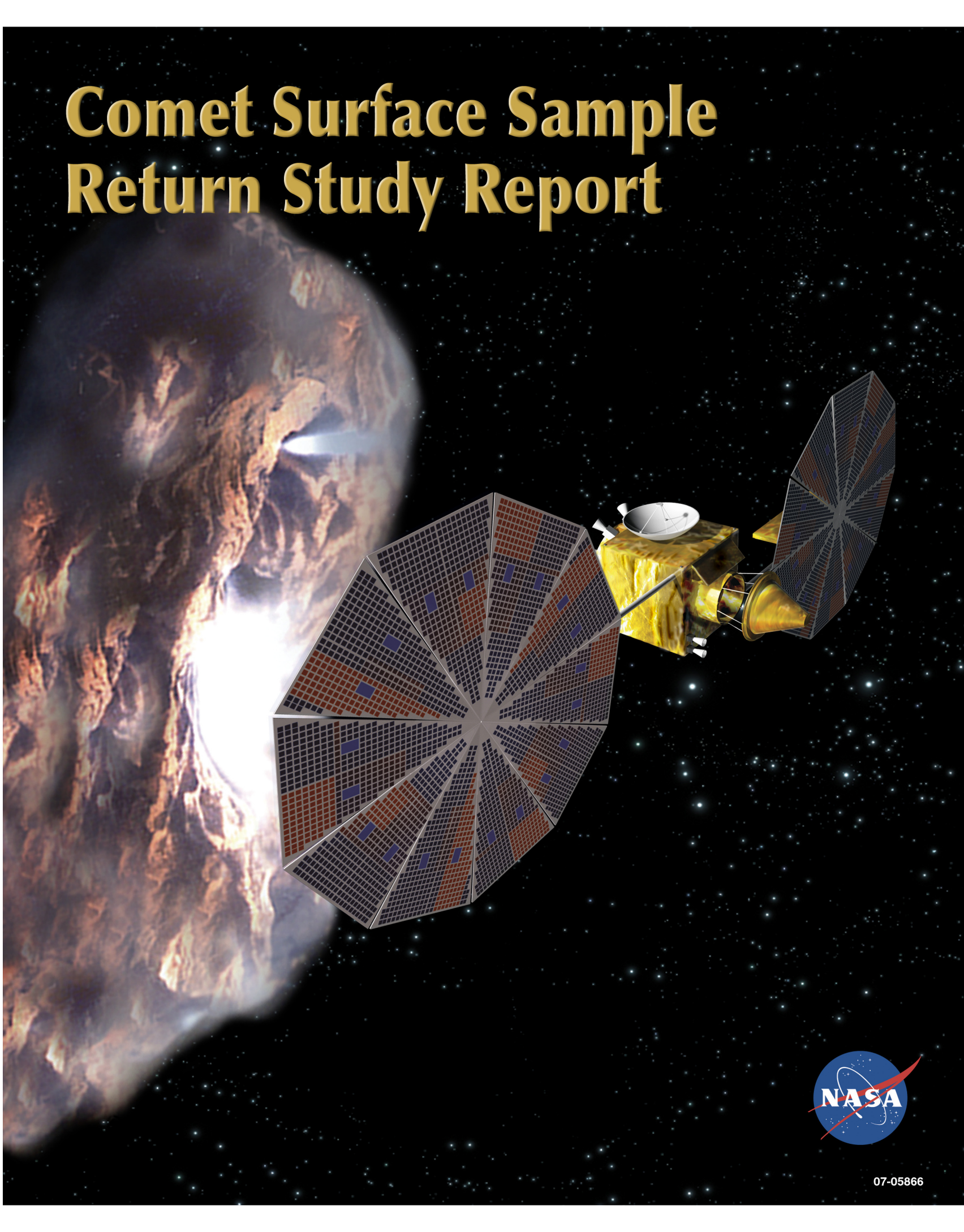

NASA

07-05866

SDO-11998
April 30, 2008

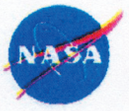

Comet Surface Sample Mission Study

Prepared for NASA's Planetary Science Division

By The Johns Hopkins University Applied Physics Laboratory

Approved By:

Glen H. Fountain
Study Lead, The Johns Hopkins University Applied Physics Laboratory

Robert D. Strain
Space Department Head, The Johns Hopkins University Applied Physics Laboratory

Hal Weaver
Science Definition Team Co-Chair, The Johns Hopkins University Applied Physics Laboratory

Mike A'Hearn
Science Definition Team Co-Chair, University of Maryland

ACKNOWLEDGMENTS

The Johns Hopkins University would like to extend a special thank you to all of the team members and to NASA's Planetary Science Division for the opportunity to investigate this amazing mission concept. The CSSR SDT gratefully acknowledges the advice it has received from colleagues in the scientific community, particularly Akiva Bar-Nun, Ben Clark, Neil Dello Russo, Wes Huntress, Uwe Keller, Toby Owen, Dina Prialnik, Scott Sandford, and Hajime Yano. Of course, these people are not responsible for any errors or omissions in this report, nor have they reviewed the final version.

The Comet Surface Sample Mission Study Team

Science Definition Team

- Mike A'Hearn (UMD): Co-chair
- Hal Weaver (JHU/APL): Co-chair
- Mike Combi (University of Michigan)
- Yan Fernández (University of Central Florida)
- Will Grundy (Lowell Observatory)
- Martha Hanner (University of Massachusetts)
- Casey Lisse (JHU/APL)
- Karen Meech (University of Hawaii)
- Joe Veverka (Cornell University)
- Paul Weissman (JPL)
- Mike Zolensky (NASA/JSC)

Engineering Team

APL

- Systems Engineering: J. C. Leary; P. A. Hill
- Mechanical Systems: C. T. Apland
- Communications: J. R. Bruzzi
- Propulsion: S. S. Bushman
- Payload: E. H. Darlington
- Mission Design: D. W. Dunham; J. J. Guzman
- Advanced Technologies: R. E. Gold
- Landing Systems: J. T. Kaidy
- Sampling Systems: W. J. Lees
- Software: V. A. Mallder
- Mechanical Design: S. Gantz
- Avionics: J. K. Ottman
- Structures: D. F. Persons
- Guidance & Control: J. C. Ray
- Power: L. M. Roufberg
- Operations & Ground Systems: E. P. Theus
- Thermal: M. J. Wirzburger
- Costing: L. S. Wolfarth

Other Team Members

- SRV: NASA LaRC (W. C. Engelund)
- Navigation & Mission Design: GRC (J. Dankanich)
- ISPT: GRC (T. Kremic)

TABLE OF CONTENTS

1.0 EXECUTIVE SUMMARY

A Comet Surface Sample Return (CSSR) mission concept study has identified viable options for a mid-class NASA mission.

- APL has led a study for NASA to determine if a CSSR mission can be executed within a cost cap of $820M in FY2007 dollars.
- A Science Definition Team (SDT) drawn from the community of comet science experts defined a set of mission science goals for a sample return mission.
- A viable mission concept has been developed that uses technologies available in the near term, assuming additional risk reduction activities are completed in the formulation phase.

The National Academy of Science's Decadal Survey (*New Frontiers in the Solar System: An Integrated Exploration Strategy*, 2003) recommended that NASA develop a medium class mission to return a comet surface sample to Earth for laboratory analysis. NASA tasked the Applied Physics Laboratory to further refine the concepts described in the Decadal Survey. As stated in the task guidelines, "The study results will include a pre-phase A fidelity plan to implement the mission concept, evaluating the cost, schedule and risk. A Science Definition Team (SDT) will be appointed by NASA Headquarters to work with mission designers and technologists. The study will take recent activities into account, assess opportunity and technological readiness, and provide estimated costs."

The study began in July 2007 with the identification of an SDT to guide the concept development. As discussed in Section 2, the SDT re-examined the scientific justification for a CSSR mission, explicitly considering the new knowledge gained during recent spacecraft missions to comets. The results from the Deep Impact mission in 2005, in combination with studies of fragmenting comets during the past two decades, strongly suggest that sampling the surface of a cometary nucleus should be much easier than previously thought. And the bounty of intriguing, new scientific results from the Stardust mission justifies taking the next logical step to a CSSR mission that would provide a more representative sample of cometary matter. In summary, the SDT reaffirms the Decadal Survey's statement that: "No other class of objects can tell us as much as samples from a selected surface site on the nucleus of a comet can about the origin of the solar system and the early history of water and biogenic elements and compounds. Only a returned sample will permit the necessary elemental, isotopic, organic, and mineralogical measurements to be performed." Indeed, both the Decadal Survey and the SDT conclude that the return of comet samples to the Earth for laboratory analysis is one of the most important objectives in all of planetary science.

The SDT finds that a CSSR mission with a single, focused objective to return approximately 500 cc of material from the nucleus will provide a major scientific advancement and will fulfill the intent of the Decadal Survey's recommendation for a New Frontiers class mission. However, the mission must be designed to prevent aqueous alteration of the sample, which would jeopardize the fundamental scientific objectives.

With guidance from the SDT, the engineering team developed a CSSR mission concept, as described in Section 3. The SDT determined that the return of a sample from any comet was of sufficient value to justify the mission and that the final choice of the target comet should be based on criteria that would reduce mission cost and risk. The initial review indicated that all potential targets are challenging from a mission design perspective. But some good candidates were identified, and we selected comet 67P/Churyumov-Gerasimenko [C-G] for this study, at least in part because the nucleus of this comet is expected to be well characterized by the Rosetta mission in the 2014 time frame, well in advance of the rendezvous and landing discussed here. The primary architecture of the mission is driven by the need to navigate in the vicinity of the comet,

descend to the surface of the nucleus to acquire a sample, and return the sample to the Earth without altering the material. Our study found that two technology options were available to accomplish these objectives: a conventional chemical propulsion system and solar electric propulsion (SEP), which has now been demonstrated by the DS1 and Dawn missions. Mission concepts built around these two options are presented in Sections 4 (SEP) and 5 (Chemical Propulsion/Ballistic Mission Design).

The technologies for either mission option are sufficiently mature that the choice between them will be based on the difference in cost and risk. Costs for both mission options were developed and are presented in Sections 4.11 and 5.11 for the SEP and chemical propulsion/ballistic mission designs, respectively. The baseline cost of a conventional chemical propulsion system fits within cost cap, while the SEP mission, though more robust with respect to launch options, is at the cap and represents a greater cost risk.

New knowledge accumulated during the past decade on the material properties of comets has significantly reduced the risk of a sample return mission. Yet, further work is required to reduce the technology risk and achieve the required (TRL6) level of maturity prior to full mission development. We strongly recommend that sufficient funds be made available during Phase A to reduce the risks associated with the sample collection system and the sample return vehicle prior to mission confirmation. This funding level, as described in Section 4, is greater than what is typically allocated for Phase A, but such an investment will pay off handsomely in the long run with respect to overall mission risk.

The mission concepts identified in this study can result in a major advancement of cometary science. The study concludes that a mission can be completed for launch on a five year development cycle and that if that five year cycle is initiated with a Phase A study no later than January 2010, a mission using either conventional chemical propulsion or SEP can be developed in time to launch to C-G. Such a baseline plan may provide a mission with the lowest risk owing to the investments already made in understanding that target's environment.

The complexity of a CSSR mission is significant. Though nearly all the component elements with the most significant development risk have now been demonstrated, the *coordination* of all these major elements (spacecraft, sampling system, and sample return vehicle) will require great care, including significant system engineering activity. The development of each element alone has low risk, but the risk of the integrated system is higher – defined as medium risk in Section 4.9. The cost of developing this CSSR mission, as established by a bottoms-up cost estimate, is clearly within the range envisioned for New Frontiers missions, but we estimate that there is a "medium" risk that this mission will exceed the cap of $820M.

2. CSSR SCIENCE OBJECTIVES

The fundamental (Group 1) CSSR mission scientific objectives are simple and straightforward:

- Acquire and return to Earth for laboratory analysis a macroscopic (≥500 cc) sample from the surface of the nucleus of *any* comet
- Collect the sample using a "soft" technique that preserves complex organics
- Do not allow aqueous alteration of the sample at any time
- Characterize the region sampled on the surface of the nucleus to establish its context
- Analyze the sample using state-of-the-art laboratory techniques to determine the nature and complexity of cometary matter, thereby providing fundamental advances in our understanding of the origin of the solar system and the contribution of comets to the volatile inventory of the Earth

2.1 The Scientific Rationale for a Comet Surface Sample Return Mission

The National Research Council's (NRC) most recent Decadal Survey of solar system science [*New Frontiers in the Solar System*, Belton et al. 2003] lists a Comet Surface Sample Return (CSSR) mission as one of the five key missions to be considered for NASA's New Frontiers (NF) program. NF comprises mid-sized space missions whose scope and budget lie between those of the smaller Discovery missions and the larger Flagship missions. Of the two NF programs recommended by the "primitive bodies" panel of the Decadal Survey, a CSSR mission was ranked higher scientifically than a Pluto/Kuiper belt explorer, but the latter was judged to be more mature technically and programmatically. With the successful launch in January 2006 of the New Horizons mission to Pluto and the Kuiper belt, a CSSR mission now becomes the Decadal Survey's highest ranked primitive bodies NF mission.

Our Science Definition Team (SDT) confirms the Decadal Survey's findings that a CSSR mission is scientifically compelling and deserves to be the next NF primitive bodies mission. Advances in our knowledge from recent missions to comets have slightly modified the details of the requirements for a CSSR mission, but our SDT reaffirms the conclusions of the Decadal Survey that bringing a surface sample from the nucleus of a comet back to Earth for laboratory analysis represents a key step toward understanding the nature of comets and the formation and evolution of the early solar system .

What role can NF-class missions play in the exploration of comets? Additional Discovery-class flyby missions will continue to reveal the diversity of cometary surfaces, as has already been observed in the four comets encountered to date. Another coma sample return mission would address whether the Stardust results can be generalized to other comets or if there is compositional diversity as well as physical diversity among the nuclei. But cometary flyby missions are intrinsically limited by their short encounter times with the cometary nucleus, on the order of tens of minutes, and by the limited payloads that can be included on those missions.

Just as exploration of the planets has moved in a progression from flybys to orbiters to landers, and perhaps one day, to sample return, the exploration of comets must now move past simple flybys to more sophisticated missions that include orbiters, landers, and sample return. While flyby missions can continue to provide important advances in our knowledge of comets, only the more advanced missions can address the most fundamental scientific questions posed by the Decadal Survey. The ESA/NASA Rosetta mission is the first to attack these more ambitious goals. A CSSR mission has the potential to be another, with sample analysis capabilities that far exceed those available from the Rosetta in situ investigations. Nucleus orbiters, landers, and

samplers may be beyond the current scope of Discovery-class missions, but they should be within the grasp of a suitably focused NF mission.

We discuss in detail below the scientific justification for spacecraft missions to comets and how a CSSR mission will dramatically improve our knowledge of these primitive bodies that are so important for understanding the origin and evolution of our solar system. Indeed, a CSSR mission is the next logical step in our journey to unravel the mysteries of comets. Eventually, the holy grail of cometary missions will be the return of cryogenically and stratigraphically preserved samples from well below the nucleus surface. That objective is clearly in the exclusive domain of a Flagship mission and would likely be one of the most valuable missions that NASA could fly within the next two decades.

2.1.1 Comets as Windows to our Past

Comets provide our best probes of the physical and chemical conditions in the outer solar system during its formation 4.6 Gyr ago. Comets are so small (the vast majority are <10 km in diameter; Lamy et al. 2004) that gravitational accretion heating has not appreciably altered cometary nuclei since their formation, unlike the case for the planet-sized objects in the solar system. Interior heating from the decay of radiogenic elements was probably also negligible for cometary nuclei, except under special conditions [Merk and Prialnik 2006].

Comets formed in the outer solar system [Dones et al. 2004; Duncan et al. 2004], from approximately the orbit of Jupiter to beyond Neptune's orbit, and have spent most of their lifetimes at cryogenic temperatures (in either the KuiPper belt or the Oort cloud), thereby making it easier to preserve volatile compounds incorporated during their formation. Comets probably formed by the accretion of smaller solid bodies, with a composition determined by the thermodynamic stability of the solid material in the nebular disk. Comets, therefore, provide our best, accessible record of the temperature, pressure, and molecular composition of the protoplanetary disk (see Fig. 2.1.1-1).

Not only does a comet provide detailed information about the conditions in the part of the protoplanetary disk where it formed, but, as shown dramatically by results from the Stardust mission [Brownlee et al. 2006], a comet can also tell us about the mixing of material from different parts of the disk and the survival of material from the interstellar medium (ISM). Stardust revealed that microscopic material is mixed over many astronomical units (AU), from far inside the orbit of Mercury to the Uranus-Neptune region and beyond, but the relative proportions of transported grains and locally condensed grains cannot be determined from the samples returned by Stardust. Several pieces of evidence, including chemical heterogeneity in the outgassing from comet 9P/Tempel 1 [Feaga et al. 2007], suggest that there was also mixing of macroscopic bodies over at least AU-sized distances.

Present-day cometary matter still shows clear signatures of its interstellar origin [Ehrenfreund et al. 2004; Bockelée-Morvan et al. 2004], firmly demonstrating its primitive nature. Furthermore, the observed compositional heterogeneity among comets [A'Hearn et al. 1995, Bockelée-Morvan et al. 2004], suggests that comets encode a record of the different temperatures and pressures throughout the nebula where nuclei formed. Comets, therefore, provide a window to our solar system's origin, which is one of the principal reasons why these tiny objects are such an important scientific priority.

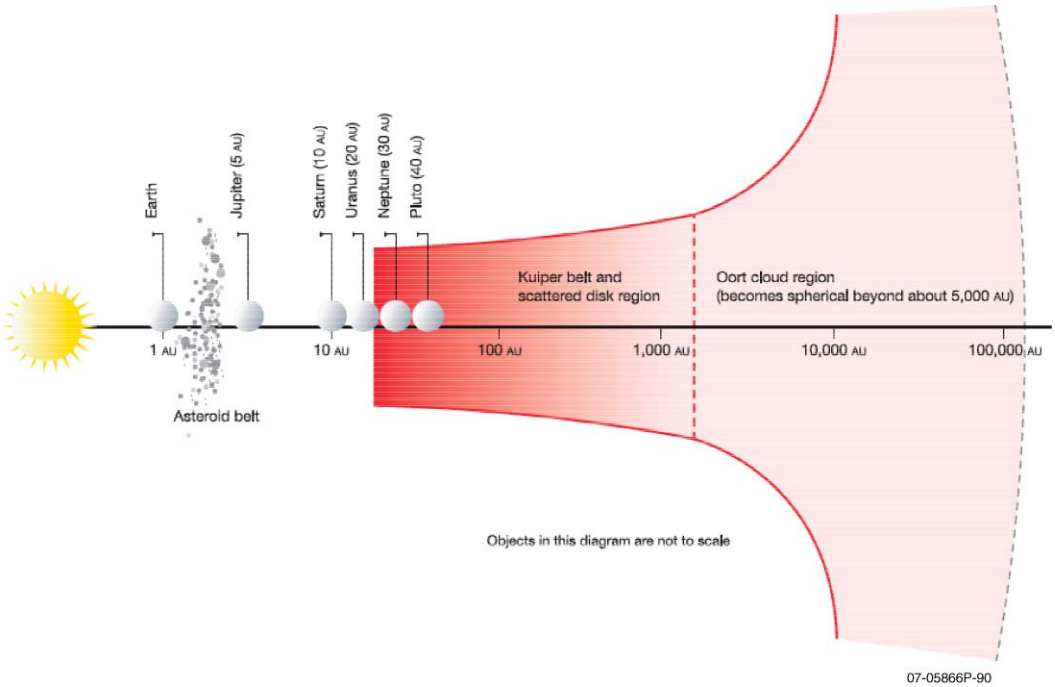

Figure 2.1.1-1. This cartoon illustrates the basic structure of the solar system. The two primary comet reservoirs are the Kuiper belt and the Oort Cloud, both at very large heliocentric distances. The Jupiter Family Comets (JFCs), or "ecliptic" comets, are now orbiting the Sun with perihelia that cross the terrestrial planets region and with aphelia inside Neptune's orbit, but they are thought to have originated within the scattered disk region of the Kuiper belt. Gravitational interactions with Neptune excited some of the scattered disk objects into orbits that ultimately caused them to be transferred into the inner solar system, where Jupiter dominated their subsequent dynamical evolution. The long period comets, also known as the "isotropic" comets, include Halley-type comets and are thought to have formed in the region of the Giant Planets where they were gravitationally scattered into the Oort cloud shortly as those planets formed. Gravitational perturbations by galactic tides, nearby stars, and Giant Molecular Clouds inject some Oort cloud comets into the inner solar system. (Adapted from Stern 2003.)

Cometary matter has certainly undergone some processing over time since formation of the solid particles from which the nuclei formed, and this must be remembered when interpreting cometary data in terms of protoplanetary conditions. This processing includes the heating of precometary grains as they pass through accretion shocks upon entry into the solar nebula, collisional heating as the grains agglomerate into cometary nuclei, modification during mutual collisions among nuclei as they are scattered within the early solar system, radiation processing (photon and charged particle) during the Sun's intense T-Tauri stage, cosmic ray and UV processing of the surface layers of nuclei during their long residence times in the Oort cloud and Kuiper belt, and thermal processing of the surface layers of JFCs during their passages through the inner solar system. While these effects cannot be ignored, the primitive record undeniably remains present in cometary nuclei.

Unfortunately, a sparse (i.e., too few comets surveyed) and incomplete (i.e., not detailed enough) observational record, and evidence of strong radial mixing of material throughout the solar nebula, have frustrated our attempts so far to make unambiguous connections between the composition of comets and their formation sites. As discussed further below, a CSSR mission can provide exquisitely detailed information on the non-volatile composition of cometary nuclei that will dwarf anything that can be achieved via remote observations. In particular, the material

returned by a CSSR mission will, for the first time, tell us exactly how complex cometary matter is. The detailed chemical and isotopic laboratory analyses performed on a CSSR sample will also enable a chronology of the matter making up a cometary nucleus, which can be used to test our models for the solar system's formation and evolution to a much greater extent than previously possible.

2.1.2 Comets and Chronology

Age dating based on studies of radioactive decay has been an invaluable tool in developing the early chronology of the solar system, from the creation of radioactive species in supernovae through the late heavy bombardment as best dated on the Moon. The techniques have been extensively applied, e.g., to chondritic meteorites. Relative ages can be determined from the extinct radioactive $^{26}Al \rightarrow {}^{26}Mg$ system, and absolute ages can be determined, e.g., from the $^{207}Pb/^{206}Pb$ ratio, which is caused by long-lived radioactivities (^{238}U). The grains that permit age dating are relatively rare, and no suitable grains have yet been identified in the samples returned by Stardust, even though many of these grains are sufficiently refractory that they should have survived the capture into aerogel. To date, there are no age determinations that can be directly associated with comets, and any such determination will require a large sample in order to include a reasonable number of the individually very small, datable, cometary grains. Determining the ages of a suite of grains from a single comet will provide crucial information about the history of the early solar system.

2.1.3 Comets as Purveyors of Water and Organics Throughout the Solar System

Comets are chock-full of water and organics, and they seed the entire solar system with these essential ingredients for life. Both reservoirs of comets (Kuiper belt and Oort cloud) are capable of impacting the planets and satellites throughout the solar system, with the spectacular collision of comet D/Shoemaker-Levy 9 with Jupiter in 1994 as the most recent example.

The potential contribution of comets to the volatile and organic inventory of the Earth and the other terrestrial planets remains one of the most interesting unresolved issues in planetary science. The deuterium to hydrogen (D/H) ratio in cometary water for three Oort cloud comets is approximately two times larger than the value in standard mean ocean water (SMOW) on Earth [Bockelée-Morvan et al. 2004], which suggests that cometary impacts could not supply more than a few tens of percent of the terrestrial water inventory if those comets are representative of the ones that impacted the Earth during its early history and if water on the primordial Earth had the same D/H ratio as the current SMOW value. However, the D/H ratio has never been measured in a JFC, and compositional diversity has clearly been observed among the Oort cloud comets. Although the D/H ratio in the hydrated minerals of some chrondritic meteorites is consistent with SMOW, which implies that impacts by the primitive asteroids could supply most of Earth's water [Robert 2001], noble gas abundance variations among the terrestrial planets are better explained by cometary impacts, assuming that noble gas trapping in laboratory comet analogs mimics that in real comets [Owen and Bar-Nun 2001].

The most accurate way to determine the connection between cometary and terrestrial matter is to perform laboratory analyses of a macroscopic sample from a cometary nucleus. The sample returned by a CSSR mission will preserve the organic content of the cometary surface layers, even if the most volatile ices are lost during the capture and return. The CSSR mission will enable the most detailed comparison yet of the atomic (including noble gas), chemical, and

isotopic compositions of terrestrial and cometary organics, which will allow a better understanding of the role played by exogenic sources for terrestrial organics. In addition, the analysis of CSSR samples should illuminate which interplanetary dust particles (IDPs) or micrometeorites captured in the Earth's atmosphere have a cometary origin. Finally, if some water ice is retained by the CSSR sample, this will enable measurement of the D/H ratio in water from a JFC to determine whether it is compatible with the terrestrial value.

2.1.4 Comets and the Giant Planets

The formation of the Giant Planets is one of the key uncertainties in our understanding of the formation of the solar system. Many theorists argue that the Giant Planets generally, and Jupiter in particular, began with the accretion of solid planetesimals to form a core of up to 10 Earth-masses. This enabled subsequent gravitational accretion to then sweep up both gas and solids. The planetesimals that formed the cores of the Giant Planets were cometary nuclei. While the Juno mission is aimed at determining whether there is a 10-Earth-mass core in Jupiter, the study of cometary nuclei is important for understanding the nature of that core and for determining the timescale on which the comets became available to create cores for the giant planets.

2.2 Decadal Survey and NASA Roadmap Recommendations for CSSR Mission

A CSSR mission is responsive to the following broad scientific questions posed by the NRC's Decadal Survey:

- What processes marked the initial stages of planet and satellite formation?
- What is the inventory of volatile compounds, especially water, across the solar system?
- What is the nature of organic material in the solar system, and how has this matter evolved?
- How do the processes that shape the contemporary character of planetary bodies operate and interact?

The Decadal Survey emphatically stated that the return of comet samples to the Earth for laboratory analysis is one of the most important objectives in all of planetary science: "No other class of objects can tell us as much as samples from a selected surface site on the nucleus of a comet can about the origin of the solar system and the early history of water and biogenic elements and compounds. Only a returned sample will permit the necessary elemental, isotopic, organic, and mineralogical measurements to be performed."

In fact, the Decadal Survey concluded that the scientific objectives of a CSSR mission are *more* compelling than those of a Pluto/Kuiper belt mission, but the latter was ranked higher because the planning for a Pluto mission was already fairly advanced at that time and uncertainties regarding the nature of the surfaces of cometary nuclei raised feasibility concerns for a CSSR mission. Those feasibility concerns have largely been dispelled by the results from the Deep Impact mission and indirect evidence from several other sources, which suggest that comets are extremely porous and essentially strengthless bodies and that it should be relatively easy to collect material from the surface of a cometary nucleus (see Fig. 2.2-1).

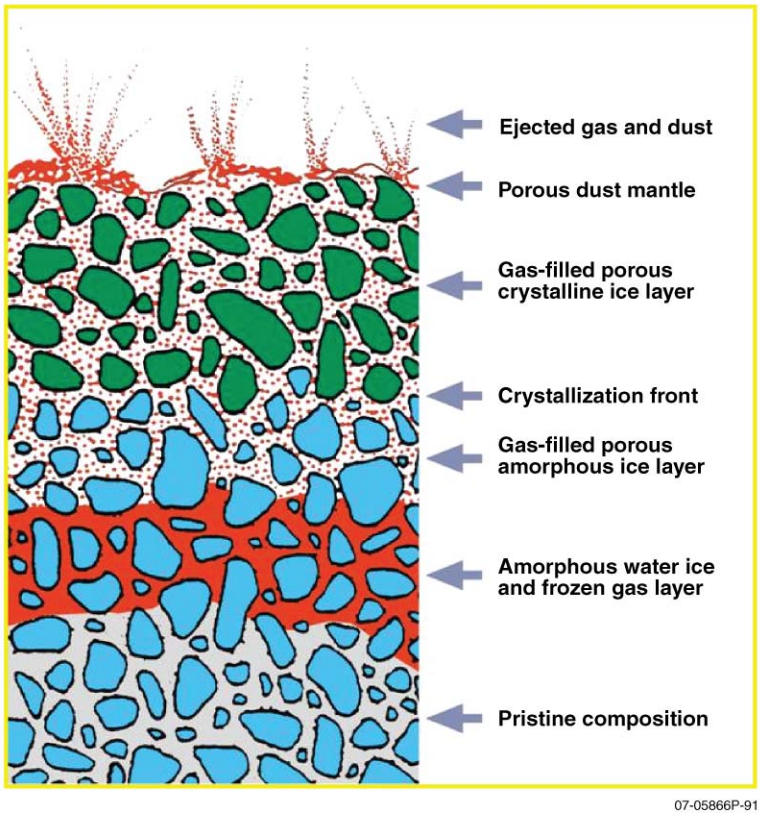

Figure 2.2-1. Cartoon illustrating a possible structure of the near-surface region of cometary nuclei. The results from the Deep Impact mission on comet 9P/Tempel 1, and indirect evidence from cometary breakup events, strongly suggest that the surfaces of cometary nuclei are extremely porous (>70% porosity) and essentially strengthless (even less cohesive than talcum powder), which should make it relatively easy to retrieve a sample for return to the Earth. The exact depth where significant ice is present is uncertain but is thought to be on the order of a few centimeters, which means that even short sample probes may collect some icy material. (Adapted from Prialnik 2004.)

The most recent NASA Roadmap for planetary exploration [*Solar System Exploration Roadmap*, 2006] reiterated the Decadal Survey's priorities, so a CSSR mission remains the highest priority primitive body mission in the NF class.

2.3 Insights from Past and Planned Comet Missions

To date there have been spacecraft flybys with high-resolution imaging of four different cometary nuclei. The results from those missions have revolutionized our view of comets, as discussed below.

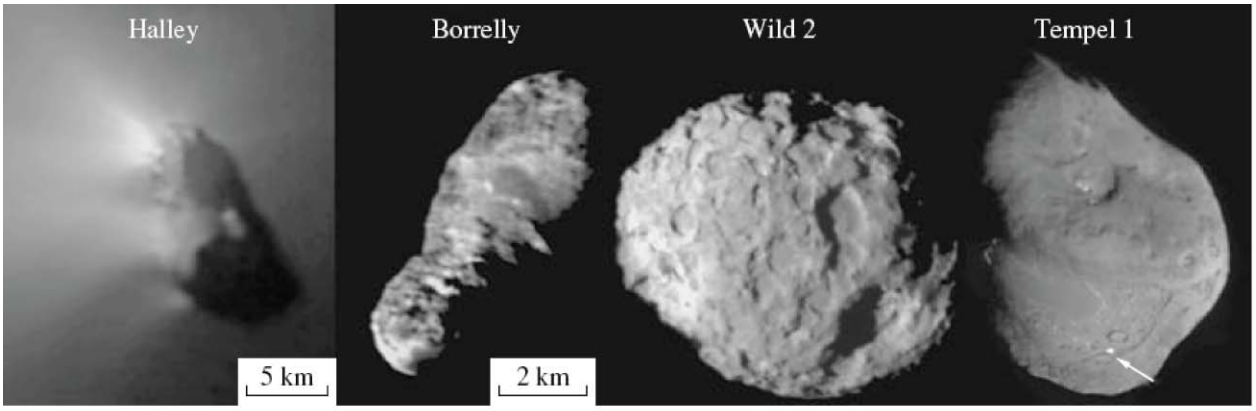

Figure 2.3-1. Visible light images of the four comets observed by flyby spacecraft. Comets 19P/Borrelly, 81P/Wild 2, and 9P/Tempel 1 are displayed with identical spatial scales, while the image of 1P/Halley is reduced by a factor of ~2.5 relative to the others. These images show the remarkable physical diversity among cometary nuclei. Nevertheless, all of these nuclei are thought to be extremely porous (porosity >70%) and to have essentially no tensile strength (i.e., they are bound only by self gravity). The arrow in the image of 9P/Tempel 1 points to the flash produced as the nucleus was impacted by a high-speed projectile fired by the Deep Impact spacecraft. (Adapted from Basilevsky and Keller 2007; all images from NASA and ESA mission websites.)

2.3.1 Results from 1P/Halley In Situ Investigations

Five spacecraft flew by the Oort cloud comet 1P/Halley in March 1986: the Soviet Vega 1 on March 6 and Vega 2 on March 9, the Japanese Suisei on March 8 and Sakigake on March 11, and ESA's Giotto on March 14. The major in situ results of the flyby missions are as follows:

The visible light cameras showed conclusively for the first time that the comet nucleus consists of a single solid body, in Halley's case an ellipsoidal object having dimensions of 15 km × 7 km × 8 km. Rather surprisingly, the observations revealed a very irregular surface that was incredibly dark, with a geometric albedo of only ~4% and with a maximum temperature that was unexpectedly hot (~380 K). Despite the high temperature, direct measurements of the gas flow by mass spectrometers confirmed outflow speeds of ~700 m/s, which is consistent energetically with a sublimation temperature of only ~ 200 K, clearly not accommodated with the dark surface. The observed gas production rates indicated that only ~10% of the sunlit surface was active, consistent with the interpretation that most of the surface of the nucleus was covered with a refractory mantle.

Water accounted for 80% (by number) of all the gases released into the coma with 10% CO from direct and extended sources, 3–4% CO_2, and smaller amounts of CH_4, H_2CO, NH_3, and HCN. A large variety of ion species produced in the coma by solar UV-induced photochemistry of the parent molecules were also detected, including H_3O^+, which is the dominant ion in the inner coma.

Many of the dust particles were the expected refractory silicates with large amounts of oxidized Si, Fe, Ca, Mg, and Na. A second population, ~30% (by mass), were organics, composed largely of C, H, O, and N, the so-called CHON particles. Thermal disruption of CHON particles might provide the sources of certain classes of gas species, such as H_2CO and the various visible carbon radical jets. There were also mixed particles of the two classes. Approximately two-thirds (by mass) of the material released into the coma was in the form of particles rather than volatile gases. A larger than expected population of very small particles, <<1 μm, contributed to the

particle size distribution function. At the opposite extreme were particles >1 cm in size, which contains most of the mass in dust particles. Neither size range was sampled by the STARDUST coma sample return mission, but both will be extensively sampled by a CSSR mission.

Most of the elements detected in the coma were present in solar abundances except for hydrogen and nitrogen, which were depleted. The D/H ratio in Halley was found to be enhanced compared to terrestrial (SMOW) values by a factor of ~2. This was later found to be consistent with remote observations of HDO in bright comets Hale-Bopp (C/1995 O1) and Hyakutake (C/1996 B2).

2.3.2 Deep Space 1 Results on 19P/Borrelly

The NASA-JPL Deep Space 1 Mission (DS-1) performed a flyby of the Jupiter family comet 19P/Borrelly with closest approach on 2001 September 22, about 8 days after perihelion, at a distance of 2171 km. The remote-sensing package on DS-1 obtained numerous CCD images of the comet and near-IR spectra of the surface [Soderblom et al. 2002]. These images provided the first close-up view of a comet's nucleus sufficiently unobscured to perform quantitative photometric studies; at closest approach, the peak resolution was 47 meters per pixel. The disk-integrated geometric albedo of Borrelly's nucleus is 0.072 ± 0.020 [Li et al. 2007], slightly larger than but comparable to that of other comets. The nucleus exhibited significant variations in macroscopic roughness, with the oldest, darkest terrain being slightly smoother. This result suggests that low-lying (low-gravity) areas have been filled with fine-grained materials that have been unable to escape the surface, as was observed at asteroid Itokawa by the Hayabusa Mission [Fujiwara et al., 2006] and at asteroid Eros [Veverka et al. 2001]. Britt et al. (2004) reported the presence of smooth plains and multiple, 100-m-high, mesa-like structures bounded by scarps. These scarps, they suggest, could be backwasting and could be the main contributor to mass loss by sublimation.

2.3.3 Stardust Results on 81P/Wild 2

Stardust is a NASA Discovery-class mission with challenging, but limited, sampling goals. The Stardust target, comet 81P/Wild 2, proved to be a geologically active and complex nucleus. During a flyby of the nucleus at a speed of 6.1 km/s and a closest approach distance of 234 km, the spacecraft successfully collected small (<100 μm) grains of coma dust via high-velocity impact into low-density silica aerogel. The mission was not intended to recover volatile samples from the comet nucleus. The Stardust collection method largely destroyed submicrometer particulate components and possibly mixed amorphous cometary materials with silica aerogel, which makes it difficult to know whether the retrieved samples are representative of the bulk nucleus.

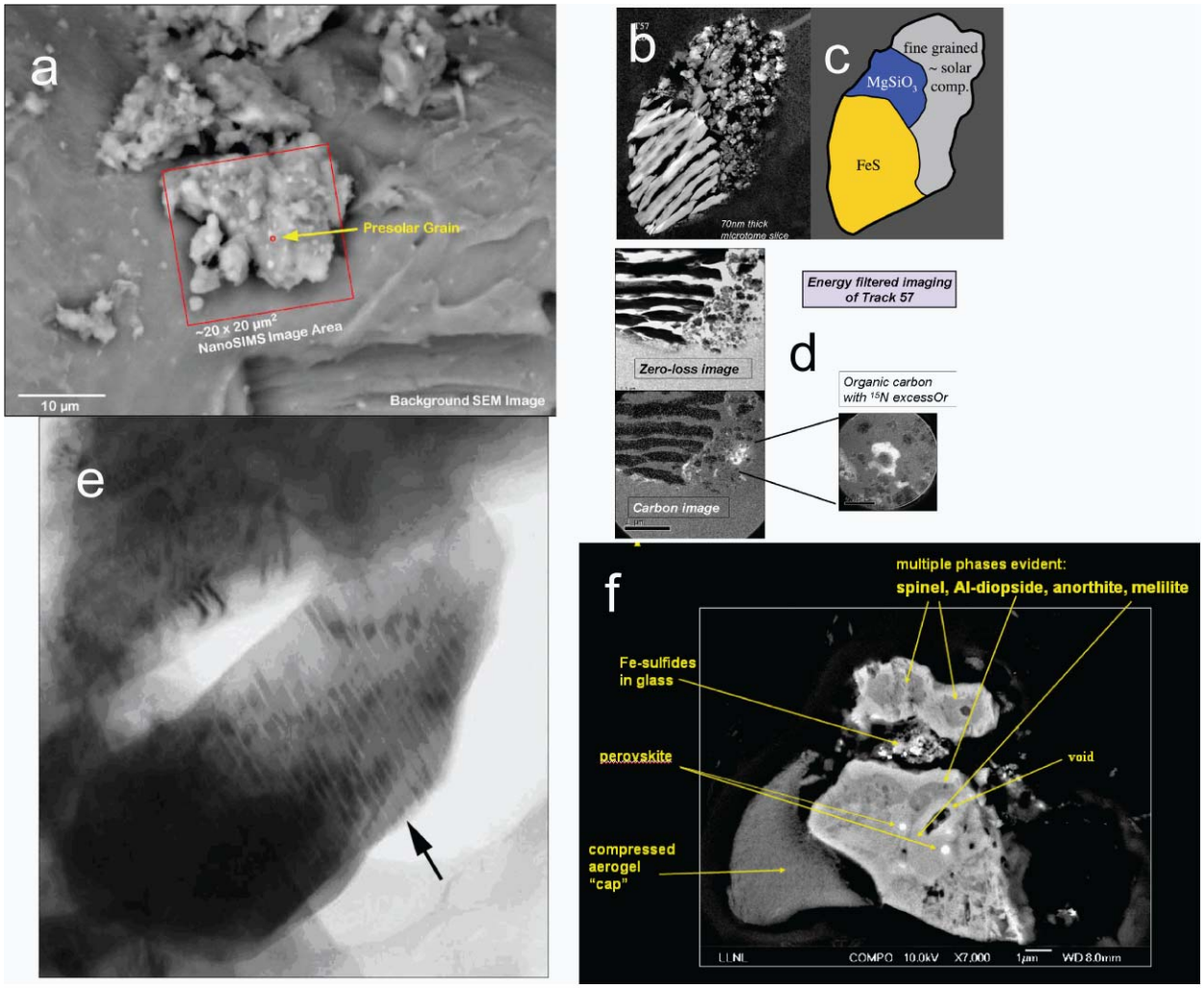

Figure 2.3.3-1. Dust particles from comet 81P/Wild 2 captured by the Stardust mission. (a) A presolar grain (image from A. Kearsley and S. Messenger). (b–d) A thin-sectioned Wild 2 grain consisting of olivine, iron sulfide, and fine-grained material. (d) A close-up of the fine-grained material, which contains abundant organics with a ^{15}N excess (indicated by the color white in the lower right portion of (d) indicative of formation in a very cold environment, such as at the edge of the protosolar disk or in a giant molecular cloud. This particle cannot have been heated appreciably either in the comet or during capture into the aerogel (images from S. Messenger and D. Joswiak). (e) Transmission electron microscopy (TEM) image of a thin-sectioned Wild 2 grain consisting of enstatite with exsolution lamellae of diopside, which had to form from a melt (image from H. Leroux). (f) Backscattered electron scanning electron microscopy (SEM) image of a Wild 2 grain consisting predominantly of refractory Ca-Ti-Al rich oxides and silicates, which must have formed very close to the early Sun (image from D. Joswiak).

Nevertheless, the returned samples have provided a new window on the early solar system. To date, most work has centered on the grains measuring a micrometer or larger in diameter, as the finer-grained materials were in many instances significantly mixed with the capture media, making their analysis difficult, though still possible. Among the recovered Wild 2 samples, demonstrably pre-solar grains are rare (<<1%), though captured cometary organics have inherited pre-solar isotopic compositions, as revealed by excesses of deuterium and ^{15}N. One big surprise of the mission has been that cometary organics were recovered, though in very limited quantities that severely limit the scope of analytical work. The amount of pre-solar material appears to increase with decreasing particle grain size. Amorphous materials appear to be rare, although the

intimate mixing of the captured cometary grains with silica aerogel has made this a controversial issue. The exact nature of cometary amorphous materials may never be known from the Stardust samples.

The returned Wild 2 grains that exceed 1 micrometer in size are crystalline and appear to have formed in a vast range of environments, not by simple annealing of amorphous nebular condensates as many expected. Some materials are organic rich, with ^{15}N and deuterium enrichments that must have formed at the edge of the solar nebula or elsewhere in the galaxy. Other grains have igneous origins and appear similar to chondrules or calcium-aluminum-rich inclusions (CAIs), and may have formed very near the early Sun. Thus, comet Wild 2 appears to have accreted from diverse materials that formed at many different locations in the solar disk, and possibly at a range of times. These diverse materials have remained distinct entities within the cometary nucleus for 4.5 billion years. Thus, this comet will inform us about a wide range of processes occurring in the early solar system, not just processes occurring in the Kuiper belt, including the origin of crystalline materials in circumstellar disks as well as indigenous cometary processes.

We now know that there was significant mixing of material across the solar nebula, and continued study of the Wild 2 samples will further illuminate that process. But the biased nature of the returned samples prevents us from understanding the full magnitude of this critical phenomenon.

When we compare the results of laboratory studies of Wild 2 materials with the spectroscopic observations of Tempel 1, we see major differences. Tempel 1 reportedly contains olivine and pyroxenes that were exclusively high in magnesium, and significant quantities of carbonates and phyllosilicates. This mineralogy suggests formation of cometary precursor materials in a rather restricted solar system environment, and considerable activity if there was liquid water on Tempel 1. By contrast, olivines and pyroxenes in Wild 2 were of the widest possible compositional ranges, and thus far the only possible products of aqueous alteration found have been very rare grains of carbonates. Possible reasons for these mineralogical differences are that these two comets had very different histories, and/or that the sampling of both comets was very limited and biased, and that the analytical techniques were so dissimilar, i.e., remote spectroscopy versus laboratory characterization. All of these explanations provide powerful justification for continued sampling of additional comets.

Stardust provided, and will continue to provide, fundamental results that could not possibly have been obtained from remote sensing or landed instruments. Stardust has also dramatically demonstrated the power, adaptability, evolutionary advances, and elegance of Earth-based instruments, which are typically large and complex and could never be carried on space missions.

2.3.4 Deep Impact at 9P/Tempel 1

On 2005 July 4, a 372-kg smart impactor, released from NASA's Deep Impact (DI) spacecraft, collided with the nucleus of comet 9P/Tempel at a velocity of 10.3 km/s, delivering 20 GJ of energy and resulting in a huge plume of dust, ice, and gas from the nucleus. Remote sensing instruments on the DI spacecraft, as well as from Earth- and space-based telescopes, observed the impact and its evolution with time.

A number of major results of the Deep Impact mission were associated with remote sensing on approach before the impact. The nucleus of Tempel 1 has an effective diameter of ~6 km with maximum and minimum observed diameters of 7.6 and 4.9 km, respectively. It is dark, like other

comets, with an average geometric albedo of 4%. The surface topography is varied. There are large smooth areas possibly indicative of surface flows. There are round features with a size distribution consistent with cratering and very unlike the bimodal distribution of round features seen on 81P/Wild 2 by the Stardust spacecraft. The overall morphology of the body is suggestive of some layering process, perhaps the result of the collisions of several (or many) precursor objects during nucleus formation. Thermal maps of the surface are consistent with a highly porous, low-conductivity body, with little or no thermal lag. The implication is that the active layer of volatile material is only a few centimeters below the visible surface. The porosity of the surface layer was >75%, according to the luminous efficiency of the initial flash. There is no bulk ice on the surface, at least at the resolution of the DI instruments, but there is abundant water ice within about 10 cm of the surface and CO_2 ice within 1 m of the surface. There were several isolated patches of surface frost, but the coverage fraction was small. The CO_2 abundance was ~7%, similar to CO at 5–10% as determined from post-impact remote observations. The spatial distributions of water and CO_2 gas in the coma are different from one another, and neither is well correlated with the dust jets. This must be considered in any "identification" of sampling sites that target "active" areas.

Analysis of the fall back of plume material, in combination with the shape model, yields a mass of the nucleus of 2×10^{16} g and a bulk density estimate of 0.4 g cm^{-3} (with a possible range of 0.2 to 1.0 g cm^{-3}). Analysis of the plume also indicates an upper limit on the tensile strength of the surface material between 200 Pa (talcum powder) and 12 kPa, which is still very weak. The dust-to-ice ratio in the plume was of order 0.1 to 1. The ejecta plume consisted of both refractory dust and nearly pure water ice particles that sublimated over time after the impact. The refractory particles were dominated by grains in the size range of 0.5 to 2.5 mm.

Spitzer Space Telescope infrared spectra of the dust excavated by the impact into 9P/Tempel 1 were similar to those obtained from very active comets, such as C/Hale-Bopp and 17P/Holmes, with even more pronounced spectral features owing to efficient particle fragmentation by the impact [Lisse et al. 2006, 2007].

2.3.5 Expected Results from Rosetta

ESA's Rosetta mission was launched in March 2004 and is currently en route to a rendezvous with comet 67P/Churyumov-Gerasimenko (C-G) in May 2014 at a heliocentric distance of 4.0 AU. The spacecraft carries 11 different scientific investigations, which include narrow- and wide-angle cameras, a visible and infrared imaging spectrometer, a UV spectrometer, a microwave sounder and spectrometer, a dust impact analyzer and accumulation sensor, a dust compositional analysis mass spectrometer, an atomic force microscope, an ion and neutrals mass spectrometer, a collection of fields and particles instruments, radio science, and a radar tomography experiment for investigating the interior structure of the cometary nucleus. In addition, Rosetta is carrying a lander, called Philae, which carries an additional nine investigations, including a drill that will retrieve samples from depths up to 70 cm below the surface for in situ analysis. The lander is expected to survive for several days up to several weeks or months. The orbiter will follow the comet through perihelion at 1.25 AU in August 2015.

Rosetta will be the first comprehensive investigation of a cometary nucleus, following it from its inactive state beyond 4 AU through its most active phase at perihelion. It will map the entire sunlit surface of the nucleus at resolutions certainly better than 1 m, possibly 10 cm, and investigate the nature and evolution of the surface topography. It will observe the onset and evolution of activity from the nucleus, both visually and compositionally, noting the change in the relative

abundances of numerous species as they evolve from the nucleus. Rosetta will map the temperatures on the nucleus surface and will determine the actual sources of cometary activity and how they work. The distribution of minerals and ices on the nucleus surface will be mapped as well as the distribution of numerous gaseous and ion species in the cometary coma. Rosetta will determine the size and velocity distributions of the dust particles released from the nucleus and their variation over time and orbital position.

The radio science experiment will measure the nucleus gravity field and its higher harmonics, as well as the mass of the nucleus. Combined with a shape model from the imaging experiment, this will yield the first direct measurement of the bulk density of a cometary nucleus. The fields and particles instruments will map the structures in the cometary magnetosphere and the interaction between solar wind and cometary neutrals and ions.

The Rosetta lander will make direct in situ measurements of the composition of the cometary surface and near-surface materials. It will obtain measurements of the physical properties of the nucleus surface materials. It will image the surface area around the lander at millimeter resolution or better. The lander also includes a transponder that will work with the radar tomography experiment on the orbiter to map the internal structure of the nucleus.

The Rosetta rendezvous with comet 67P/C-G will certainly be a watershed event in cometary science, and we eagerly await dramatic breakthrough discoveries in 2014. Even in this context, however, the scientific importance of a CSSR mission remains compelling. The in situ analysis of cometary samples by Rosetta is not even in the same league as the detailed and comprehensive analyses that can be performed on CSSR samples at sophisticated Earth-based laboratories.

2.3.6 Outstanding Unresolved Issues

Despite the revolutionary advances provided by the previous spacecraft missions to comets, many fundamental questions remain unanswered. What is the nature and source of cometary activity? Is the activity associated with vents, geysers, fumaroles, or something else? How does the energy exchange between the incoming solar radiation and the near-surface materials work? What is the nature and evolution of cometary land forms? What causes comet fragmentation events?

The spacecraft images of cometary nuclei strongly suggest that geological processes are operating on the surfaces of nuclei. What are those processes and how do they produce the observed land forms? What is the internal structure of the cometary nucleus? Is it indeed a rubble-pile, as proposed by many researchers, or is it more aptly described by one of several other models (e.g., onion skin, talps, fractal, icy-glue, etc.)?

How complex is cometary matter? Do comets harbor the precursors of biological molecules? Did comets supply a significant fraction of the terrestrial water and organics? What is the detailed composition of the cometary volatiles and how are they distributed versus depth in the nucleus? What is the detailed composition and mineralogy of cometary dust? What is the nature and abundance of materials from the inner regions of the solar nebula, whose presence in comets is suggested by analysis of the Stardust samples?

Most of these questions can be addressed by missions such as Rosetta and the CSSR mission discussed here, and we need to take those steps to make significant further progress in cometary science. However, some of these questions can only be resolved by an ambitious Flagship mission that can return a cryogenic sample from deep within a nucleus to Earth for detailed analysis.

A cryogenic comet sample return mission should certainly be near the top of NASA's priories for Flagship missions during the next two to three decades.

2.4 The Role of Remote Observations of Comets

Remote observations have always played, and will continue to play, an important role in the study of comets. Remote spectroscopic studies are responsible for the discovery of many new molecules in comets, and remote photometric observations have been successfully employed to measure the sizes, shapes, colors, and rotational properties of cometary nuclei.

Spacecraft missions generally have a complementary and synergistic relationship with remote observations. Much more detailed information on specific targets can be obtained from a spacecraft mission, and that ground truth can be used together with remote observations to explore the properties of the entire population of comets.

2.4.1 Cometary Volatiles from Earth-Based Facilities

The volatile composition of comets, that is, the inventory of ices captured within cometary nuclei, is a probe of both the comet's formation environment and its subsequent evolution over the age of the solar system. The temperatures and pressures in the regions where comets formed, and the subsequent thermal evolution of comets, play a critical role in determining which ices are retained in cometary nuclei. Researchers have already identified approximately two dozen "parent" molecules in comets [Bockelée-Morvan et al. 2004], ranging from extremely volatile species like carbon monoxide (CO) and methane (CH_4), which freeze out only for temperatures below 35 K, to plain water (H_2O) ice, which is the dominant volatile constituent in cometary nuclei and has a sublimation temperature in space of ~180 K. Infrared, radio, and ultraviolet remote measurements of comets show an interesting diversity in composition among the dozen or so Oort cloud comets observed during the past decade that may reflect varying physical conditions throughout the regions where comets formed. Systematic optical surveys of many comets during the past several decades have shown abundance variations among the radicals CN, C_2, C_3, and NH, including the finding that roughly half of the Jupiter family comets, but very few Oort cloud comets, are significantly depleted of carbon-chain molecules [A'Hearn et al. 1995].

Despite the remarkable advances enabled by remote compositional measurements of comets, the true complexity of cometary matter can never be ascertained this way. As molecules become more complex, so do their spectral signatures. The relatively sparse spectral features of simple molecules give way to a forest of overlapping lines from different species that cannot be untangled even using spectral resolving powers exceeding a million. And when the resolution is high enough to resolve the lines separately, the sensitivity required to detect the lines is usually well below the available limits, except possibly for the very brightest comets. We must, therefore, rely on cometary samples measured in situ or, preferably, returned to Earth for laboratory analysis to measure the most complex species in comets. Identification of the most volatile species will require a cryogenic sample return capability, which is generally acknowledged to be in the domain of a Flagship-class mission, but a CSSR mission should be capable of providing compositional information on all species whose volatility is comparable to that of water, including many complex organics.

2.4.2 Earth-Based Investigations of Dust

The dust released from comets is typically observed remotely at visible and infrared wavelengths. The visible scattered radiation allows one to determine albedo, phase function, and polarization for the dust, setting limits on the composition and size distribution of the optically dominant grains. Observations of the infrared thermal emission from the dust are more diagnostic. The thermal spectral energy distribution allows us to model the temperatures and size distribution of the dust, while infrared spectroscopy can be used to identify the mineral composition of the dust.

Thermal infrared spectroscopy of several comets having strong emission peaks indicates a complex mineralogy for cometary silicates, including grains that must have formed under a wide range of physical conditions. The emission features in cometary infrared spectra suggest the presence of various silicates, including fosterite (Mg-rich olivine), fayalite (Fe-rich olivine), amorphous silicates, and diopside (Ca/Al-rich pyroxene). The refractory Si:Mg:Fe:Ca:Al abundances estimated for these materials, based on analysis of the Spitzer spectra of comet 9P/Tempel 1 immediately following the projectile impact, are consistent with solar system abundances determined from the Sun and from C1 chondrites [Lisse et al. 2007]. The dust spectra of Hale-Bopp, which is the best-studied comet to date at thermal infrared wavelengths, are quite similar to those of Tempel 1, although the Tempel 1 spectrum has much more detailed spectral structure.

However, our knowledge of comet dust composition from remote sensing is limited because the thermal infrared spectra of most comets do not have enough spectral structure to permit detailed mineralogical identifications. Also, full modeling to pin down the temperature, size distribution, and porosity for each of several grain components, in order to determine abundances, is only possible with complete 5- to 35-μm spectra having high contrast features. Cold dust, or a component present only as large, optically thick particles, can be masked by the emission from smaller, warmer grains. Moreover, the carbonaceous material in the dust cannot be well characterized from remote sensing.

IDPs collected at Earth can also provide information about probable cometary dust composition, if one can identify which types of IDPs are actually from comets. The anhydrous chondritic aggregate IDPs are the most likely candidates, based on their high atmospheric entry speeds, porous structure, small grain size (0.1–0.5 μm), and high carbon content. These heterogeneous aggregate particles are a mix of crystalline and non-crystalline silicates of both pyroxene and olivine composition, FeNi sulfides, carbonaceous material, and other minor components. The carbon is distributed as a matrix surrounding the mineral grains, and much of the carbon is in an organic phase. The crystalline silicates have a high abundance of the Mg-rich minerals forsterite and enstatite, consistent with the infrared cometary spectra. The non-crystalline grains are primarily GEMS (glass with embedded metal and sulfides). These are glassy Mg-silicate grains 0.1–0.5 μm in size with embedded nanometer FeNi and iron sulfide crystals.

The composition of the anhydrous chondritic aggregate IDPs collected in Earth's atmosphere is generally consistent with the Stardust results for the Wild 2 particles analyzed to date. The Wild 2 particles captured in the aerogel appear to be fine-grained heterogeneous aggregates, containing olivine, pyroxene, Fe-Ni sulfides, and carbonaceous material. While the Wild 2 grains and anhydrous chondritic IDPs contain a large fraction of Mg-rich olivine and pyroxene, these minerals also show the widest range of compositional variations in both cases.

However, we cannot be certain that any given IDP is cometary, and we may be overlooking true cometary particles in other IDP subgroups classified as "asteroidal." There may be some cometary particles that do not survive atmospheric entry, including some organic materials.

2.4.3 Population Studies Using Remote Observations

One of the key contributions of remote observations is the ability to investigate *many* comets so that their properties as a population can be addressed, something that is impractical to do with spacecraft missions. Remote observations are currently being used to measure the bulk physical characteristics of comet nuclei, e.g., in order of decreasing knowledge: size, shape, albedo, rotation, spin state, and color. Through 2007, reasonably accurate size estimates had been determined for nearly 80 cometary nuclei, and, over time, many more comets should be added to the list. Roughly two dozen cometary nuclei have been monitored well enough to estimate axis ratios, but detailed shape models exist only for the four nuclei already visited by spacecraft. Detailed rotational information is available for even fewer comets, and only a handful of those are well enough documented to determine the spin state, including two cases that provide evidence for a rotational period that changes over time. Albedo and color measurements are available for ~20 comets, but there are inconsistencies among the color measurements for some nuclei, possibly owing to unrecognized coma contamination. The phase function behavior of cometary nuclei generally cannot be investigated by remote means.

In summary, important strides have been made using remote observations to address the properties of cometary nuclei as a population, and further progress should be possible in the future. But in situ spacecraft mission results are needed to establish the ground truth for individual nuclei that allow the results from remote observations to be reliably extended to comets that cannot be visited by spacecraft.

2.5 CSSR as the Next Big Step in Comet Exploration

As emphasized by the Decadal Survey, understanding comets is key to understanding how the solar system formed. Since comets seeded the entire solar system with water and organics, elucidating the nature of cometary matter (e.g., the D/H ratio of cometary water, the complexity of cometary organics, etc.) will likely be a fundamental step toward explaining the origin of life on Earth and possibly elsewhere.

Despite the wealth of new information on one particular JFC provided by Stardust, the limitations of that mission's collection technique invites the next step in cometary exploration beyond what will be achieved by that or any other current or planned mission. The Stardust collection method largely destroyed most of the impacting particles (raising the issue of whether the collected samples are truly representative of the bulk of the nucleus) and thoroughly mixed amorphous cometary materials with silica aerogel; information on the bulk of the fine-grained amorphous cometary materials may not be recoverable from these samples. A CSSR-type mission is thus required that will make a deliberate effort to collect fine-grained and non-crystalline materials, as well as labile organics at low temperatures.

Stardust collected only grains measuring up to tens of micrometers in size [Zolensky et al. 2006]. Returning a much larger sample mass to Earth would provide larger particles, millimeter-size rocks, and rare components (such as zircon crystals) that would finally permit age dating and isotopic analysis to establish whether there was live ^{26}Al or ^{60}Fe in the accreted comet, which could serve as a source of internal heat. In addition, we have found that practically every grain of

Wild 2 is different from every other grain, which suggests that a much larger sample would be more representative of the mineralogy and composition of a particular comet, and presumably comets in general. Owing to the apparent heterogeneity of comets, as revealed by studies of returned Wild 2 grains, our understanding about the early solar system should increase proportionally with an increase in returned sample volume.

It is essential that the returned sample from a CSSR mission not come into contact with liquid water at any time during or after the mission. We know from the Halley and Wild 2 results that comets contain a major component of nanophase materials, which will be exceptionally susceptible to aqueous alteration. If captured cometary water ice were permitted to melt during any phase of the mission (or during sample recovery or curation) and interact with the cometary solids, aqueous alteration of the returned sample would forever erase any record of amorphous nebular condensates and yield a completely erroneous view of the physical and chemical history of the comet. Any collected water ice must either be maintained in a frozen state during the mission and subsequent curation, or a system must be set up to ensure that the vapor pressure from the ice does not rise high enough to cause aqueous alteration of the solid sample. If possible, it is preferred that any water ice collected during the CSSR mission be maintained in the solid state, so that cometary water can be directly examined in laboratories on Earth.

Organic materials are now known from the Stardust mission [Sandford et al., 2006] to be present in abundance in cometary samples, and these may include molecules made and/or modified in stellar outflows, the interstellar medium, and the protosolar nebula, as well as by parent body processing within the comet [Delsemme 1992]. The presence of organic compounds in comets is of astrobiological interest because cometary delivery of organics throughout the solar system may have played an important role in the origin of life on Earth (e.g., in the era of the Late Heavy Bombardment and the subsequent rise of life) and possibly elsewhere (e.g., the icy Jovian and Saturnian moons; Chyba and Sagan, 1992). The majority of the organic material found in meteorites is in insoluble macromolecular phases. In contrast, it is striking that the Wild 2 samples show evidence of relatively labile organics [Sandford et al., 2006]. In addition to the predominantly refractory organics that have been preserved in aerogel, the captured Wild 2 particles contained an organic component that was volatilized during impact and diffused into the surrounding aerogel. In terms of sample heterogeneity, the organics found in Stardust samples are similar to stratospheric IDPs and primitive meteorites. However, they exhibit a greater range of compositions (higher O and N concentrations) and they include an organic component that is poor in aromatics and also a more labile fraction (possibly the same material). In general terms, the organics in Wild 2 samples are even more "primitive" than those in meteorites and IDPs, at least in terms of being highly heterogeneous and unequilibrated. Unfortunately, this heterogeneity has been severely affected by the Stardust mission collection process, which will *not* be an issue for samples collected by a CSSR mission.

The much larger sample volume returned by a CSSR mission, carefully maintained below the freezing point of water ice, will permit a thorough analysis of labile species with high to moderate sublimation temperatures that have not been preserved in any comet samples available to date. A CSSR mission will also enable, for the first time, a sensitive search for minor but critically important cometary organic components expected to be present, such as amino acids, which is not possible for the small sample returned by Stardust.

It is only with a carefully preserved, macroscopic comet nucleus sample that we can apply the full power of laboratory analytical techniques to the investigation of the elemental, molecular, isotopic, and mineralogical content of the returned sample. With samples in the laboratory,

we can achieve unprecedented sensitivity: trace elements and isotopes can be measured that can be used for geochronology and assessment of the importance of cometary impacts to the terrestrial volatile inventory, analyses can be repeated where unexpected results are obtained, and analyses can continue for many years in the future in response to new questions as they arise. With a substantial (approaching 1 liter in volume) cometary sample returned from a CSSR mission, we will finally have the means to determine the true complexity of cometary matter, thereby gaining a more profound understanding of early solar system processes.

2.6 Target Selection for a CSSR Mission

The CSSR SDT provided the mission engineering team with a list of nine potential targets for a CSSR mission. These objects were selected mainly because they might potentially satisfy the dynamical constraints for a rendezvous mission (e.g., the perihelion distance, aphelion distance, and orbital inclination were favorable and would not impose unrealistic launch C_3 or spacecraft delta-V requirements), and they were already fairly well characterized by previous observations. However, the CSSR target will be extremely well scrutinized during the rendezvous phase of the mission, even if the object's properties were not well measured from previous observations, and the SDT ultimately concluded that any bona fide comet could be a suitable CSSR mission target. We therefore strongly recommend that NASA give proposers flexibility in their target selection for a CSSR mission.

We selected 67P/C-G as the target for the current study for two reasons: (1) it is a viable target for both ballistic (chemical propulsion) and solar electric propulsion (SEP) missions, thus allowing us to compare those two options, and (2) the nucleus of C-G will be extremely well characterized by the Rosetta mission, which should provide some risk mitigation for the CSSR mission.

2.7 Science Requirements for the CSSR Mission

As is common practice for NASA space missions, the SDT defined a set of prioritized, high-level scientific requirements for a CSSR mission. The "Group 1" objectives are the "science floor"; if the mission cannot accomplish the Group 1 objectives discussed below, the mission will be judged a failure scientifically. Conversely, if a mission successfully accomplishes the Group 1 objectives, the mission can be judged successful because exciting, breakthrough science will have been achieved.

However, it is important that any CSSR mission selected by NASA adopt a more ambitious set of objectives as its "baseline." In addition to accomplishing the Group 1 objectives, the selected CSSR mission should be designed so that it can achieve all of the "Group 2" scientific requirements discussed below.

Finally, there are many scientific objectives that could potentially be addressed by a CSSR mission, but which are clearly of lower priority than the Group 1 or Group 2 objectives. The SDT encourages NASA to request that proposers be responsive to the Group 3 objectives mentioned below, but it should also be made clear that Group 3 goals must be descoped when necessary to ensure that the mission can be accomplished on time and within the original budget, while still achieving all the Group 1 objectives and as many of the Group 2 objectives as feasible.

2.8 Group 1 Objectives: Science Floor (Must Do)

2.8.1 Return a macroscopic (≥500 cc) sample from the surface of a comet to Earth with no aqueous alteration; the returned sample volume can be reduced to ≥250 cc in exchange for substantially lower temperatures (i.e., at least to preserve water ice) that are justified for preservation of the sample

The 81P/Wild 2 grains returned by Stardust were generally submicrometer to nanometer-sized, and much less than a total of 1 mg of sample material was retrieved. The Stardust, Giotto, and Vega spacecraft were operated more than 100 km from their targeted nuclei, deliberately out of the reach of larger spacecraft-threatening grains. IDPs also are 100 μm and smaller; larger micrometeorites generally melt during atmospheric entry. Thus, we currently know essentially nothing about coarser-grained cometary materials, a situation that can be rectified by the sample returned by a CSSR mission.

While one might have anticipated the micrometer-sized materials from Wild 2 to be a homogeneous collection of commonly formed minerals (Mg-rich olivine and pyroxene, Fe-Ni sulfides, etc.), in reality the collected grains have a fantastic degree of variability. Practically every recovered Wild 2 grain has proven to be different from all the others, which suggests that larger, coarser-grained samples might show even greater variability. This extreme mineralogic and petrologic sample variability presumably derives from a vast range of sample formation sites and grain histories, certainly before, and possibly after, comet accretion. Far from having formed from materials that originated in the outer early solar system, the materials in Wild 2 appear to have sampled the entire early solar system as well as its surroundings. In order to ensure that the sample is providing an unbiased survey of the vast range of cometary grain types, it is imperative that the CSSR mission return a much larger sample than was obtained by Stardust.

In considering how much material should be returned by the CSSR mission, the SDT attempted to balance technical feasibility and the needs of the scientific community, including long-term archiving of the sample. To permit useful, repeatable analyses of rare but critical organic materials, such as amino acids, we estimate that a sample volume of at least 500 cc is sufficient. Of course, there is some arbitrariness in that specific value, but the SDT concludes that returning a 500-cc sample is technically feasible and satisfies the scientific objectives of the CSSR mission. A volume, rather than a mass, requirement is used because determining the density of the sample is problematic and verification that the proper amount of sample is captured is probably easier with a volume requirement.

The data from a large sample, collected from a well-characterized site on the nucleus, would be much easier to interpret than the Stardust data. The increased sample volume and the "gentle" collection technique employed should ensure that the CSSR sample is far more representative of the bulk nucleus than can be claimed for the dust grains collected by Stardust. The CSSR sample data would also contain more rare grain types, which would inform us about the full variety of early solar system processes and environments. A large sample might include pebble-sized materials and coarser-grained crystals. Such samples would present a greater opportunity to locate samples suitable for age dating and other isotopic work impossible for micrometer-sized samples. The Wild 2 samples analyzed so far appear to contain a low concentration of preserved presolar grains. A larger sample from the nucleus would be expected to yield a far greater abundance of these critical materials as well.

Wild 2 samples are now known to contain a significant amount of both labile and refractory organic materials, although the majority of the labile materials must have been destroyed during sample collection. The wide range of molecular structure evident in the C- and N- X-ray Absorption Near Edge Structure (XANES) spectra of the relatively small set of comet 81P/Wild 2 particles analyzed to date is intriguing. Whereas evidence of some connection between some of the comet particles and primitive chondritic organic matter exists, many of the particles exhibit chemical structure completely foreign to that of primitive chondritic insoluble organic matter (IOM) [Cody et al. 2007]. This high degree of variation in functional group distribution is also reflected in a enormous scatter in these particles' elemental chemistry, i.e., N/C and O/C [Sandford et al., 2006]. Thus, despite this destructive collection process, organic species not previously observed in extraterrestrial materials have been observed among the best preserved Wild 2 grains [Cody, 2007], a result that hints at the far deeper record of early solar system organic chemistry that would be revealed by a carefully maintained, larger sample from a comet nucleus.

To maintain the mineralogical integrity of amorphous or anhydrous inorganic phases and critical organic compounds, the samples must be protected from inadvertent reactions with liquid water. If water ices were to be collected, and this ice were to melt in the presence of amorphous or anhydrous crystalline cometary materials, the resulting aqueous alteration would fundamentally alter the anhydrous phases (including many organics), probably making the original mineralogy of the comet nucleus irretrievable. For example, fine-grained glasses and ferromagnesian silicates would be quickly converted into phyllosilicates and oxides. Metals and sulfides would likewise be completely converted into new phases. Labile organic species would also be processed, destroying their unique record of the evolution of organics in early solar system. Thus, the sample must be maintained in a completely dry state during the entire mission, including SRC atmospheric entry, recovery, and curation. Only this precaution will ensure that the sample will not suffer chemical reaction after sampling.

One way to accomplish this requirement would be to vent the collected sample to space during the cruise phase, essentially freeze-drying it. But it would be better if the sample could be returned in the frozen state, retaining at least its water ice component. Based on literature surveys and consultations with colleagues, the SDT finds that maintaining the sample at ≤263 K (i.e., ≤ −10°C) should prevent aqueous alteration and might possibly retain some of the water ice in the sample. A possible strategy that both mitigates the risk of aqueous alteration and improves the possibility of retaining ice in the sample is to have at least two sample compartments, both maintained at ≤263 K but venting one to space and keeping the other one sealed. In addition, the incorporation of carefully selected witness samples in the sample return chambers would permit one to recognize any unforeseen mineralogic changes that might have occurred in the collected comet sample during the spacecraft cruise and Earth return phases.

Adopting a low-temperature sample return constraint places stricter requirements on the spacecraft design, operation, recovery operation, curation, handling, and analysis. However, the potentially large scientific benefits provided by returning a cold sample may outweigh the challenges. For this reason, we recommend that the returned sample volume can be reduced to ≥250 cc in exchange for maintaining the sample at cryogenic temperatures (e.g., ≤150 K, so that a solid ice sample is depleted to depth of less than a millimeter over the entire mission).

If the strategy of allowing the sample to vent to space is adopted, an additional requirement is that the sample must be protected against pyrolysis. That is, the sample temperature cannot be allowed to rise so high that labile organics are lost. This is a somewhat ill-defined concept, and the SDT recommends that the sample never be allowed to warm above 30°C (300 K) at any time

after the sample has been collected from the comet because that limit should permit the retention of most organic species that are stable under standard laboratory conditions.

2.8.2 Determine the geomorphological context of the sampled region

Understanding the geomorphological context of the sampled region is critical to the success of the CSSR mission. Was the sample retrieved from an active or inactive region on the nucleus? Where was the sample located relative to various land forms on the surface? What variations in solar illumination did the sample experience as the nucleus rotated? How did the sampled region compare (e.g., in shape, surface texture, color, albedo, etc.) to the rest of the surface of the nucleus? It will be difficult to determine the applicability of the sample analysis results to comets in general until these questions are answered.

The Giotto images of the nucleus of comet 1P/Halley near closest approach provided a spatial resolution that varied between 50 m and 110 m over the nucleus. The highest resolution images revealed an irregular surface with valleys, hills, and circular features that had some similarities with impact craters [Reinhard 1986]. However, the resolution was insufficient for determining details of the structures or their origins, and much of the surface was only observed at kilometer-scale resolution [Keller et al. 1986].

Observations of the nucleus of comet 19P/Borrelly by the Deep Space 1 (DS-1) camera revealed a nucleus with a complex surface morphology: the surface was variegated and rough with pits, bumps, and ridges on a 200 m scale, and there were significant albedo variations. At the closest approach distance of 2171 km, the highest resolution achieved was ~50 m/pixel. There was no clear evidence for impact craters down to a resolution of 200 m, but rounded depressions were seen [Soderblom et al. 2002]. There was possible evidence of smooth plateaus, which might be similar to the smooth regions seen on 9P/Tempel 1 with Deep Impact (DI), but the resolution differences between DS1 and DI make direct comparison difficult.

Prior to returning comet and interplanetary dust samples to Earth, the Stardust spacecraft flew past the nucleus of comet 81P/Wild 2, with its navigation camera achieving a highest resolution at closest approach of 14 m/pixel. The surface of the comet was covered with rounded depressions, some bounded by steep cliffs.

The cameras on the Deep Impact spacecraft produced images with resolutions approaching ~3 m over small portions of the surface and ~10 m over larger regions, and all the images show intriguing patterns (e.g., evidence for layering) and interesting land forms.

Many of the features seen in the four nucleus encounters may be similar in morphology, but, it is very difficult to make comparisons owing to the large differences in resolution among the different missions. One thing is certain: as the spatial resolution has improved, more intricate details of the surface are revealed, indicating that there is still much to be gained by pushing the resolution further.

For the CSSR mission, global images of the nucleus should be obtained with a resolution somewhat higher than that of previous missions in order to define the context of the sampled region relative to those other missions. The sampled site itself should be imaged at a spatial resolution comparable to the physical size of the sampling device.

The SDT considers the following to be one possible way of meeting the context requirement: image the entire sunlit nucleus at a resolution better than 1 m and perform visible characterization of the sampled region with a spatial resolution better than 1 cm. A resolution of 1 m should be sufficient to establish the global context of the sampled region and is probably good enough to

determine whether the various features on the surface are the result of outgassing vents or impact craters. Taking visible images of the sampled region to a resolution of 1 cm should provide information on the texture of that part of the nucleus (i.e., fine- vs. coarse-grained, whether or not pebbles or rocks are nearby, etc.). However, the SDT recognizes that other approaches could also be used to establish the context of the sampled region, and proposers should be given the flexibility to apply different techniques.

2.8.3 Maintain samples in a curation facility without degradation for ≥2 years

A sample of comet nucleus on Earth will be largely uninformative unless it can be safely and reliably maintained and handled for many years in a non-reactive, contamination-free environment. NASA's existing Curation Facility, at the Johnson Space Center (JSC), has 40 years of experience in the careful maintenance, sampling, and allocation of astromaterials. In line with recent experience with the Stardust and Genesis sample return missions, we recommend that the CSSR mission fully fund the field recovery of the sample by JSC personnel, and the curation of the sample at the JSC facility for 2 years following Earth return. The latter would include the acquisition of new equipment and skills necessary for the curation and handling of the samples. We also recommend that NASA assume the burden of funding the curation and distribution of samples after the 2-year period, for as long as NASA determines there is still value in maintaining the samples (e.g., in anticipation of improved laboratory analysis capabilities).

For a dry returned sample, the techniques for sample handling are fairly well established and understood. However, if the CSSR mission returns a cold or cryogenic sample, curation will be considerably more challenging. The only experience with a frozen sample has been the Tagish Lake meteorite [Brown et al. 2000], which was curated in a frozen state successfully for 6 years, and subsampled only a few times under very limited circumstances. It is clear that the particular needs of a frozen comet nucleus sample will necessitate the acquisition of new skills and facilities for NASA. Curation of frozen samples is a well understood process at several existing ice core laboratories in the United States and abroad, and JSC has already begun to explore what such a facility would entail. The greatest challenges will arise from the extreme requirements for sample contamination control, well above what is routinely practiced at ice core laboratories. These requirements will be significantly more severe for a true cryogenic sample, which we are encouraging, though not making part of the baseline mission. It may also be necessary to handle and allocate volatiles derived from the captured samples.

In addition, it would be advantageous for NASA to provide the opportunity of new funding to astromaterials analytical laboratories to support upgrading their facilities to handle frozen samples, where necessary. The vast majority of planetary science analysts are unfamiliar with the special requirements presented by frozen samples. While not all techniques will require that samples remain in a frozen state, many techniques will require this precaution.

2.9 Group 2 Objectives: Science Baseline (Highly Desirable)

Of the many possible additional goals for a CSSR mission, the following group 2 objectives are the most important scientifically. All of them should be part of the *baseline* for any proposed CSSR mission.

2.9.1 Capture gases evolved from the sample, maintaining their elemental and molecular integrity

Comets are approximately half ice by mass. The majority of the C, N, and O atoms (most abundant after H and He) derived from the protosolar nebula and stored in comets reside in volatile species (e.g., H_2O, CO, CO_2, CH_4, C_2H_6, CH_3OH, NH_3, etc.) whose relative abundances and isotopic concentrations are key to understanding the role of comets in transporting water and organics in the early solar system. Returning a sample of the volatile fraction of the surface sample is thus a highly desirable goal of the CSSR mission.

It will, however, not be possible to return the volatile fractions in their original frozen state given the technical and budget constraints of a CSSR mission. The plan, therefore, would be to collect the gases in a separate chamber (e.g., flask) as they sublimate from the original sample, using a technique that preserves the elemental and molecular integrity of the evolved gases. Approximately 500 cc of gas storage volume is possible using the baseline CSSR engineering design described below. Fractionation effects may cause the relative abundances of gases evolved from the sample to be very different from the abundances in the condensed phase in the nucleus, which will limit the interpretation of the results. The elemental abundances may be similarly fractionated. However, the isotopic abundances should be essentially unaltered, and those results alone could have important cosmogonic implications (e.g., the relative isotopic abundances bear on the issue of whether cometary impacts contributed significantly to the volatile inventory of the Earth and the other terrestrial planets). It is particularly important scientifically to return a sample containing H_2O, either in the condensed or gaseous phase, so that the D/H ratio in cometary water from the targeted comet can be compared to the value in standard mean ocean water (SMOW) on the Earth.

2.9.2 Return material from a depth of at least 10 cm (≥ 3 diurnal thermal skin depths) if the sampled region has a shear strength no greater than 50 kPa

The primary goal of the CSSR mission is to return a bulk sample that is representative of the non-icy composition of the nucleus. A key aspect of that goal is to acquire an unaltered sample of the organic components of the nucleus. The organic material is expected to be complex, with a broad range of substances of different thermal stability. Perhaps the best way to ensure collection of a cometary sample whose organic composition has not been appreciably altered by repeated passages of the comet through the inner solar system is to acquire at least part of the sample from well below the surface of the nucleus.

Observations of cometary nuclei from Earth and from space probes tell us two important facts. First, the temperature of the nucleus surface is hot; the subsolar temperature measured by Deep Impact for P/Tempel 1 was 326 K at 1.5 AU from the Sun, and a comet near 1 AU could have a subsolar temperature close to 400 K. Second, cometary activity seems to be concentrated in limited active areas. Thus, much of the comet surface is not necessarily being eroded in the current epoch and may have been exposed at the surface for a geologically long time.

Thus, even the relatively involatile organic material in the outermost surface layer may have been altered by the elevated temperature and by an unknown, but possibly long, exposure to the space environment. The physical structure of this devolatized surface may also be altered (e.g., sintering, erosion, micrometeorite bombardment, etc.). Comparing a sample from ~10 cm depth with a sample from the outermost surface will help us to understand how the surface has been

modified and serve as a constraint on interpretations based solely on the outermost surface material.

Two results from the Deep Impact experiment make this scientific objective feasible. First, thermal inertia measurements imply that the diurnal thermal skin depth is probably only a few centimeters. Thus, a depth of 10 cm will be insulated from the high subsolar temperature of the surface. Second, the development of the post-impact ejecta implied that the strength of the outer layers of the nucleus is quite low, probably ≤50 kPa, and is consistent also with a low bulk density of the material. Hence, the mechanical process of drilling or coring to a depth of ~10 cm should be straightforward.

The CSSR study team considers acquisition of a subsurface sample to be an important science goal. However, the technical difficulty of guaranteeing that the depth requirement could be met on a surface of unknown strength led the SDT to place it as a Group 2 science objective, not a Group 1 objective. The SDT considers this to be a realistic Group 2 objective if the strength of the material is similar to that inferred for 9P/Tempel 1, i.e., the tensile strength is ≤50 kPa.

2.9.3 Determine whether the sample is from an active region of the nucleus

Understanding the activity context of the sampled region is important. Our current picture of the thermal and erosional behavior of a nucleus suggests that an area with significant subliming gas (an "active" area) will be thermally and structurally different from an area with relatively little or no subliming gas (an "inactive" area). The detailed thermophysical distinctions between active and inactive areas have not yet been measured, which is why this objective is part of Group 2, not Group 1. An actively sublimating region may shed material so rapidly that its surface material has only recently been exposed to the space environment and may thus be relatively less modified from its primordial state by evolutionary processes. While unlikely to be absolutely pristine, the surface of an active region will likely have suffered less from the effects of cosmic rays, solar wind particles, UV photons, and heating.

Since active areas turn on and off diurnally and seasonally and are influenced by insolation, monitoring the nucleus for sufficient time to determine the rotational, seasonal, and heliocentric contexts of the sampled region should be important for discovering whether a sampled region could be an active area. The rotational context would involve knowing if and how the nucleus is in non-principal axis (NPA) rotation and could be determined in approximately 20 rotation periods (although this would depend on the details of the rotation and might require perhaps more time). Once the direction of the angular momentum is established, the seasons on the nucleus can be predicted and a judgment can be made as to how much of the seasonal variation needs to be observed. For example, a nucleus in simple rotation with the axis perpendicular to the orbit plane might need less monitoring than a nucleus in an energetic NPA rotation with the angular momentum vector parallel to the orbit plane. Depending on the circumstances of the sampling, the variation of activity with heliocentric distance may also need to be monitored since ostensibly inactive areas could become active areas simply due to increased insolation.

Diverse methods could be used to potentially identify and map active areas, but they all depend on assumptions about characteristics of active areas, which are largely unknown. At least three relatively simple observational techniques are available for identifying active regions. First, optical imaging of the surface at ~1 m resolution might be capable of detecting small, icy regions on the nucleus simply by virtue of albedo differences; fresh ice or snow would be brighter than the dark ("dirty") mantle covering most of the nucleus. Second, if dust jets are detected, they

could be observed as the nucleus rotates and the appearance and disappearance of these jets over the limb could be used to determine the source of the jets at the surface. Finally, a relatively simple infrared imaging bolometer could be used to distinguish hot (~300 K) mantled regions from cold (~180 K) icy spots on the nucleus, if sufficient spatial resolution is available. A reasonable trade-off between instrument complexity and sensitivity to icy regions suggests that an imaging bolometer having a spatial resolution of ~10 m at the surface might allow icy regions to be detected.

2.10 Group 3 Objectives: Other Meritorious Goals

There are many other meritorious scientific objectives that could be added to a CSSR mission, but those are clearly a lower priority than the Group 1 and Group 2 objectives. The Group 3 objectives should not be required of the baseline mission, and the descope plan that will be required for any CSSR mission should reflect the lower priority of the Group 3 objectives. Nevertheless, proposers should be encouraged to consider innovative ways to squeeze more science out of the mission.

In general, Group 3 objectives might include any in situ measurements that characterize the physical and chemical nature of the nucleus. There is, however, one particular objective that the SDT wishes to highlight as the highest priority within Group 3:

2.10.1 Sample Multiple Locations

To distinguish the potentially very different effects of recent radiolysis, photolysis, and thermal mobilization from more scientifically interesting influences of the protoplanetary nebular environment, it would be advantageous to collect and return samples from multiple sites on the nucleus, ranging from freshly exposed to more highly evolved material. Determining which sites on the nucleus are "active" versus "evolved" may be problematic (see previous discussion), although the long rendezvous times for a CSSR mission should make the identification of active regions much easier than it was for previous flyby missions. In any case, comparing results for samples that are returned from different sites, all of which are well characterized optically, will clearly provide valuable information on compositional variability across the surface of a nucleus.

2.10.2 Other Objectives

Some other potential Group 3 objectives that would yield significant advances in cometary science include (arranged roughly from highest to lowest priority, although the SDT as a group did not express strong preferences):

- Sample to a depth ≥50 cm
- Preserve stratigraphy of the sampled region (even gross [~3 cm scale] resolution is valuable)
- Perform thermal mapping of the entire nucleus (which should aid in identification of icy terrain)
- Perform remote compositional observations of the surface of the nucleus, including the sampled area
- Perform remote compositional observations of the coma, including near the sampled area

- Perform dust measurements using a nephelometer (note that the methods used to measure dust fluxes during previous spacecraft flybys of comets will not generally be applicable to a CSSR mission)
- Investigate potential flyby opportunities of other comets (especially) and asteroids, which might provide substantial scientific return with little or no risk to the primary mission.

2.11 Traceability between Science Objectives and Required Measurements

In this section, we discuss the measurements that must be made to achieve the scientific objectives of the CSSR mission. We describe both the techniques and the instruments that could be used for making the required measurements.

2.11.1 Traceability Matrix

A "traceability matrix" provides a concise way of illustrating the path between the science objectives of the mission and the measurements that provide the data needed to accomplish those objectives. The table below is the traceability matrix for the CSSR mission considered here. The following subsections provide further discussion of the various measurements that will be made to accomplish the scientific objectives of the mission in time-ordered sequence starting with the initial reconnaissance of the nucleus and ending with the storage of the sample in the curation facility.

2.11.2 Characterization of the nucleus

Intensive monitoring of the nucleus is required to create a detailed shape model, determine its rotational properties, map surface features, measure albedo variations, create a thermal map, and search for sources of activity. All of these tasks can be accomplished with only three instruments: a narrow field of view visible light camera (NFV), a wide field of view visible light camera (WFV), and a thermal infrared camera (IRC). The performance requirements of these instruments are presented in section 4.2.

Science Objective	Measurement Objective	Measurement Technique
1.1 Return a macroscopic (≥ 500 cc) sample from the surface of comet to Earth with no aqueous alteration; sample volume can be reduced to ≥ 250 cc if cold sample (preserving water ice) is returned	• Collect at least 500 cc from the surface of the nucleus, maintaining T ≤ 263 K throughout the mission to prevent aqueous alteration • Prevent pressure rise above sample that could cause aqueous alteration	• A sample acquisition system (SAS) employing slow-turning drills within cylindrical containers collect ≥ 500 cc of nucleus surface material without appreciably heating the material or altering the mineralogical or chemical content • Drills have capability to collect material having a wide range in porosity (0-90%) and tensile strength (10 Pa – 10^7 Pa) • Use of two dual-pair drill systems provides redundancy and capability to sample to different depths • Sample is stored in a sample return vehicle (SRV) where the temperature is maintained at or below 263 K throughout the mission using primarily radiative cooling during the cruise phase and phase change coolant material during the Earth landing phase • Pressure monitoring and pressure relief valves allow evolved gases to be vented to space before aqueous alteration can occur; vent to space if P ≥ 1 mbar
1.2 Determine the geomorphological context of the sampled region	• Map entire sunlit side of nucleus with spatial resolution ≤ 1 m, S/N ≥ 25 for geometric albedo ≥ 0.01, and no saturation for albedo ≤ 1 • Observe sampled region before and after sample acquisition with a resolution ≤ 1 cm	• Narrow field visible (NFV) imaging system with FOV = 20 mrad, IFOV = 20 µrad is used to determine shape model of nucleus from standoff distance of 50 km • Wide field visible (WFV) imaging system with FOV = 350 mrad and IFOV = 350 µrad is used to support proximity ops during descent to nucleus; also serves as backup to NFV for producing shape model • Sample microcams (SMCs) are used to observe the sampled region and verify sample collection success
1.3 Maintain samples in a curation facility without degradation for ≥ 2 years	• Store samples in a clean (class 100, or better) curation facility, always maintaining T ≤ 263 K	• Upgrade current Curation Facility at NASA JSC to create cold cleanroom (T ≤ 263 K) where samples can be stored for 5 years or longer
2.1 Capture gases evolved from the sample, maintaining their elemental and molecular integrity	• During the cruise phase, collect any gases evolved from the sample and maintain them in their original molecular form	• Use metal flasks (to prevent photon and particle irradiation) with clear paths to the samples to collect any sublimating gases • Flasks are connected to valve system that allows isolation from sample, if desired, and venting to space, if desired
2.2 Return material from a depth of at least 10 cm (≥ 3 diurnal thermal skin depths) if the sampled region has a shear strength no greater than 50 kPa	• Sample nucleus material at depths ≥ 10 cm	• Use of short (10 cm) and long (15 cm) drills allows penetration below the surface if tensile strength is ≤ 50 kPa
2.3 Determine whether the sample is from an active region of the nucleus	• Determine whether the sample site is the source of dust jets, which are presumably active regions • Determine whether there is exposed ice at the sample site that could produce gas and dust activity • Produce thermal map of the nucleus with spatial resolution of ≤ 50 m, temperature resolution of ± 3 K at 170 K, and a single observation dynamic range covering 150 K to 400 K with S/N ≥ 5	• Use NFV images to map jets back to their source regions on the nucleus, which are presumably active • Use NFV to search for bright albedo regions that could be associated with ice, hence activity • Use a microbolometer-based infrared camera (IRC) with FOV = 520 mrad and IFOV = 4 mrad to produce thermal maps of the nucleus with a spatial resolution of ≤ 50 m at a standoff distance of 10 km • Use the IRC to search for cold regions (~170 K) on the nucleus that might be icy, hence active • Use IRC to map hottest regions on the nucleus that might be devoid of volatiles, hence inactive

Figure 2.11.1-1. Traceability for Science Objectives.

The NFV has a resolution of 1m/pixel at a distance of 50 km and is expected to be the workhorse for the characterization of the nucleus. The nucleus of 67P/CG is an ellipsoid with an effective diameter of 3.44 km (i.e., the diameter of a sphere with the same volume), principal axes having dimensions of 4.6 × 3.7 × 2.9 km, and a rotational period of 12.6 hr [Lamy et al. 2007]. During the rendezvous phase of the mission, when the spacecraft is standing off the nucleus by ~50 km for an extended period of time, the NFV could take a mosaic of the nucleus approximately every half hour, which corresponds to a rotation by ~15 deg in cometocentric longitude. Each mosaic, which would be comprised of 25 separate images obtained in a 5×5 spatial pattern, would result in a data volume of ~160 Mb, assuming a lossless onboard compression ratio of ~2. A full map including all longitudes could be acquired by taking 24 such mosaics in a single 12 hr period for a total data volume of 3.84 Gb. Managing the storage and downlinking of these data volumes should be relatively straightforward, as the baseline design employs dual 16 Gb solid state recorders (SSRs) and a data downlink rate ranging from 2.5 Mbps (earlier) to 0.5 Mbps (later) during the first 50 days of the reconnaissance phase.

The mosaic imaging sequence could be repeated as many times as necessary until confidence is gained in the fidelity of the surface map produced by combining all the imaging data. Perhaps a suitable shape model could be obtained in only a day or two for observations of 67P/CG, which will have already been extremely well characterized by the Rosetta mission. In that case, the NFV would be used to verify that the shape model, rotational properties, geomorphology, etc. derived from the Rosetta data were still valid. For the more general case of a nucleus that has not been so well characterized previously, the nucleus would be imaged for at least 20 rotational periods spanning the better part of a month.

The intense monitoring phase would begin shortly after perihelion, when the comet was still moderately active, typically when the comet is within ~2.5 AU of the sun. The same NFV images used to create the shape model would also be used to search for active regions on the nucleus using two techniques: (1) icy patches on the nucleus might reveal themselves by having a much higher reflectivity than surrounding regions, and (2) the positions of dust jets could be mapped back to their origin on the surface by monitoring their appearance and disappearance over the limb of the nucleus.

The IRC would be used to map the temperature over the visible nucleus at a resolution of ~170 m at a standoff distance of 50 km from the nucleus. However, it should be possible to move in to a distance of ~10 km from the nucleus for at least one complete rotational period of the comet, at which time the nucleus will slightly underfill the IRC FOV and a thermal map can be obtained at ~35 m/pixel. If there are regions on the nucleus where patches of ice are ~30-40 m in extent, they should be easily detectable as low intensity spots in the IRC images. Even if ice is not detected, the IRC should provide extremely valuable data on the thermal properties of the nucleus.

During the reconnaissance phase, the WFV serves mainly as a backup for the NFV. If the NFV should fail, the standoff distance could be lowered to ~10 km and maps could be obtained at a slightly degraded resolution of 3.4 m by the WFC. At a standoff distance of 10 km, the nucleus of WFV almost exactly fills the FOV, so the number of mosaic points could be significantly reduced (e.g., 2×2 at most).

2.11.3 Sample Site Selection

After the final nucleus shape model is produced and the activity across the surface is mapped, it is time to select a sample site. Both scientific and technical issues must be addressed when selecting a suitable sample site. Clearly the topography of the sampled area must be conducive to proximity operations and touch-and-go operations. That is, the spacecraft health and safety must be ensured at all times during the sample collection process. Thus, a sample site must be selected from regions on the nucleus that are essentially flat over spatial scales of at least 50 m, which is the accuracy to which the spacecraft can be commanded during the descent to the nucleus and is roughly 20 times the spatial extent of the spacecraft after the solar arrays are folded up.

Once this engineering requirement is satisfied, other criteria for sample site selection can also be considered. Some scientific criteria for selecting sample sites include whether the region shows activity or evidence of ice (i.e., perhaps those areas are more "pristine" than others), or whether the region is near an "interesting" geological structure. But one might also decide that acquiring a sample containing ice is too risky owing to potential aqueous alternation during the return to Earth, in which case the sample might be selected from the hottest and/or least active region on the surface.

The SDT recommends that proposers be given flexibility in determining their sample selection sites. Proposers should discuss their rationale for site selection, and the adopted strategy can be judged during the proposal review process.

Once the sample sites are selected, at least two practice runs are planned to ensure that the selection site is suitable. During these rehearsals, the WFV and onboard lidars and Doppler radar systems will be used to monitor and guide the spacecraft during proximity operations around the nucleus, as described in detail in Section 4.4.9.

2.11.4 Sample Acquisition

The specification of a robust sample acquisition process that preserves the elemental, chemical, and mineralogical integrity of the sample is critical to the success of the mission. The huge advantage that a CSSR mission has relative to a Stardust-like mission is the opportunity to perform a "gentle" acquisition of the sample. The strategy adopted in this study is to collect samples using drills encased within cylindrical containers during a "touch-and-go" operation, as described in section 4.2.2. The CSSR sample acquisition system (SAS) is comprised of two pairs of drills, each pair containing one short and one long drill. During an acquisition sequence, both the short and long drills within a single pair turn slowly, moving material up the shaft while they penetrate the surface to a depth of 100 mm and 150 mm, respectively. Assuming each drill is filled to capacity, the sampling would yield 250 cc and 380 cc, respectively, of comet surface material and would provide the potential for measuring differences between the samples collected from the two depths. The second pair of drills provides redundancy in case the first pair fails, as well as an opportunity for collecting more samples if the original pair succeeds. A pair of sample microcams (SC1 and SC2, see section 4.21) will be used for optical verification that the drilling operation collected the required volume of sample material.

After sample collection, the drill head retreats, rotates 180°, and is placed, along with the samples, in the sample return vehicle (SRV). After releasing the drills, the drill head moves away from the SRV, rotates back 180°, and then seals each drill/sample with a hermetically sealed cap. The SAS is then ready to be jettisoned or to attempt a second sampling using the second drill pair.

2.11.5 Sample Maintenance during the Cruise to Earth and Possible Comet Monitoring

The fundamental objectives of the CSSR mission are jeopardized if the sample is not stored carefully. In particular, aqueous alternation must be avoided at all cost, as discussed in previous sections. The SRV used for this CSSR study is based on a design being developed for sample return from Mars, as described in detail in Section 4.2.3.

The SRV is instrumented to monitor the pressure and temperature near the sample throughout the entire cruise and until the sample is returned to Earth. The temperature of the sample will not be allowed to rise above 263 K (-10 C) at any time during the mission to ensure that labile organics are preserved. During the cruise phase, radiative cooling will be used to keep the temperature at ~135 K, which should be cold enough to maintain water ice in the sample for the ~12 year cruise. During atmospheric entry and return to Earth, a phase change material in thermal contact with the sample will be used to maintain the sample at or below the 263 K requirement.

Within the SRV, a flask system with valves, as described further in Section 4.2.3, either captures gases evolving from the sample or vents them to space. In either case, the system is designed to ensure that the evolved gases from the sample cannot reach a high enough pressure to cause aqueous alteration of the sample. Each sample container can be separately controlled, and the strategy adopted here is to seal one of the samples in a pair (i.e., either the "short" or "long" sample) and to vent the other one to space. A similar strategy would be adopted for the second pair of samples, assuming those were collected, except reversing the sealed versus unsealed relative to that used in the primary sample containers. This strategy should increase the probability that at least one sample is returned without any aqueous alteration and at least some remnant of the icy component of the sampled region is captured for analysis on the Earth.

The flasks are designed to maintain the compositional integrity (i.e., molecular composition) of the evolved gases. While the relative abundances of any gases in the flask may be quite different from abundances in the original frozen sample owing to fractionation effects during sublimation, the isotopic composition of the gases, which can be measured to unprecedented sensitivity by laboratory analysis, should provide extremely valuable information on the geochronology of the sampled material and on the role of comets in providing volatiles to the Earth.

During the cruise back to Earth, infrequent, but regular, monitoring of the comet using the NFV should be attempted to provide a more complete record of the comet's behavior. For example, changes in activity, especially those associated with the sampled region, could be documented over a large portion of the comet's orbit, and this would be valuable for establishing the context of the sample.

2.11.6 Sample Return to Earth

As already mentioned above, the samples must always be maintained at a temperature at or below 263 K, even during atmospheric entry and while the SRV is sitting on the ground. In addition, this temperature must be maintained during the recovery of the sample from the SRV (estimated to take up to 1 day from the landing to recovery of the SRV by ground personnel), during the transfer of the samples to the curation facility (which should be completed within 1 day), and during the storage of the samples at the curation facility for at least 5 years (only the first two years of costs should be borne by the CSSR proposal team; NASA should cover the costs for the longer term storage of the samples).

Throughout the recovery process, great care must be exercised to prevent contamination of the sample. The SRV is hermetically sealed and provides protection for the sample, and one possible strategy would be to transport the entire SRV in a refrigerated truck to the curation facility where the disassembly of the SRV and extraction of the sample could be performed in a clean-room facility (class 100 or better) maintained at a temperature at, or below, 263 K. However, maintaining cold temperatures within the SRV for a day or more may not be feasible, and an alternative strategy would be to set up a field laboratory at the landing site where the sample extraction from the SRV could be performed and the sample placed temporarily in a small, clean (class 100 or better), cooled ($\leq$ 263K) container for transport to the curation facility.

The NASA team at the Johnson Space Center (JSC) led the collection of the samples returned from the Stardust and Genesis missions, and the current study assumes that a similar JSC team will lead the recovery and storage of the CSSR samples. The JSC team will be assisted by the NASA Langley Research Center (LRC) team that designed and built the SRC and by support personnel at the Utah Test and Training Range (UTTR), where this study assumes the SRV will land on Earth.

2.11.7 Laboratory Analysis of Samples

The laboratory analysis of the returned sample is the most important scientific objective of the CSSR mission, and the necessary resources must be allocated to ensure that the bulk of the sampled material is thoroughly analyzed with state-of-the-art laboratory equipment within 2 years of the return to Earth. The members of the CSSR science team who are expert at sample analysis should manage and lead the initial laboratory analysis program.

This study assumes that the current NASA JSC curation facility will be upgraded to accommodate the requirements for storing and handling the CSSR samples. In addition, the JSC curation facility must establish policies and procedures for distributing samples to other laboratories for analysis without altering the samples. Funding to accomplish these objectives should be provided by the CSSR project for a period of 2 years. The SDT recommends that NASA assume the cost for maintaining and distributing the samples for at least another 3 years to enable analysis by even more capable laboratory equipment that is developed during that time.

Finally, in addition to funding members of the CSSR science team to analyze the samples within the first two years after the return of the sample to Earth, the SDT also recommends that NASA establish a separate CSSR Data Analysis Program, funded at ~$2M/year, to enable research and analysis on the samples for at least 5 years following the return of the sample to Earth.

3. MISSION ARCHITECTURE ASSESSMENT

Sample return from a Jupiter Family Comet is technically demanding, requiring a highly capable launch vehicle, large onboard ΔV capability, and multiple mechanisms for sample acquisition and handling.

- The CSSR architecture is selected based on the science objectives, technical feasibility, risk, and cost.
- Architecture maximizes flexibility while staying within the specified cost cap.
- Key mission architecture trades reflect the technical risk areas for the mission: target selection, propulsion technology, proximity operations strategy, and sample acquisition and handling.

The Comet Surface Sample Return (CSSR) Mission Study consisted of two phases, as shown in Fig. 3-1. During Phase I, discussed here, major trades affecting mission architectures were identified, evaluated, and narrowed down to focus the detailed design in Phase II, as described in Sections 4 and 5.

Architectural Identification and Evaluation Process. The CSSR Science Definition Team (SDT) defined clear, simple science objectives surrounding acquisition and return to Earth of a macroscopic sample from a well-characterized region on the surface of a comet nucleus. However, this simple science objective requires a technically challenging mission. Rendezvousing with a comet and returning a sample to Earth requires a large launch vehicle for high C_3 values and a spacecraft with extensive ΔV capabilities. Mission designs require operations at large heliocentric and geocentric distances. Proximity operations around a small body in a poorly understood environment present further challenges that are unique for each comet. Investigations during the past decade strongly suggest that the surfaces of comets are porous with negligible

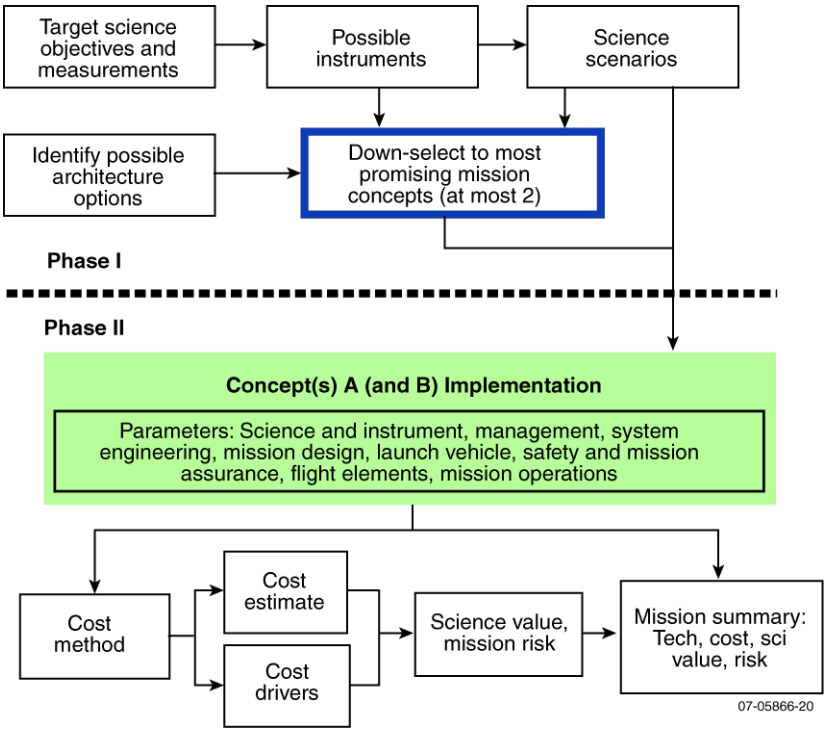

Figure 3-1. The structured approach used in Phase I for architecture definition resulted in a robust mission set for detailed analysis in Phase II.

strength, which should facilitate sample acquisition, but there is no guarantee this is true for every location on every cometary nucleus, and the sampling mechanism must be designed for worst-case scenarios. Despite these challenges, all the risks are manageable. Risk tolerance defined the trade decisions outlined in Figure 3-2 and discussed in the following sections.

Trade	Decision	Benefits
Target Selection	C-G[a] selected as prime with Wirtanen backup	Rosetta should provide details that lower mission risk (e.g., shape model, environments, surface properties)
Propulsion Technology	Carry both chemical and electrical propulsion systems forward through costing	Demanding mission provides unique case where there is no clear cost/risk minimum
Sample Acquisition	Redundant pairs of drills (10 cm and 15 cm in length)	Active drills are single design that facilitates sampling a wide range of surface properties; two depths provide stratigraphic information
Sample Handling	Temperature maintained ≤–10ºC; volatiles captured	Temperature ≤–10ºC minimizes aqueous chemistry and volatile capture flasks mitigate loss of cryogenic storage; highest temperature allowable to meet science requirements (and therefore lowest cost)
Sample Return Vehicle Design	Mars Sample Return (MSR)-type design	Ballistic return eliminates spin table and parachutes; feeds forward into MSR mission; thermal requirements easier to meet than with Stardust heritage design
Multiple vs. Single Spacecraft	Single spacecraft used for all operations	Single spacecraft solution is lower cost
Proximity Operations Strategy	Incorporate NEAR and Hyabusa lessons learned; add lidar and Doppler radar triads; add terrain-relative optical navigation	Ensures velocities are nulled and optical navigation system provides robust backup

[a]Churyumov-Gerasimenko.

07-05866P-38

Figure 3-2. The CSSR mission trades provide the lowest cost and lowest risk technical solution.

3.1 Target Selection

By selecting a well-characterized target (e.g., 67P/Churyumov-Gerasimenko [C-G]), the overall mission risk is reduced. For example, many recent missions have provided valuable information about cometary properties and environment. Deep Impact, Stardust, etc., have all resulted in major increases in the understanding of what can be expected for the CSSR mission, lowering the overall mission risk. Specific to this study, the Rosetta mission is expected to develop very detailed models of the cometary environment and surface properties, which will help in mission planning. The selection of C-G as the prime target also facilitates an interesting technical trade to directly compare a ballistic trajectory using chemical propulsion and a low-thrust trajectory using electric propulsion. However, the mission risk incorporated in this study assumes no prior knowledge of the target body, thus resulting in a conservative risk posture that should be lowered by a mission including knowledge gained from a previous comet encounter.

All Jupiter Family Comets (JFCs) were considered in order to gain an understanding of the range of possible options for the lowest cost mission. Most comets were rejected immediately owing to unfavorable perihelion distances <0.7 AU or >1.6 AU, aphelion distance >5.9 AU, or inclinations >15°. Figure 3-3 shows the key orbital characteristics and constraints when consider-

ing the targets for the nine targets ranked most favorable by the SDT and ten other targets considered most likely to be accessible.

For the ballistic mission launching between 2014 and 2017, the analysis found only three targets with reasonable launch energy (C_3), post-launch delta-V requirements, and mission durations (C-G, Wirtanen, and 2004 R1 McNaught) providing two backup launch opportunities but confirming the limited choices available for targets. Another driver was the requirement that the 6 months of comet operations be performed within a heliocentric distance of 3.0 AU to minimize the mission risk. The low-thrust mission is much more forgiving and provides access to many more targets and regular (usually yearly) launch opportunities.

Comet	Apparitions	Perihel., AU	Aphel., AU	Incl., deg.
9P/Tempel 1 [1]	2016 Aug. 2, 2022 Mar. 4	**1.54**	4.75	10.5
19P/Borrelly [2]	2015 May 29, 2022 Feb. 2	**1.31**	**5.90**	**29.3**
81P/ Wild 2 [3]	2016 July 20, 2022 Dec. 15	**1.59**	5.31	3.2
67P/Churyumov-Gerasimenko [4]	2015 Aug. 13, 2021 Nov. 2, 2028 Apr. 9	1.21	5.70	3.9
21P/Giacobini-Zinner [5]	2018 Sep. 10, 2025 Mar. 25	1.01	**5.98**	**32.0**
22P/Kopff [6]	2015 Oct. 25, 2022 Mar. 17	**1.56**	5.33	4.7
6P/d'Arrest [7]	2015 Mar. 2, 2021 Sep. 17	**1.35**	5.64	**19.5**
43P/Wolf-Harrington [8a]	2016 Aug. 19 (before 2019 Mar.)	**1.36**	5.34	**16.0**
43P/Wolf-Harrington [8b]	2025 Aug. 5 (after 2019 Mar.)	**2.44**	**6.22**	9.3
46P/Wirtanen [9]	2018 Dec. 12, 2024 May 19	1.05	5.13	11.8
73P/Schwassmann-Wachmann 3-C	2017 Mar. 17	0.97	5.21	11.2
41P/Tuttle-Giacobini-Kresak	2017 Apr. 11	1.05	5.12	9.2
103P/Hartley 2	2017 Apr. 20	1.07	5.89	13.6
P/2001 Q2 Petriew	2018 Jan. 27	0.93	5.27	14.0
79P/du Toit-Hartley	2018 Sep. 13	1.12	4.77	3.1
P/1999 RO28 LONEOS	2019 July 1	1.12	5.73	7.5
P/2003 H4 LINEAR	2015 Apr. 24, 2020 Oct. 5	1.17	5.02	2.6
P/2004 R1 McNaught	2015 Aug. 14, 2021 Jan. 26	0.97	5.22	4.9
P/2000 G1 LINEAR	2016 Mar. 15, 2021 July 11	1.00	5.10	10.4
15P/Finlay	2014 Dec 27, 2021 July 13	0.99	**6.02**	6.8

07-05866P-39

Figure 3-3. JFCs are demanding targets limiting mission accessibility using ballistic mission designs and chemical propulsion. Values in bold red were considered too difficult to achieve; and values in orange were demanding but possible. The original target priority provided by the SDT is shown in square brackets. However, the SDT later decided that any comet, in principle, could serve as a suitable CSSR target, and the entire list of known JFCs was considered, with some of the more favorable CSSR candidates listed here. Baseline and backup targets are highlighted in yellow. Although C-G has rather unfavorable perihelion and aphelion distances for a ballistic mission, detailed analysis showed that the C_3 and ΔV requirements could still be met.

3.2 Spacecraft Architecture

By using the spacecraft to ascend and descend to the nucleus, costs are minimized when compared to a separate landing/sampling craft. The large (on the order of Rosetta) arrays that are required for both mission architectures add complexity to a single spacecraft descent, but the dual-axis gimbal allows the array to be rotated into a safe position during sampling. The communications subsystem is augmented to facilitate direct-to-Earth communications at a variety of spacecraft orientations that will be encountered during the long thrust periods of the low-thrust

mission and during proximity operations. The rest of the spacecraft (e.g., avionics, power, guidance and control) has been simplified to focus the technical team on the many items required for a CSSR mission. Spacecraft details for the electrical and chemical propulsion designs can be found in Sections 4 and 5, respectively.

3.3 Proximity Operations

A layered Height and Motion System provides a robust approach for ascent and descent to the comet nucleus. While proximity operations, including an inertial landing on a small body, have been demonstrated by the NEAR mission, a triad of lidars and Doppler radars are incorporated into the design to provide improved landing safety by ensuring all velocities are properly nulled prior to surface contact. A terrain-relative optical navigation system will also be employed as an additional safety measure. Lessons learned from the NEAR and Hyabusa missions have been incorporated, allowing a lower risk proximity operations strategy. The unique factors associated with approach of a comet nucleus (e.g., outgassing) have also been folded in to conservatively estimate the mission risk. Proximity operations are discussed in detail in Section 4.

3.4 Sampling System

A versatile active sampling system (redundant drill sets) provides a wide range of surface properties while ensuring a bulk sample return. Alternative designs were investigated, but most had significant shortcomings. Corers did not have the ability to ensure sampling over the entire range of potential cometary surface properties. "Sticky" pads were also ruled out by the SDT due to possible interference with the science investigation since the sticky substance is usually organic. Other solutions are envisioned, but a point design was selected to facilitate study closure. Coupled with a sample return vehicle design that feeds forward into a future MSR mission, the sampling system provides verified acquisition, storage, and return of at least a 500-cc sample maintained <–10ºC throughout. Lower temperatures were examined, but they introduced an excessive amount of cost risk for a mid-level mission. Utilization of the Stardust heritage return capsule design was investigated, but thermal concerns resulted in the selection of the MSR-type design. Further work in this area is recommended. Section 4 provides the sampling system details.

4. MISSION IMPLEMENTATION

The CSSR mission implementation minimizes risk while satisfying all baseline science objectives.

- The CSSR low-thrust trajectory, electric propulsion design reduces mission risk by providing regular (yearly) launch opportunities and robust in-flight options to mitigate anomalies.
- Single spacecraft architecture reduces cost risk compared to multiple platform missions.
- MSR-style SRV provides technology advancements for future missions.
- Flexible sampling system facilitates return from a wide range of surface properties.
- Robust descope methodology provides programmatic flexibility.

Comet Surface Sample Return (CSSR) provides a bulk sample return using simple interfaces and flight-proven designs wherever possible. CSSR is developed with proven processes incorporating lessons learned from many past missions.

4.1 Mission Architecture Overview

CSSR science objectives drive the need for a complex mission design and spacecraft. To this end, a single spacecraft architecture using electric propulsion has been defined incorporating a Mars Sample Return (MSR)-style sample return vehicle (SRV) and a drill-based sample acquisition system (SAS) to provide a robust mission with flexibility and risk mitigation options.

Draft Level I and Additional Driving Requirements. The science investigation and measurement requirements are described in Section 2. The science instruments and accommodation requirements described are representative; actual instruments will be selected through a process defined by NASA Headquarters. Beyond the payload accommodation requirements, the draft Level 1 CSSR requirements are:

- Monitoring the target comet for >20 rotations in the period from −10 days to +100 days around perihelion passage
- Mapping the target comet surface to ≤1 m/pixel resolution
- Returning a surface sample of ≥500 cc from the target comet to Earth (Utah Test and Training Range, UTTR) for laboratory investigation
- Preserving the comet sample organics and volatiles at a temperature ≤−10°C at a pressure of 1 bar
- Single fault failure tolerant design
- Sampling a selected area on the comet within 50 m (1-σ radial)
- Capable of descending to the surface for sample capture at least three times

4.2 Science Investigation

4.2.1 Science Instruments

The representative science payload discussed below directly addresses the required measurement objectives. Figure 4.2.1-1 lists the key instrument characteristics and Fig. 4.2.1-2 shows the payload block diagram. Discussion of how the instruments are used to achieve the mission scientific objectives and instrument measurement approaches are provided in Section 2.

The Long-Range Reconnaissance Imager (LORRI) on the New Horizons spacecraft [Cheng et al. 2007] was designed for a long-duration outer solar system mission, and the requirements are very similar to those of CSSR. The two primary imagers use LORRI focal plane units (FPUs), i.e., charge coupled device (CCD) detectors and their associated electronics boards. These can be built to print but component obsolescence makes some redesign likely.

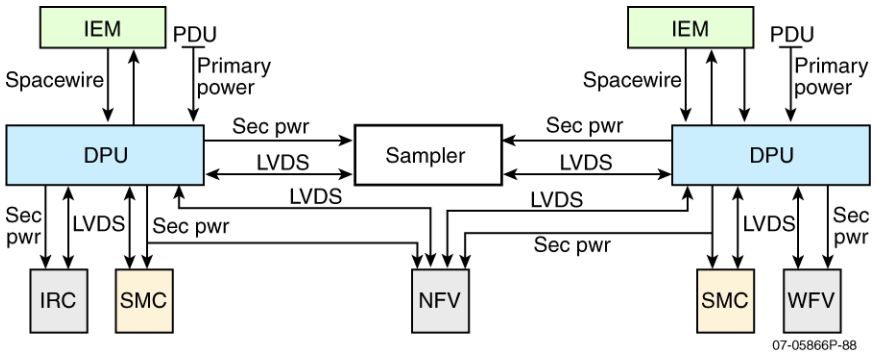

Figure 4.2.1-1. The CSSR payload is single-fault tolerant in providing the science floor.

Sensor	FOV (deg)	Resolution (radians)	Dynamic Range	Mass (kg)	Size (cm)	Power (W)	Sens (Wm^{-2})
NFV	1.2	30×10^{-6}	10^3–10^6	2.5	10×10×25	2	8×10^{-15}
WFV	20	5×10^{-4}	10^3–10^6	2.0	8×10×20	2	2×10^{-15}
IRC	30	5×10^{-3}	10^2	2.5	10×10×15	5	ΔT=3 @ 170 K
SMC1	30	1×10^{-3}	10^3–10^4	1.5	10×10×15	5	2×10^{-14}
SMC2	30	1×10^{-3}	10^3–10^4	1.5	10×10×15	5	2×10^{-14}
Temp	2 + 2 Thermistors		16 b/s	0.1	1×1×1 ea	0.1	0.1 K
Press	2 + 2 MEMS		16 b/s	0.1	1×1×1 ea	0.1	0.01 bar
DPU1	Rate is per sensor		1.3 Mb/s (Data Rate)	2	30×30×51	13 (40 peak)	N/A
DPU2	Burst rate per image		1.3 Mb/s (Data Rate)	2	30×30×51	13 (40 peak)	N/A

07-05866P-89

Figure 4.2.1-2. The CSSR payload accommodation requirements are modest. The NFV and WFV both use 1024 x 1024 pixel CCDs. The IRC employs a 160 x 120 pixel microbolometer array. The NFV sensitivity ("Sens") assumes an exposure time of 10 s, while the WFV value is for an exposure time of 1 s. The IRC is designed so that it can simultaneously measure ice at 170 K and hot mantle material with a temperature above 400 K. The two sample microcams (SMC1 and SMC2) are attached to the sampler unit and employ CMOS detectors.

The optics for the narrow field visible (NFV) camera uses a reflective Richey-Chretien design similar to a miniature LORRI, with a 65-mm aperture. It can be fabricated using ordinary materials such as aluminum. The wide field visible (WFV) camera is similar to the refractive imagers on NEAR and MESSENGER but intermediate in size between the two. A spectral filter would be used to adjust sensitivity and reduce chromatic aberration effects with radiation-tolerant glass optics. The design would be similar to the MESSENGER wide-angle camera with a single filter, but the difference in size and focal length would mean that it would not be built to print. The thermal infrared camera (IRC) is based on commercial refractive designs with microbolometer arrays. The detector and electronics from the Mars Odyssey THEMIS instrument, with simple imaging optics, provide an alternative path to meet the thermal imaging requirement (at a slightly higher cost).

The DPUs to control and power these three imagers are functionally redundant and MESSENGER-derived, with only the NFV cross strapped. The DPU basic design has extensive APL flight heritage. The IRC is connected to one DPU, and the WFV is connected to the other. The IRC interface is new. Each DPU also controls half the redundant sampler mechanisms and one sample monitoring camera (SMC). Thus, the SMCs, the sampler drive mechanisms, and temperature and pressure sensors are all controlled from both DPUs.

The temperature and pressure sensors are simple in design, using a microelectromechanical system (MEMS) pressure sensor and thermistors. They are redundant for temperature and are split between the DPUs for pressure.

The SMCs consist of two microcams with refractive optics and light-emitting diode (LED) illumination. They are necessary to inspect the collected samples for volume and integrity. The cameras are based on a compact detector electronics design developed at APL and an existing radiation-hardened CMOS (complementary metal oxide semiconductor) detector. The optics would be refractive using a new design with fixed focus and aperture. The illuminators would also be new.

4.2.2 Sample Acquisition System

The SAS must be capable of extracting a sample from a comet whose surface strength properties can vary by 6 orders of magnitude from several tens of pascals for unconsolidated ice crystals to tens of megapascals for water or carbon dioxide crystalline ice. The unknown nature of the comet surface dictates that the SAS be capable of collecting a sample throughout the entire range of potential comet surface strength properties, which may result in sacrificing collection optimization at the extremes for more reliable capability throughout the entire range including the extremes. This section describes the trade study results and presents a solution capable of collecting a surface sample from a comet regardless of the surface that is encountered.

The SAS operates a pair of Ø63.5-mm drills simultaneously that are designed to penetrate the surface to a depth of 100 mm and 150 mm, respectively. Assuming each drill is filled to capacity, the sampling would yield 250 cc and 380 cc, respectively, of comet surface material and the potential for a stratigraphic difference between the 100-mm and 150-mm sampling depth. The SAS has a primary and an identical secondary pair of drills should a second sampling attempt be desired (Fig. 4.2.2-1). The SRV contains four sample receptacles that are capable of receiving and returning to Earth the primary and secondary, just the primary, or just the secondary set of drilled comet surface samples.

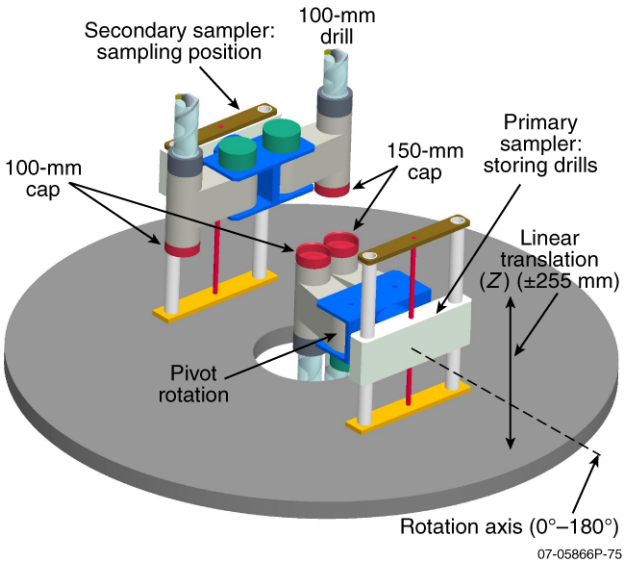

Figure 4.2.2-1. The SAS is fully redundant and uses a single mechanism for acquisition and stowage.

A touch-and-go sampling technique is selected for the CSSR mission. The comet selected for the CSSR mission is significantly smaller than the Earth, Moon, or Mars; thus the SAS will be required to collect a sample in a micro-gravity deep space environment. Whatever surface properties are encountered, a force will be required to drive the sampler into the comet surface. There is essentially no gravitational force at the comet surface to prevent the sampler from lifting the spacecraft off the comet surface instead of penetrating the surface with the samplers as on high-gravity bodies like Earth. There are essentially two options to overcome the lack of gravity and to generate this force:

1. The spacecraft can generate force by using its mass and velocity (i.e., its momentum) to impact the comet. The impact is capable of generating a force for a short period of time. The impact determines the amount of force available to the samplers as well as a limitation on the duration of the sampling event to several seconds. This solution is baselined.
2. The spacecraft could be equipped with an anchoring system that firmly attaches the spacecraft to the comet surface. However, given the unknown nature and characteristics of the comet surface, landing a spacecraft and designing an effective system to anchor and eventually release it was considered too complex and risky for the mission.

The samplers are composed of a drill that rotates inside a thin tube. The cut/extracted material will be captured inside the tube until it is compacted to capacity. The stage to which the drills are attached is designed to limit the maximum force placed on the drills to prevent them from stalling or any mechanism from being damaged during the sampling impact. In addition, the entire SAS is isolated from the spacecraft via shock mounts to prevent a hard strike from transferring loads into the spacecraft. After sample collection, the drill head retreats, rotates 180°, and places the drills and samples in the SRV. After releasing the drills, the drill head moves away from the SRV, rotates back 180°, and then seals each drill/sample with a hermetically sealed cap. The SAS is then ready to be jettisoned or to attempt a second sampling using the second drill pair. The sampling sequence is outlined in Fig. 4.2.2-2.

Time (sec)	Altitude (m)	Action
−10000	+1000	Final orbit—complete SAS primary sampler system checkout
−100	+1	Engage primary up/down mechanism force control
−5	+0.5	Start primary 100- and 150-mm drills
0	0	Surface contact/penetration
+5	−0.150	Sampled full depth, stop drills
+105	+1	Disengage primary up/down mechanism force control
+1000	+1000	Position primary up/down mechanism to mid-travel
+1100	>1000	Rotate primary drill head +180°
+1200		Store primary drills in SRV
+1210		Release 100- and 150-mm drills and move primary up/down mechanism to mid-travel point
+1300		Rotate primary drill head −180°
+1400		Stow drill caps in SRV
+1405		Release drill caps
+1500		Translate primary up/down mechanism to deployment position.
This completes the primary sampler cycle. A second sample will complete the same cycle with the secondary sampler system, if required.		

07-05866P-83

Figure 4.2.2-2. The sampling timeline is simple and provides sufficient margin to ensure a sample is acquired safely.

4.2.3 Sample Return Vehicle

The SRV design is based on the concept developed for the Mars Sample Return Earth Entry Vehicle (MSR EEV) [Mitcheltree et al. 2001]. This architecture is focused on a low-risk, robust, and simple operations approach to safely return samples to Earth. The same approach is applied here to CSSR to provide a low-cost, highly reliable solution that leverages heavily on the technology development experience of MSR.

The SRV is a scaled version of the MSR EEV (Fig. 4.2.3-1). The entry is completely ballistic, relying on no parachute or other deployments prior to impact at the landing site. This provides a very robust design, which greatly simplifies the entry operations, thus reducing overall risk. The SRV is passively stable in the forward orientation and passively unstable in the backward orientation. This unique approach makes it possible to ensure the vehicle can self-orient to nose-forward under all separation or entry contingencies, including tumbles. Additional risk mitigation features include:

- Proven flight-heritage components for critical subsystems
- Flight-proven, aerodynamically stable 60º half-angle sphere cone forebody similar to that used for Genesis and Stardust capsules
- An integrally hinged lid to ensure that the sealing surfaces are accurately mated
- Fully redundant sets of lid locking pins
- Redundant battery-powered beacons to locate the SRV if radar tracking fails

The mission will conduct independent entry analyses using state-of-the-art, flight-validated codes (POST, LAURA, DPLR) to ensure an accurate end-to-end simulation of the SRV entry, descent, and landing. The entry simulations and computational fluid dynamics (CFD) analyses will encompass trajectory, aerodynamic, and aeroheating solutions through all flight regimes

from free-molecular hypersonic flow through subsonic terminal descent. Landing site support, including planning, vehicle tracking, and recovery, will be provided by the UTTR.

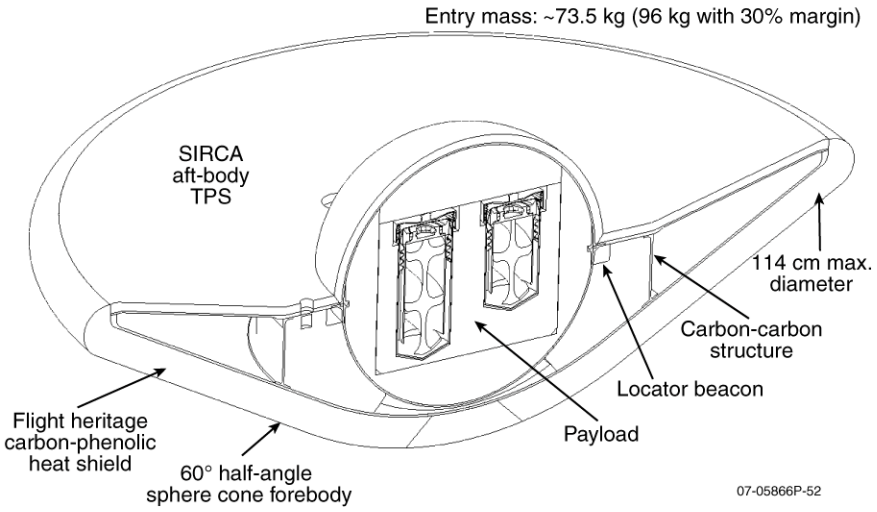

Figure 4.2.3-1. The SRV design feeds forward into the Mars Sample Return program.

NASA Langley Research Center (LaRC) has led the unparachuted sample return architecture development for MSR EEV since 1999. Technology development conducted previously for MSR EEV directly applies to the CSSR SRV and includes the following:

- Penetrometer drop tests and site surveys to characterize the soil conditions inside the UTTR landing footprint
- Validation of analytical methods to predict impact loads for high-velocity landings at UTTR
- Probabilistic risk assessments comparing parachuted landings, mid-air recoveries, and unparachuted landings for both water and land recoveries
- Full-scale drop tests at UTTR

The early design and development phase of the CSSR SRV will be focused on addressing the following trade studies and analyses:

- Configuration/payload layout
- Mechanical systems, including lid closure and latching
- TPS selection and sizing
- Forebody attach points (to spacecraft)
- Structures and materials
- Impact modeling
- Thermal (post-landing) analyses
- Entry conditions (e.g., entry flight path angle)
- Landing site prediction and targeting

The project will also complete early (Phase B) risk-reduction testing, including additional drop and impact tests. Aerodynamic and aerothermal analytic model performance will also be validated with the use of ballistic range and wind tunnel testing.

4.2.4 Sample Volatile Capture

Preservation of the volatile components of the comet surface sample is vital to understanding the true nature of the comet surface. The surface sample will be taken at very low temperature; however, during the sample mission return cruise phase and reentry to Earth, the temperature of the sample will rise and some volatiles may escape. A volatile capture flask is attached to the sample cell to ensure that these volatiles are not lost.

The volatile capture flasks are closed volumes in the SRV that are connected to each of the cells that hold the comet samples for return to Earth. There is a check valve between the sample cell and the volatile capture flask and a powered overpressure valve between the volatile capture flask and a vent to space. The passive check valve only allows gasses at higher pressure in the sample cell to flow into the volatile capture flask but does not allow flow in the other direction.

During the outbound cruise phase of the mission, the overpressure valve is powered to open it to space. This ensures that the volatile capture flask is fully empty and evacuated. At the comet, the overpressure valve is unpowered. In this state, it is a passive valve that will not allow the pressure in the volatile capture flask to rise above a preset limit.

After taking the sample and placing it into the cell, the sample cell is sealed. Therefore, any evolved gasses will raise the pressure in the cell and the gasses will flow through the check valve into the volatile capture flask. If the quantity of volatiles is large, the pressure in the volatile capture flask will rise; if it exceeds a preset value, it will open the overpressure valve to release some of the volatiles to space. This will ensure that the pressures within the volatile capture flask remain within safe levels.

When the SRV is brought into the laboratory after landing on Earth, the vent is connected to the laboratory gas sample system and the overpressure valve is powered to transfer the volatile sample into the ground analysis instruments.

4.3 Mission Design and Navigation

Key driving requirements for the mission design and navigation, flowed down from or in addition to those in Section 4.2.2, include the following:

- Launch opportunities every 1–2 years
- Launch on Atlas V
- Launch period 21 days
- Trip time minimized (less than 10 years preferred)

With the success of Deep Space One (DS-1) and with the current flight experience of Dawn, solar electric propulsion (SEP) is becoming a more mature technology for space exploration. The smaller mass ratios (propellant to launch mass) obtained for missions to the short period comets and other demanding targets offer many advantages. The study baselines NASA's NEXT (NASA's Evolutionary Xenon Thruster) engine to investigate not only mass performance but also some other important parameters such as the return speed. It should be noted that considerable efforts have been made to make the NEXT engine not only better in performance (thrust and Isp) as compared to NSTAR but also better tested, better documented, and easier to fly. It is indeed an important investment that NASA has made. CSSR can provide an excellent opportunity to leverage this important NASA technology investment. A mission using the NEXT engine will also open the door to the possibility of having one spacecraft bus for a wide variety of missions to the main belt asteroids, to the comets, and beyond. Moreover, the solar array

technology keeps improving (smaller array sizes to deliver a given power) and, in combination with the NEXT engine, will enable larger scientific payloads.

The comet 67P/Churyumov-Gerasimenko (C-G) provides an excellent target for a sample return mission. It is well observed and will be visited by the Rosetta spacecraft. As seen by Hubble's Wide Field Planetary camera, the nucleus measures 5 × 3 km and has an ellipsoidal shape. It rotates once in approximately 12 hours. Rosetta will perform analyses on the dust grains and the gas flowing out from the cometary nucleus. The physics of the outer coma and the interaction with the solar wind will also be studied [Fiebrich et al. 2004]. Although no sample will be brought back to Earth, Rosetta and its lander will characterize the comet shape, its mass properties, and its gravity field. With these pieces of information, the risk of landing and bringing a sample back will be significantly reduced.

To construct the mission design, very conservative assumptions were used. First, for the solar array modeling, Dawn's solar array parameters (the coefficients that describe the array performance as a function of distance) were used. Since this mission will not launch until approximately 2015, better performance can be expected. A solar array degradation of 2% per year was enforced in conjunction with a 90% duty cycle for the thruster. Furthermore, in terms of power, at least 250 W were reserved for housekeeping. For the launch mass, the NASA Kennedy Space Center (KSC) launch curves (which already have contingency built in) were used. For the NEXT engine data, NASA John H. Glenn Research Center (GRC) ion engine curves are used. Finally, although other dates were explored, in accordance with the guidelines specified for the study, launch dates ±1 year from 2016 are presented here.

Under the assumptions discussed above and for the C-G target, the resulting spacecraft is a 17.4-kW (at 1 AU, beginning of life [BOL]), 1+1 NEXT system (one engine is used with one as a spare and to alleviate any potential throughput concerns) with 405 kg of xenon (including 15% contingency). For comparison, Dawn is a 10.3-kW system and its tank holds about 425 kg of xenon. Using triple junction gallium arsenide arrays, as shown in the power section, the sizes of the arrays needed to provide the required power are not much larger than Rosetta arrays. A representative trajectory for 2015 is shown in Fig. FO 4-1A. Note the presence of two orbits about the Sun before the comet encounter. The phases and their durations are also shown in Fig. FO 4-1A. Note the presence of generous coast times in the mission phases. Extended coast times make the design robust to unexpected periods of missed thrust. The distances and the Sun-Earth-Probe angle are in Fig. FO 4-1B. The power (after degradation of 2% per year and a 90% duty cycle), thrust magnitude, thrust angle definition, and angles are, respectively, in Figs. FO 4-1C, 4-1D, and 4-1E.

To construct multi-year launch windows, the number of "phasing orbits" around the Sun is varied. As a result, different years can be used for the launch. The initial period of the heliocentric orbit is set by the launch vehicle. To set the initial period and the number of phasing loops needed to reach C-G (and to use the same spacecraft configuration for two consecutive years), an Atlas 521 is used in 2015 and an Atlas 531 in 2016. (Specifically, what changes is the number of solids, *x*, on the Atlas 5x1 rocket.) The benefit is that it is possible to launch the same spacecraft with about the same mass margin for 2 years in a row. This strategy, in turn, simplifies systems engineering and programmatic constraints. Since the spacecraft fairing is the same, mating of the spacecraft to the vehicle will be the same each year.

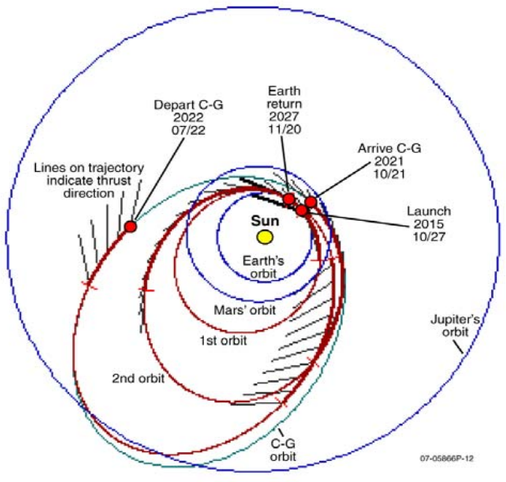

A. CSSR low-thrust trajectory (ecliptic view).

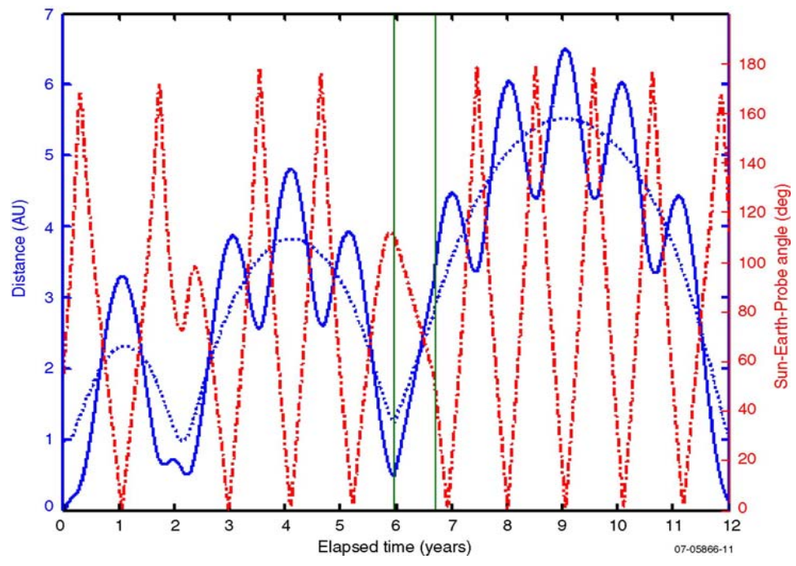

B. Low-thrust trajectory solar distance and Sun-Earth Probe angle.

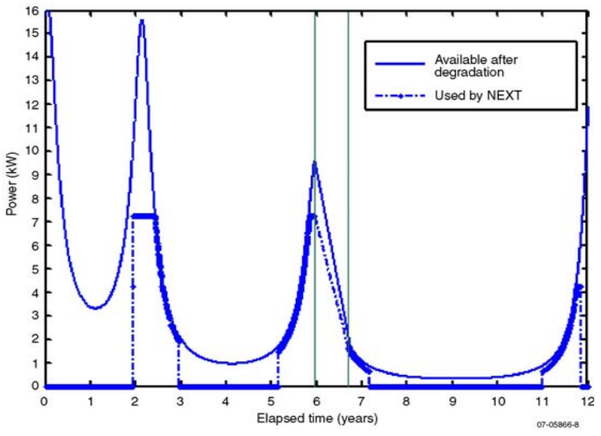

C. CSSR low-thrust trajectory power available and power used (30% margin worst-case).

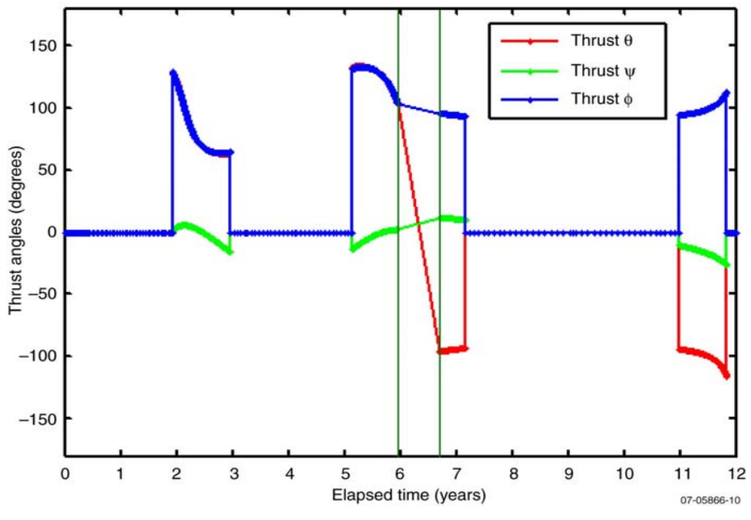

D. Thrust angle definition throughout the low-thrust trajectory.

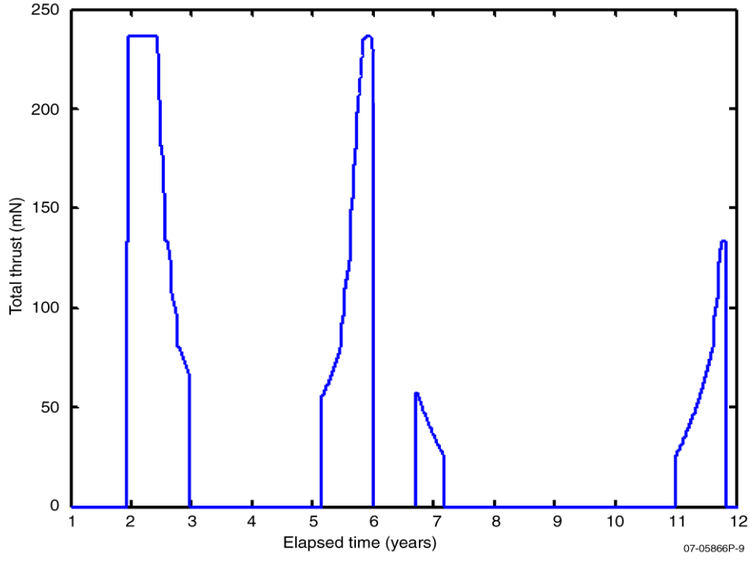

E. The CSSR thrust magnitude allows use of the NEXT 1+1 system.

Foldout 4-1. Low-thrust mission design.

The resulting launch windows are presented in Figs. 4.3-1 and 4.3-2. Although only 20-day windows were considered, each year, a 30- to 40-day launch window should be possible by allowing the current generous mass margin to vary. When compared to the chemical trajectories, the velocities at infinity on the approach hyperbola are smaller, which will make the reentry speeds more manageable and simplify the thermal design of the thermal protection system for the SRV. Additional propellant can be used to make the reentry speeds smaller. Other comet targets should be accessible with the resulting spacecraft bus [Sims 2000].

Launch Date 2015	C_3 (km^2/s^2)	Launch Mass (kg)	Launch Asymptote Declination (deg)	C-G Arrival 2021	C-G Departure 2022	Earth Arrival 2027	Arrival V_∞ (km/s)	Xe Load with 15% Contingency (kg)
10.27	43.56	1867.0	24.1	10.10	07.09	11.20	8.94	371.5
10.28	43.43	1872.9	23.8	10.10	07.09	11.20	8.94	371.8
10.29	43.43	1872.9	23.5	10.08	07.09	11.20	8.94	373.2
10.30	43.43	1872.9	23.5	10.08	07.09	11.20	8.94	371.7
10.31	43.43	1872.9	23.4	10.08	07.09	11.20	8.94	370.3
11.01	43.43	1872.9	23.3	10.08	07.09	11.20	8.94	369.2
11.02	43.43	1872.9	23.2	10.08	07.09	11.20	8.94	368.3
11.03	43.43	1872.9	23.1	10.08	07.09	11.20	8.94	367.5
11.04	43.43	1872.9	23.0	10.08	07.09	11.20	8.94	366.8
11.05	43.43	1872.9	22.8	10.08	07.09	11.20	8.94	366.3
11.06	43.43	1872.9	26.7	10.08	07.09	11.20	8.94	365.9
11.07	43.43	1872.9	22.4	10.08	07.09	11.20	8.94	365.6
11.08	43.43	1872.9	22.2	10.08	07.09	11.20	8.94	365.3
11.09	43.43	1872.9	22.0	10.08	07.09	11.20	8.94	365.3
11.10	43.43	1872.9	21.7	10.08	07.09	11.20	8.94	365.3
11.11	43.43	1872.9	21.5	10.08	07.09	11.20	8.94	365.3
11.12	40.96	1984.7	21.2	10.09	07.09	11.20	8.90	404.1
11.13	40.96	1984.7	21.1	10.09	07.09	11.20	8.90	404.1
11.14	40.96	1984.7	20.9	10.09	07.09	11.20	8.90	404.3
11.15	39.69	2043.6	20.7	10.09	07.09	11.20	8.90	404.5

07-05866P-76

Figure 4.3-1. The baseline CSSR launch window provides a 20-day opportunity to launch on an Atlas 521 and a 12-year mission.

Launch Date 2016	C_3 (km^2/s^2)	Launch Mass (kg)	Launch Asymptote Declination (deg)	C-G Arrival 2021	C-G Departure 2022	Earth Arrival 2027	Arrival V_∞ (km/s)	Xe Load with 15% Contingency (kg)
10.27	51.98	1869.7	26.1	08.23	07.09	11.20	8.92	324.3
10.28	51.98	1869.7	26.4	08.23	07.09	11.20	8.92	318.6
10.29	51.98	1869.7	26.6	08.23	07.09	11.20	8.92	313.6
10.30	51.98	1869.7	26.7	08.23	07.09	11.20	8.92	309.2
10.31	51.98	1869.7	26.9	08.23	07.09	11.20	8.92	305.4
11.01	51.98	1869.7	26.9	08.23	07.09	11.20	8.92	302.0
11.02	51.98	1869.7	26.9	08.23	07.09	11.20	8.92	299.1
11.03	51.98	1869.7	26.9	08.23	07.09	11.20	8.92	296.5
11.04	51.98	1869.7	26.8	08.23	07.09	11.20	8.92	294.4
11.05	51.98	1869.7	26.8	08.23	07.09	11.20	8.92	292.7
11.06	51.98	1869.7	26.7	08.23	07.09	11.20	8.92	291.3
11.07	51.98	1869.7	26.5	08.23	07.09	11.20	8.92	290.4
11.08	51.98	1869.7	26.3	08.23	07.09	11.20	8.92	289.8
11.09	51.98	1869.7	26.1	08.23	07.09	11.20	8.92	289.6
11.10	51.98	1869.7	25.8	08.23	07.09	11.20	8.92	289.8
11.11	51.98	1869.7	25.5	08.23	07.09	11.20	8.92	290.3
11.12	51.98	1869.7	25.1	08.23	07.09	11.20	8.92	291.3
11.13	51.98	1869.7	24.7	08.23	07.09	11.20	8.92	292.6
11.14	51.98	1869.7	24.3	08.23	07.09	11.20	8.92	294.2
11.15	51.98	1869.7	23.9	08.23	07.09	11.20	8.92	295.8

07-05866P-77

Figure 4.3-2. The backup CSSR launch window provides a 20-day opportunity to launch on an Atlas 531 and an 11-year mission.

During the thrusting phases, the CSSR trajectory has been designed with a 90% duty cycle. As a result, there will be time to collect housekeeping and navigation data while not thrusting (even though the spacecraft design allows communication while thrusting). Significant navigation experience for spacecraft using ion engines has been collected by DS-1 and is currently being collected via Dawn's flight experience. This experience gathered by the Jet Propulsion Laboratory (JPL) navigation team should be leveraged for CSSR. For proximity operations, if Rosetta is successful, the navigation team will also have additional data to use in their gravity force modeling and associated computations. Moreover, as done with other missions, to increase the accuracy of the interplanetary navigation (and the subsequent arrival to the target, and return to Earth), Very Long Baseline Interferometry (VLBI), Delta-Differential One-way Range (ΔDOR) tracking data will be incorporated into the orbit determination process.

In many cases, SEP has been shown to be an enabling technology for comet sample return missions [Sims 2000]. For C-G, a much lighter spacecraft can be launched with about the same mass margins (and perhaps even more when the SRV thermal design is assessed in more detail) as a chemical propellant configuration. In the bigger picture of NASA space exploration, performing this mission with the NEXT engines will open the door to many other targets. Combined

with gravity assists, other targets in the solar system (e.g., Titan) may also become accessible with a NEXT 1+1, 17-kW spacecraft [Benson 2007].

4.4 Flight System Design and Development

Discussion of the flight system design and development approach, including the use of new versus existing hardware and software and fault tolerance, is included within the following sections. The manufacturer and flight heritage information provided assumes that the spacecraft is being built today. This information is representative, and it is expected that a project will leverage additional advancements and flight heritage that occur between now and project start.

The technology readiness level (TRL) for each component is estimated based on current technology. All components are considered TRL>6 except for the SAS, SRV, height and motion subsystem (H&MS), and the NEXT system as there are no additional exotic requirements and existing representative heritage components for each subsystem. For any component considered TRL<6, technology development required to bring the level to TRL 6 by Project Confirmation is described in Section 4.8. The technology costs are included in the total project cost where applicable.

4.4.1 Flight System Overview

Key features and benefits of the flight system are listed in Fig. 4.4.1-1. The spacecraft design heavily leverages heritage from previous and current APL missions: MESSENGER [Leary et al. 2007], STEREO [Driesman et al. 2007], New Horizons [Fountain et al. 2008], and Radiation Belt Storm Probes (RBSP). Design flexibility allows commonality on the avionics, telecommunications, and guidance, navigation, and control (GN&C) subsystems between the low-thrust architecture presented here and the ballistic architecture presented in the following section. As shown in the block diagram (Fig. FO 4-2A), CSSR is single fault tolerant. The avionics design incorporates a fully redundant main processor (MP) architecture providing command and data handling (C&DH), GN&C, and autonomy over all of the spacecraft subsystems and instruments. The telecommunications (RF) subsystem is block redundant, providing telemetry during all mission-critical events and ensuring that the spacecraft is able to receive commands during all normal modes and mission phases. The GN&C subsystem provides three-axis stabilized, zero-momentum pointing throughout the mission using an Inertial Measurement Unit (IMU), star trackers, and reaction wheels. The H&MS is the part of GN&C that allows safe spacecraft guidance and control during comet proximity operations. Both spacecraft architectures are powered by large dual-axis gimbaled solar arrays that are required for both mission designs (that go out beyond 5 AU) and can be rotated into a safe position during sampling. The thermal control subsystem for both designs provides a low-risk design approach using multi-layer insulation (MLI), heaters, radiators, and louvers (low-thrust design). The low-thrust mission propulsion system leverages NEXT heritage electric propulsion technology for ΔV maneuvers and a single-mode chemical propulsion system for attitude control during proximity operations. The mechanical spacecraft designs for both the ballistic and low-thrust missions are simple and efficient, with a center cylinder as the primary load-bearing structure that interfaces directly with the launch vehicle. Lessons learned from previous missions are incorporated to simplify development, integration and testing (I&T), and flight operations. The design is compatible with all evolved expendable launch vehicles (EELVs), although the Atlas 521 is baselined for SEP design to reduce the cost risk of the mission. The mass and power budgets are shown in Fig. FO 4-2B.

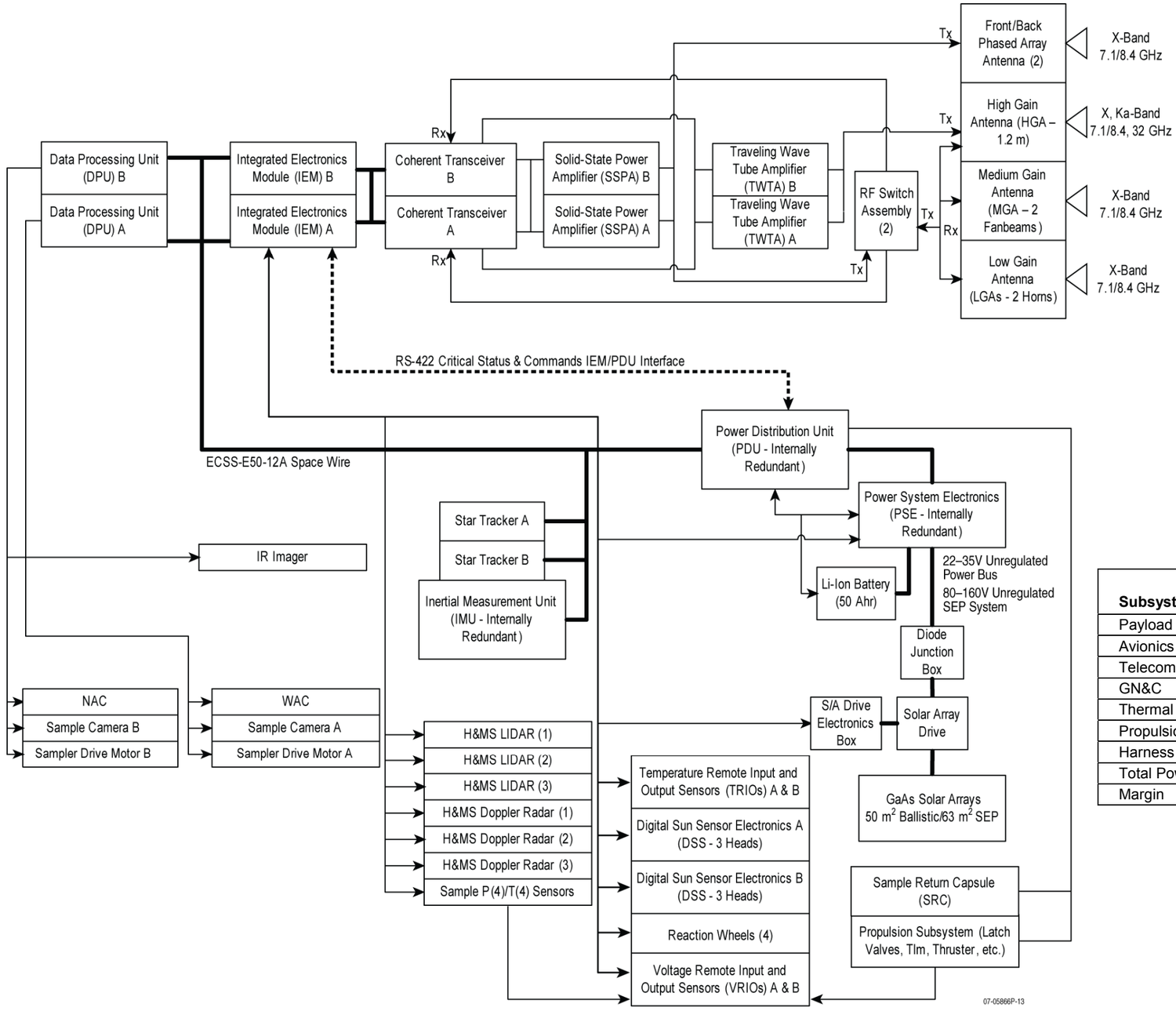

Subsystem	CBE Mass (kg)
Payload	127
Avionics and Power	227
Telecommunications	38
GN&C	52
Thermal	98
Propulsion	167
Structure	236
Harness	27
Total Dry Mass	972
Propellant & Pressurant	468
Total Wet Mass	1440
Max Launch Mass	1865
Dry Mass Margin	30%

07-05866P-94a

Subsystem	Cruise Power (W)	Orbit Power (W)	Sampling Power (W)
Payload	1	21	13
Avionics and Power	74	74	67
Telecommunications	68	187	68
GN&C	85	85	121
Thermal	152	123	138
Propulsion	2	2	2
Harness	6	7	6
Total Power	386	500	416
Margin	36%	Max range cruise is worst-case	

07-05866P-94b

Foldout 4-2. Low-thrust mission implementation system characteristics.

70-m Equivalent Ka DSN Capability During Orbit and Critical Events Only	Reduces onboard requirements (HGA size, power); reduces DSN time to satisfy requirements; 34-m baseline for cruise reduces mission cost
Front/Back Phased Array Antennas	Facilitates higher bandwidth communications during electric propulsion thrusting and proximity operations; eliminates the need for an antenna gimbal
Ballistic-type SRV	Eliminates the need for a parachute and spin table; feeds forward into MSR program
UltraFlex Solar Arrays	Reduced S/C launch mass; leverages NASA exploration investment
Height and Motion System	Provides improved accuracy for sampling site; ensures S/C velocities are nulled during proximity operations, simplifying sampling scenario and eliminating the need to land; autonomous abort capability reduces mission risk
Sample Acquisition System	Active drills facilitate sampling over a wide range of surface properties; allows “touch and go” sampling, eliminating the need to land; single mechanism used to acquire and to store the sample
Solar Electric Propulsion System	Allows for multi-year launch window; provides mitigation to post-launch anomalies; facilitates use of smaller launch vehicle; NEXT leverages NASA investment

Figure 4.4.1-1. The CSSR architecture features provide multiple benefits. 07-05866P-87

4.4.2 Propulsion Subsystem

The propulsion subsystem is divided into two parts: a NEXT ion thruster system for ΔV and a conventional hydrazine system for attitude control.

4.4.2.1 NEXT Ion Propulsion System

The NEXT ion propulsion system will provide the primary propulsion to propel the spacecraft to the destination comet and return the spacecraft to Earth vicinity for sample delivery. The total ΔV provided by the ion propulsion system is approximately 11.5 km/s. The study team has defined a two-string system, referred to as a 1+1 system, in which the primary string provides all the propulsion and the second string provides block redundancy. This block diagram for this 1+1 ion propulsion system is shown in Fig. 4.4.2.1-1, the components of which are described in more detail below. The NEXT thruster has a maximum input power of approximately 6.9 kW. As the spacecraft travels farther from the Sun, solar array power drops off. The NEXT system throttles as the power drops below 6.9 kW.

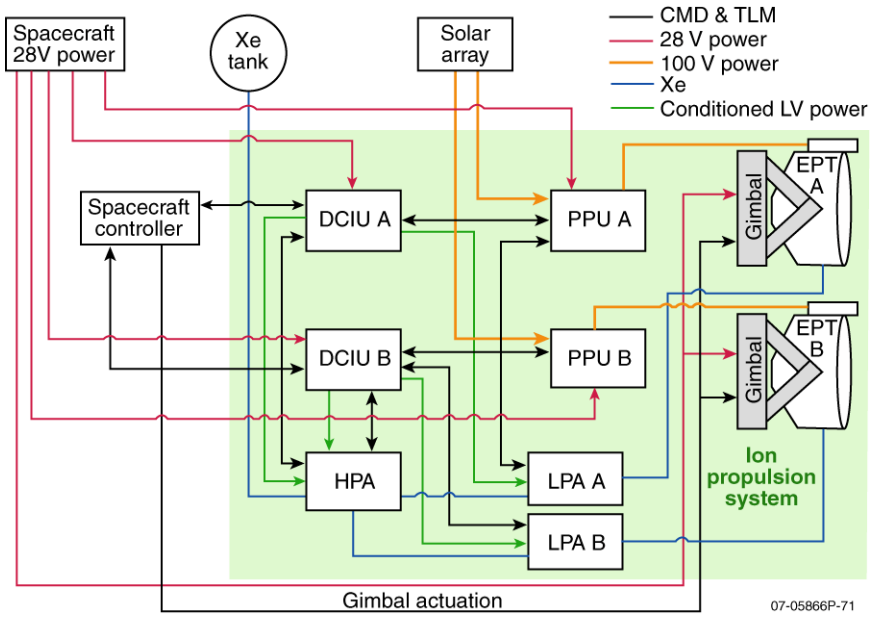

Figure 4.4.2.1-1. The ion propulsion system schematic illustrates the simplest 1+1 baseline configuration.

The NEXT ion propulsion system is under development within the In-Space Propulsion Technology (ISPT) project under the NASA Planetary Science Division. The NEXT project is due to complete technology development to TRL 6 in 2008. This level of progress satisfies the standard mission announcement of opportunity requirement that all technologies be at TRL 6 by the mission confirmation review. Each of the NEXT system components is described below. The NEXT system will undergo a major system integration test in early 2008, with each of the sub-system products integrated into a single string of the propulsion system. Multi-string testing is also planned to validate the propellant management system capabilities with multiple operating thrusters.

The NEXT thruster provides 235 mN of thrust, at a specific impulse above 4170 s and efficiency >70%, at the maximum input power of 6.9 kW. It can throttle down to approximately 550 W, with associated decreases in thrust and specific impulse. The NEXT thruster, shown in Fig. 4.4.2.1-2, has been developed to the prototype level: a flight-equivalent advanced engineering model. The prototype model thruster has completed performance acceptance and qualification-level environmental tests. The NEXT thruster is designed and fabricated by Aerojet General, a proven spacecraft propulsion system provider.

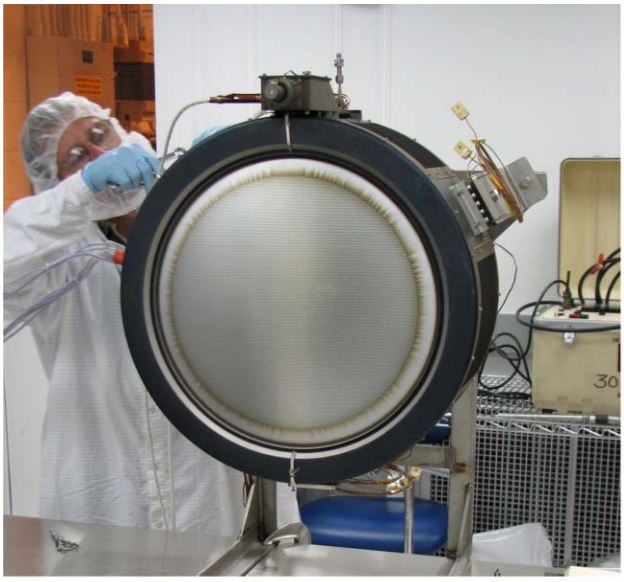

Figure 4.4.2.1-2. NEXT prototype model (PM) ion thruster shown in test.

A primary measure of ion thruster capability is in lifetime, expressed in terms of propellant (xenon) throughput. The ISPT requirement for NEXT thruster throughput capability is 300 kg of xenon. The on-going long-duration test has surpassed 270 kg as of the end of 2007. In situ test diagnostic data and supporting thruster life analyses indicate that the first failure of the NEXT thruster (caused by defined wear mechanisms) will not occur prior to 730 kg throughput. This provides a qualified capability of over 480 kg after applying a 1.5 qualification factor. Given successful demonstration of the expected NEXT thruster lifetime, considerable margin will exist above the 405 kg of xenon required for deterministic ΔV over the launch opportunity for this mission concept.

An integrated thruster performance and wear model has been developed to predict NEXT thruster performance as a function of throttling profile, specific to potential missions, while monitoring service life margin for the primary thruster failure modes. The model was developed using methodology described in the NEXT thruster service life assessment [Van Noord 2007]. Additional modeling capability has been added, permitting prediction of ion optics aperture erosion and its impact on thruster performance. The model is currently in the process of validation and incorporates the most up-to-date findings from the NEXT Long-Duration Test [Herman et al. 2007]. To date the Long-Duration Test has demonstrated 14,360 hours of operation, 294 kg of xenon throughput, and 1.19×10^7 N·s of total impulse with negligible performance degradation.

The CSSR mission profile assumes a 1+1 NEXT thruster configuration in a high-thrust throttling profile with a thruster throughput requirement of 405 kg. Figure 4.2.2.1-3 illustrates the thruster input power and ion optics' accelerator grid groove depth throughout the mission. Accelerator grid groove erosion wear-through is the first failure mode for most mission applications and is the case for the CSSR mission. The maximum groove depth is predicted to be 40% of the accelerator grid thickness at the end of the mission, leaving 60% margin.

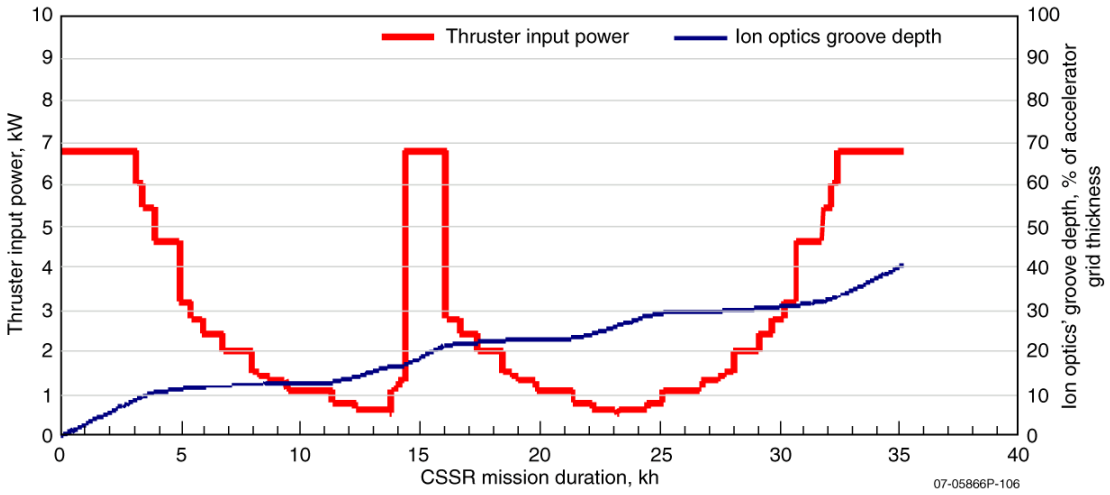

Figure 4.4.2.1-3. CSSR thruster throttling profile input power as a function of mission duration. The optics' accelerator grid groove depth, first failure mode, is plotted for the mission profile.

Modeling of all other thruster wear-out modes indicates greater margin than the ion optics' accelerator groove erosion service life capability. Figure 4.2.2.1-4 demonstrates NEXT cathode capability and keeper wear, indicating a conservative estimate of 25% barium depletion and 20% keeper depth erosion as the worst cases for the neutralizer and discharge cathodes, respectively. Other thruster performance parameters not shown, such as electron-backstreaming margin and purveyance margin, indicate more than sufficient margin at the end of the mission to have a negligible impact on thruster performance and operability.

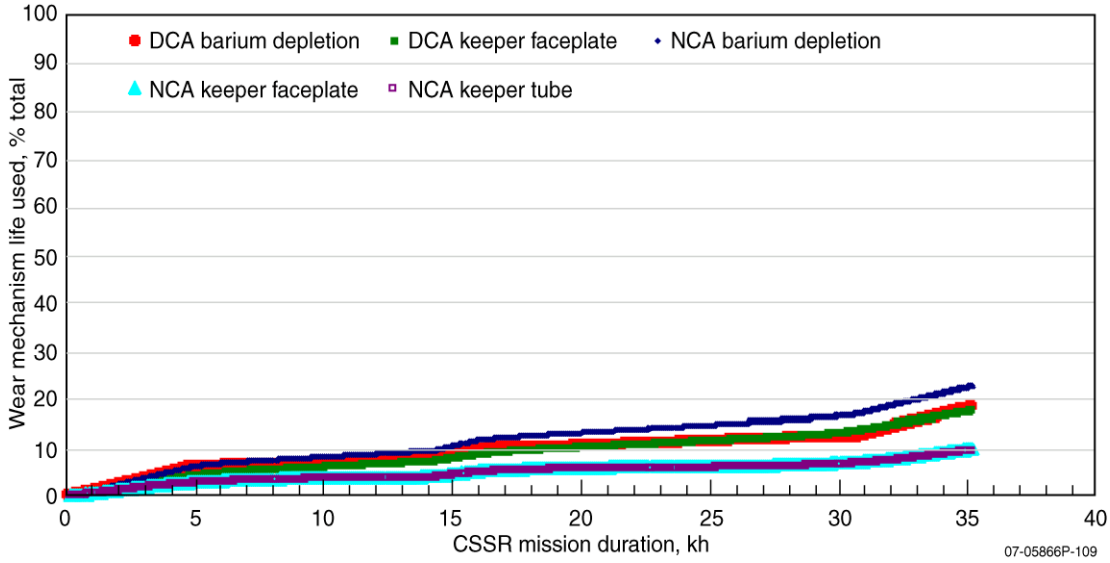

Figure 4.4.2.1-4. NEXT discharge and neutralizer cathode barium depletion and keeper erosion for the CSSR mission profile.

The application of the NEXT thruster integrated performance and wear model indicates the first failure mode for the CSSR mission profile using a 1+1 configuration to be charge-exchange

groove erosion through the ion optics' accelerator grid. After completion of the CSSR mission, approximately 40% of the single NEXT thruster service capability will have been used.

The life capability required for this mission concept, including a 1.5 qualification factor, will not be demonstrated by test until late-2010 or later. If the thruster capability has not been validated to the level required, this can be mitigated through various approaches. A second operational thruster, operating serially with the first thruster, can be added to the system to divide the throughput between two primary thrusters (similar to Dawn). A third thruster string (with PPU) can be added, accomplishing the same result, likely increasing mission performance as well. Operationally, balancing the xenon throughput between the primary and spare thrusters in a 1+1 system will increase the reliability and probability of completing the required ΔV.

The power processing unit (PPU) accepts the input power from the solar array and converts it to the power characteristics required by the thruster. The PPU can operate over an input voltage range of 80–160 V, such that the spacecraft does not need to regulate ion propulsion power over the range of heliocentric distances expected. The PPU performs the power throttling for the thruster as well. Efficiency is nearly 95% at full power and is above 90% over the 1-kW to 7-kW input power range.

The NEXT PPU has been developed to the engineering model level by L3 Communications ETI, who also built the NASA SEP Technology Application Readiness (NSTAR) PPU that flew on NASA's DS-1 mission. The NEXT design maintains elements of the NSTAR PPU topology, with incorporation of a modular beam supply to improve performance over the broad throttle range. The NEXT PPU has also been developed using modern electronics packaging techniques to improve the manufacturability of the unit. Functional testing of the engineering model PPU integrated with the protoflight model thruster has been completed. The PPU will undergo qualification-level environmental testing and electromagnetic interference/electromagnetic capability (EMI/EMC) testing later in 2008.

The primary elements of the xenon propellant system are a xenon propellant tank and the NEXT high-pressure and low-pressure assemblies (HPA and LPA, respectively). The xenon tank selected is the composite overwrap tank developed for the Dawn mission, which was manufactured by Carleton Technologies, Inc. This tank has a maximum propellant capacity of 450 kg. The current xenon load for the CSSR mission, including margin, is 420 kg. While a delta-qualification may be necessary, the cost savings associated by manifesting a commercial off-the-shelf (COTS) tank with flight heritage is considerable. The primary flow control component of the HPA and LPA is a Moog Proportional Flow Control Valve (PFCV). In the HPA, parallel-redundant PFCVs are used to regulate the xenon tank pressure to a nominal 35 psia inlet pressure to the LPA. The LPA distributes and controls the xenon flow to the three inlets to each thruster (main discharge, discharge cathode, and neutralizer cathode). The flow control loop for each of the three feeds consists of a PFCV, a pressure transducer, and a thermally controlled orifice. The PFCV variable orifice is controlled through changes in input current to throttle the flow across the ranges required for thruster start and throttled operations. The NEXT HPA and LPA have been developed to the engineering model level by Aerojet General. Each assembly is tested and calibrated as an assembly. The flight-like EM HPA and LPA have successfully completed qualification-level environmental tests and are integrated into the NEXT system integration test for final functional validation. In addition to the primary elements described above, the propellant system includes latch valves and service valves as required to meet safety requirements, isolate thrusters, fill and drain the system, and purge the thruster cathode assemblies.

Each ion thruster is mounted on a dedicated gimbal to maintain thrust vector control throughout the mission. The NEXT gimbal provides over 17° angular authority at the primary axes. A high-fidelity breadboard unit was completed by Swales Aerospace under the NEXT project and serves as a baseline for flight system development. The gimbal structural concept has been validated, as this unit was integrated with the PM thruster for qualification-level vibration testing.

The digital control interface unit (DCIU) is an electronics unit dedicated to the control of the ion propulsion system PPU and propellant control assemblies. The DCIU accepts high-level commands from the spacecraft, dictating the desired ion propulsion operations. For this mission concept, the DCIU controls only the PPU and LPA within the same thruster string. The NEXT project has developed a simulator for the DCIU to support integrated system testing. A flight unit development, including flight-level software, is required as part of the spacecraft development program. The Dawn project incurred cost growth in developing the DCIU. This was attributed to the complexity of controlling multiple thruster strings within a single unit. The approach for this concept, with separate DCIUs dedicated to each thruster string, reduces the likelihood of encountering this issue.

The ion propulsion system elements must be developed and thoroughly tested prior to delivery early in the spacecraft I&T sequence. In addition, the ion propulsion system will be tested as an integrated propulsion system prior to delivery. Finally, there are a number of long-lead procurement elements within an ion propulsion system, including thruster materials, PPU EEE parts, xenon tank, and propellant system flow control components. These factors will add schedule risk to the propulsion work breakdown structure (WBS) element, resulting in possible late delivery to spacecraft I&T. The ion propulsion system will likely require long-lead authority in Phase B. Sequencing of design reviews within the overall program will be critical.

4.4.2.2 Blowdown Hydrazine Attitude Control System (ACS)

The blowdown monopropellant hydrazine system provides attitude control capability for the spacecraft. The system consists of 18 0.9-N (0.2-lbf) thrusters and components required to control the flow of propellant and monitor system health and performance. The blowdown system, shown in Fig. 4.4.2.2-1, will be procured as a complete system from a subcontractor.

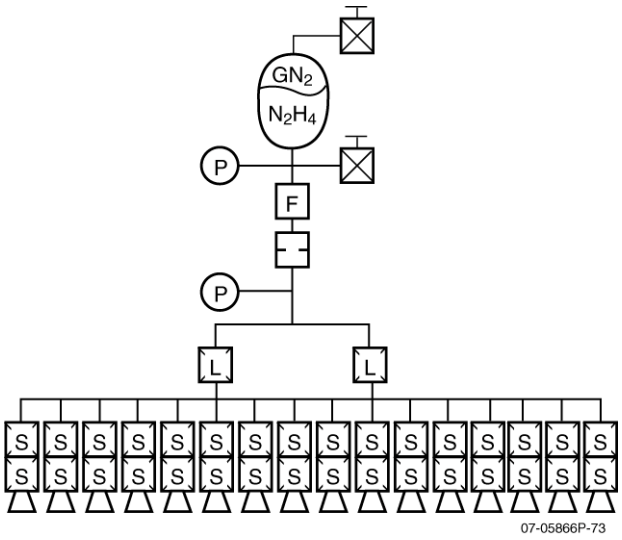

Figure 4.4.2.2-1. CSSR incorporates a simple blowdown hydrazine monoprop system for attitude control and proximity operations.

The baseline hydrazine load for CSSR is 63 kg of hydrazine, which translates to 73 m/s ΔV (including 15% margin). The selected tank can accommodate 67 kg of hydrazine. Several flight-proven options exist for each component of propulsion subsystem. A representative set of heritage components has been identified for preliminary performance evaluation and demonstrates that system requirements can be achieved. The propellant and helium pressurant, separated by a fully reversible elastomeric diaphragm, are stored in one spherical titanium tank. As the mission progresses and propellant is expelled, the tank pressure decreases. Accordingly, the steady-state thrust will decline. This thrust range will be sufficient to perform all anticipated maneuvers over the spacecraft's lifetime. The baseline thrusters are of the catalytic monopropellant hydrazine type. When the thruster valves open, propellant flows through the thruster into a catalyst bed, which has been preheated by series-redundant heaters. The hydrazine spontaneously decomposes into hot gases, which expand through a nozzle and exit the thruster, producing thrust. The thruster valve is spring-loaded such that the valve closes automatically when the solenoid is not energized. Latching valves isolate the thrusters from the tank for safety and system reliability (i.e., in case of a thruster leak), while manual service valves are used for testing and loading the system on the ground. Pressure transducers are used together with temperature telemetry to gauge propellant and monitor system performance in flight. Filters ensure propellant purity. The surge suppression orifices keep transient pressures within appropriate levels.

Blowdown monopropellant systems are well characterized and well understood and have significant flight history. However, there is schedule risk, as titanium shortages have resulted in an 18-month lead time for many propellant tanks. Thrusters require a lead time of 12 months. The primary spacecraft structure must ship to the propulsion system supplier 3 months before the start of I&T. If the structure is not ready, we will be forced to provide potentially costly tooling.

4.4.3 Communications Subsystem

The telecommunications subsystem design (Fig. 4.4.3-1) is driven by two major requirements: (1) to provide a downlink capability of 750 Mbits/day during the comet mapping phase of the mission, and (2) to provide a significant downlink capability (one image every 30 min, ~1–3 kbps) with the Earth at an arbitrary direction in the spacecraft coordinate system during comet approach and landing. In addition, the SEP mission requires communications to an arbitrary Earth pointing vector during the thrust periods traveling to and from the comet. The telecommunications subsystem should also minimize mass, power, and cost, and provide a redundant, fault-tolerant communications capability throughout all mission phases. Telecommunications operations are designed for 3-dB telemetry margin and 6-dB command margin with simultaneous command, telemetry, and ranging capability considered nominal. Modes of communications are planned by spacecraft state and mission phase to optimize operational safety and data delivery.

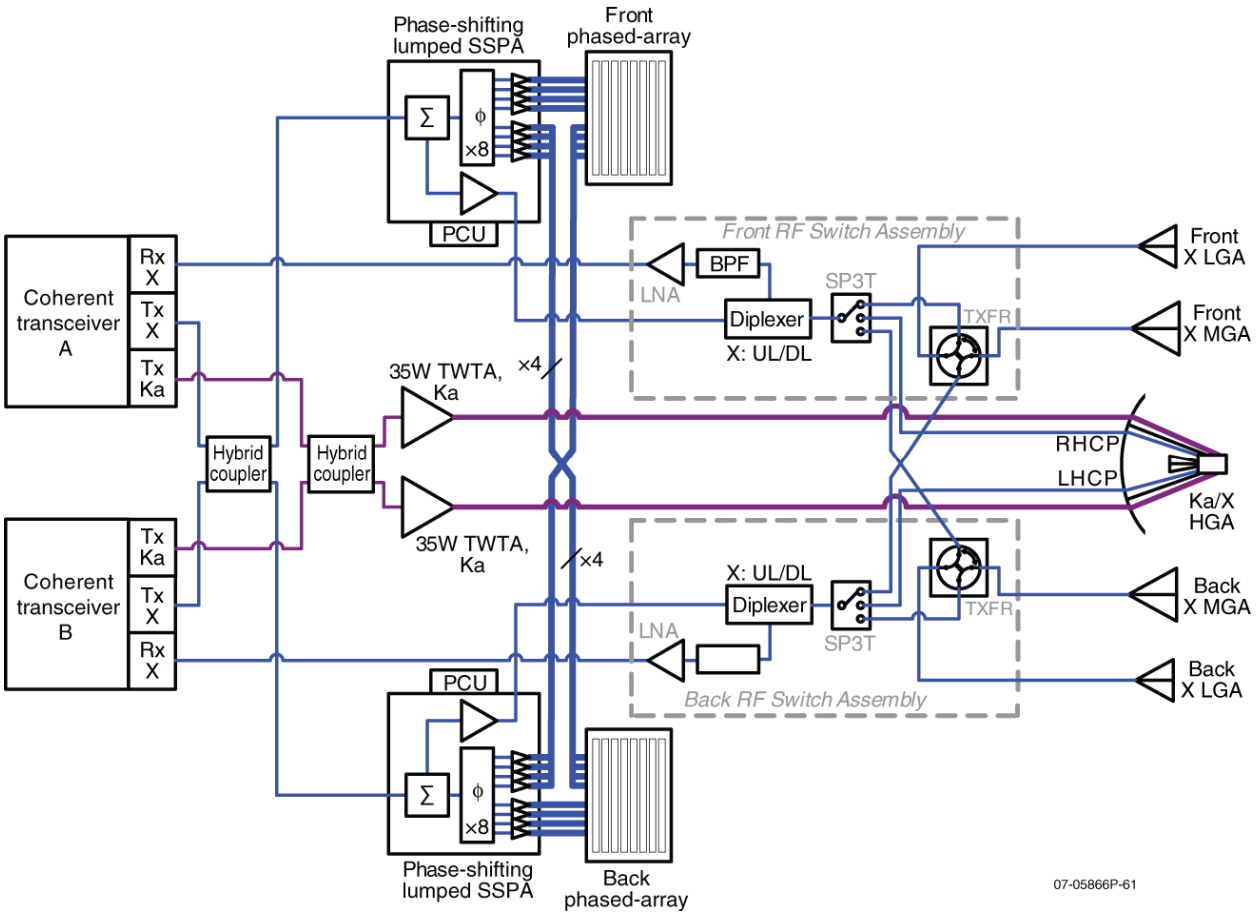

Figure 4.4.3-1. The CSSR telecommunications block diagram highlights a flexible architecture that maximizes bandwidth during all mission phases.

Mapping data delivery is accommodated through a dual-band (X/Ka) spacecraft body-mounted 1.2-m high gain antenna (HGA). The primary downlink is via Ka-band using dual-redundant traveling wave tube amplifiers (TWTAs). X-band is used for uplink, backup high gain capability, and lower gain and low-power situations (including emergency communications) via two fanbeam medium gain antennas (MGAs) and two low gain antennas (LGAs). Science collection will occur for 16 hours each day while operating at the comet, with the remaining 8 hours used for data downlink, which is enabled by the freedom to change spacecraft attitude to direct the HGA toward Earth. In addition, the HGA is fed by redundant sides of the telecommunications subsystem via opposite polarizations, allowing single antenna polarization diversity combining on the downlink for a potential increase in data rate of >2.5 dB, when additional power amplifier power is available.

During periods when the spacecraft pointing vector cannot be changed to accommodate communications, such as during comet approach and landing and during SEP thrust periods, one-dimensional electronically steered X-band phased arrays will be used in conjunction with spacecraft roll to provide significant downlink capability. A deployed and gimbaled dish was also considered for this purpose, but in order to reduce the risk and mechanical complexity of a gimbaled design, which is of particular concern during comet landing, the phased-array approach was preferred. The MESSENGER flight-proven phased arrays also exhibit graceful degradation in

performance with component failure, as opposed to an "all or nothing" gimbal mechanism. Dual-redundant and cross-strapped solid-state power amplifiers (SSPAs) implementing eight distributed phase-shifting amplifier chains are used to drive the phased arrays, with a parallel and selectable lumped amplifier chain used to drive the other X-band antennas.

Switch assemblies allow both transmit and receive capabilities through the same antenna path and for antennas on either side of the spacecraft to be routed to either of the two X/Ka-band coherent transceivers. The APL coherent transceiver is New Horizons heritage with the addition of a Ka-band exciter stage and phase-coherency between uplink and downlink frequencies. The transceiver design allows two-way coherent carrier tracking and ranging in addition to heritage noncoherent navigation. Each redundant transceiver includes an X-band digital receiver for uplink commanding and provides both a Ka-band signal for primary data downlink and an X-band signal for lower rate, lower gain communications. The cross-strapped subsystem design allows a transmit path through either of the transceivers, TWTAs, SSPAs, and antennas while maintaining a receive capability simultaneously in both transceivers via different antennas.

The Ka-band functionality is descopable, but the Ka-band HGA downlink provides ~3 times the data downlink capability of an X-band system with the same antenna size and power dissipation. Recent upgrades of the Deep Space Network (DSN) have made operational use of Ka-band available to users. Mars Reconnaissance Orbiter (MRO) recently completed a demonstration of this capability. Close attention is paid to data rate margin throughout the mission to ensure link performance accommodates the atmospheric effects of weather.

4.4.4 Power Subsystem

The power subsystem for the SEP mission is very similar to that for the ballistic mission (Section 5.4.4). They both use peak power tracking and the same photovoltaic array technology (see Section 5 for a discussion of specific technical issues). However, the solar array wings and power electronics are larger for the SEP mission. Total solar array blanket area on both solar array wings is approximately 63 m^2 for this mission. Another difference is that the solar array voltage is higher for the SEP mission. This is because power from the solar array is directly fed (via switched power services in the power system electronics [PSE]) to the SEP PPUs, which operate over a specified input voltage range of 80 V to 160 V. Feeding S/A power directly to the PPUs minimizes power processing and wiring losses and is the same architecture used on the DS-1 and Dawn spacecraft.

Because the solar array for the SEP mission has a higher voltage, additional precautions are taken to prevent electrostatic discharge (ESD) on the solar array, including minimizing potential gradients, increased separation, and protective coating/grouting where appropriate. The PSE, including the PPT modules, must accommodate the solar array input voltage, and this requires parts qualified for the higher voltage and circuit layout techniques to withstand the voltage. In addition, the solar array drive slip rings for the SEP mission are designed to withstand the higher solar array voltage.

For portions of the SEP mission, the battery helps to level the load on the solar array, as the power to the electric thrusters is typically set near the maximum that the solar array can accommodate (given the other loads and losses). As spacecraft bus loads such as heaters vary, the battery will cycle accordingly. However, the same battery size used for the ballistic mission can easily accommodate the battery electrical cycling required for the SEP mission since the driver sizing the battery is 1 hour of spacecraft support during descent/ascent operations.

4.4.5 Structural/Mechanical Subsystems

The CSSR structure design is simple and efficient. The primary load path is a 94-cm-diameter aluminum honeycomb, aluminum facesheet composite center cylinder, which interfaces with the launch vehicle using its attached separation ring. The propulsion tanks and the interface structure for the SAS and the SRV are mounted directly to the cylinder. Three bulkhead panels, spaced 90° apart, run down the length of the cylinder between top and bottom decks. Equipment is then mounted to the four panels that close out the prismatic rectangular structure. Attaching the highest mass components (tanks, SAS, and SRV) directly to the cylinder and reacting the loads from the equipment and solar arrays directly into the cylinder enables a structure that is 9% of the launch mass. The cylinder is 193 cm tall, and the structure box is 140 cm tall, 143 cm wide, and 158 cm deep. The honeycomb cylinder is a common element among domestic geosynchronous communication satellites, and the box structure is very similar to the flight-proven STEREO structure. Figure 4.4.5-1 shows the spacecraft layout with dimensions.

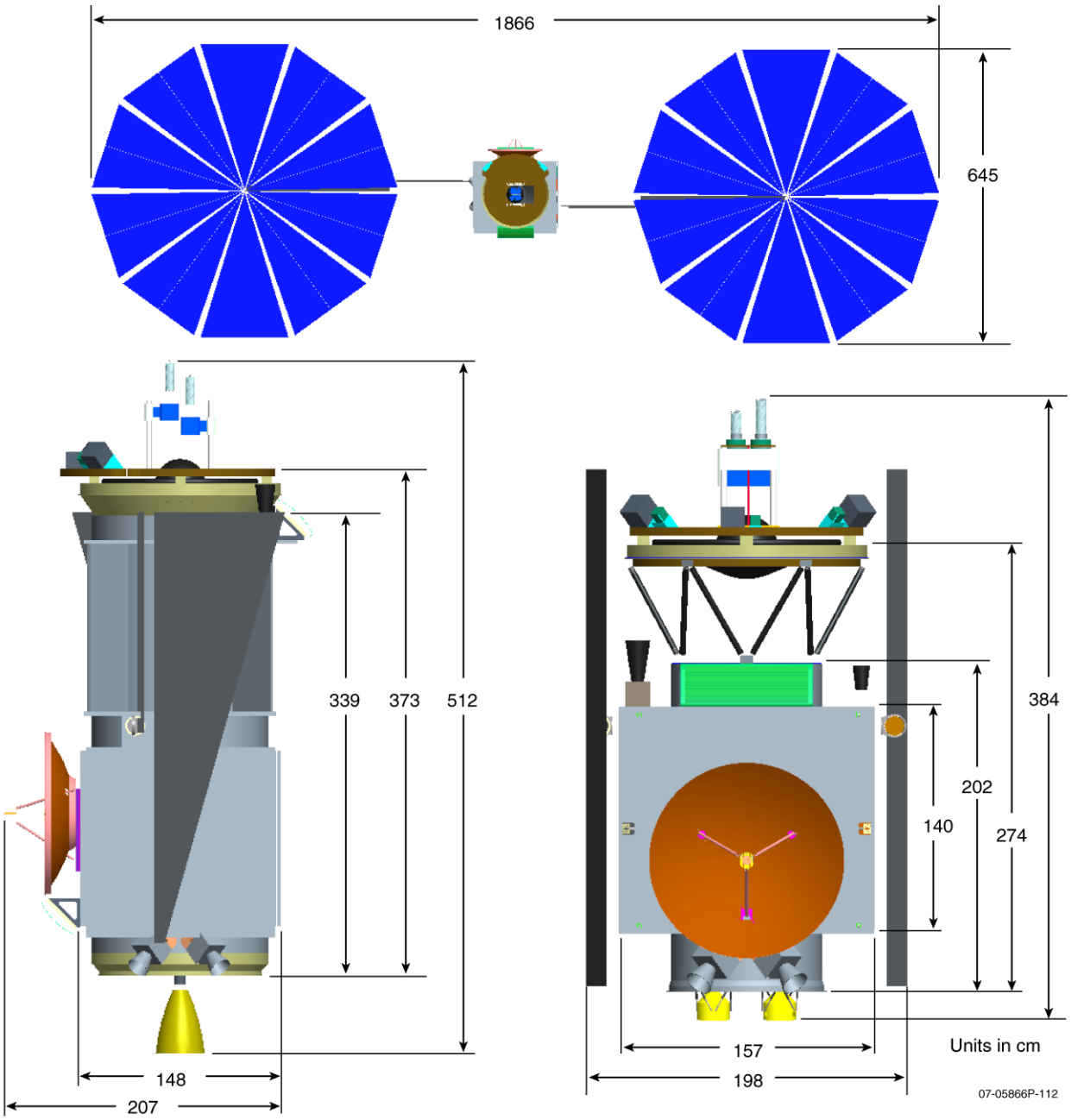

Figure 4.4.5-1. The CSSR spacecraft bus layout with dimensions (chemical propulsion on the left and electric propulsion on the right).

The only mechanisms on the bus are associated with the solar arrays. The solar array selected for the CSSR mission consists of two ATK-built UltraFlex wings, very similar to the wing in development for the CEV mission. Each of the solar array wings is pointed by a two-axis gimbal. The two-axis gimbals allow efficient energy collection and off-pointing the arrays, which minimizes loads on the array during sampling operations and minimizes sampling-induced contamination on the arrays. During launch, the lower array tie-downs mount through the equipment panels into the bulkheads, which react load to the center cylinder. The upper array tie-downs mount to brackets attached to the payload support structure, which reacts loads back into the

center cylinder. CSSR takes advantage of the CEV wing development. The CEV array size is similar, and the load requirements (3 g, each axis when deployed) envelop those for CSSR during sampling (0.15 g at spacecraft center of gravity [CG]). The UltraFlex wings boast reduced mass (~50% of conventional arrays). They lower spacecraft inertia because of their circular shape, which puts the CG of the wings closer to the spacecraft. The industry-best mass per power contributes significantly to spacecraft mass reduction on this deep space mission. The lower mass and inertias contribute significantly to the stability of the spacecraft during proximity operations because they minimize CG shifts when off-pointed.

During launch, the SAS and SRV are protected from contamination by a shroud, which is separated by pyrotechnic actuators and separation springs. The panel that accommodates the SAS and the panel that restrains the SRV are attached to a rigid spacer, which is mechanically isolated from the spacecraft using shock mounts. The rigid spacer ensures co-alignment between the SAS and SRV during sampling and sample stowage operations. The shock mounts limit the loads into the SAS and acceleration seen by spacecraft appendages. Following sampling operations, the panel that accommodates the SAS and the height and motion sensing equipment is jettisoned from the spacecraft by pyrotechnic actuators and separation springs. Prior to reentry operations, the spacecraft is spun to 2 rpm, and the SRV is jettisoned from the spacecraft by pyrotechnic actuators and separation springs. The pyrotechnic actuators, incorporated into hold-down and release mechanisms, have heritage from many APL spacecraft (e.g., TIMED, MESSENGER, STEREO).

4.4.6 Thermal Control Subsystem

The CSSR SEP thermal control subsystem provides a low-risk design approach using passive thermal control, including heat pipes, louvers, and MLI. Waste heat from most bus electronics will be distributed throughout the MLI-covered structure and louvers will be placed on the bus radiators, reducing the need for heater power. Bus electronics are directly coupled to the structure, and heat dissipated by the electronics is spread throughout the structure by conduction and thermal radiation.

The propulsion components are isolated from the bus and controlled with heaters. High-power bus electronics like the SSPAs and TWTAs will be placed on a heat pipe radiator panel in order to reduce the required radiator area and heater power. The PPUs are extremely high power and will be controlled separately. There is one operating PPU and one spare. They will be attached to a separate radiator panel with a heat pipe network to spread the heat evenly, no matter which unit is operating. The outside of the heat pipe panel will have louvers that will reduce the required heater power when the SEP engines are off or in standby. Fig. 4.4.6-1 shows the block diagram of the thermal control system. The bus consists of nine thermal zones that are independently controlled. The temperature of each zone is shown in Fig. 4.4.6-2.

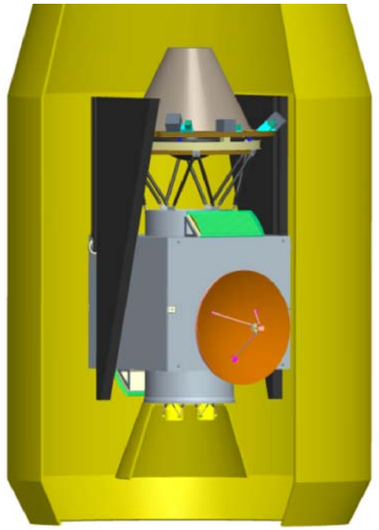

A. The spacecraft can be stowed in the smallest Atlas V 5M fairing.

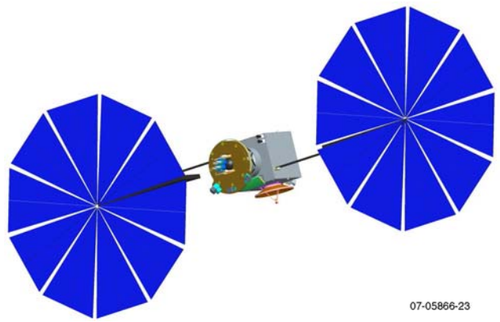

B. Two-axis gimbals allow complete freedom in pointing the UltraFlex arrays.

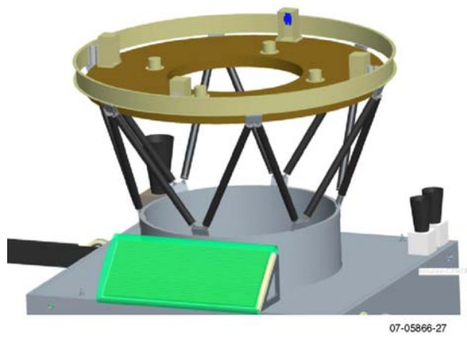

F. The SRV deploys with a simple pyrotechnic actuator and separation spring system.

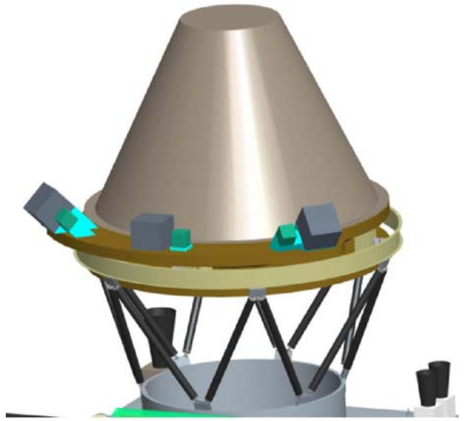

C. The deployable shroud protects the sampling mechanism and the sample return vehicle's sample magazine from contamination during launch and initial cruise phase.

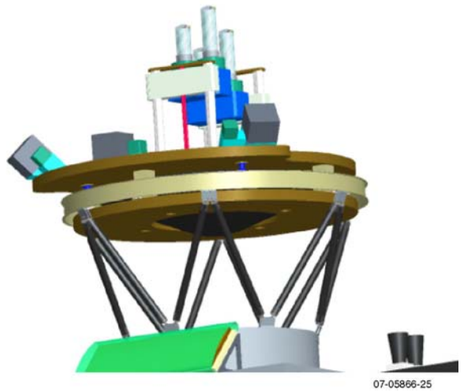

D. The sampling mechanism, shown in pre-sampling configuration, is thermally isolated from the bus. Its placement protects the bus from contamination during sampling operations.

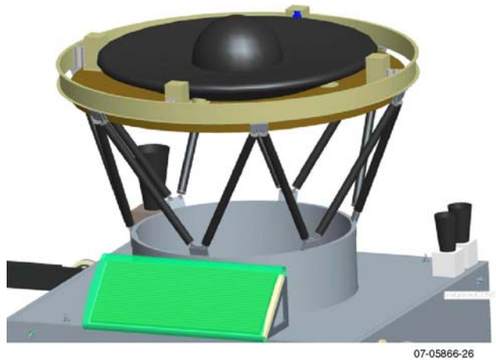

E. The sampler support panel separates from the spacecraft, reducing mass for the cruise back to Earth. Jettisoning the panel allows a near-complete field of view to cold space for the SRV, preserving the sample.

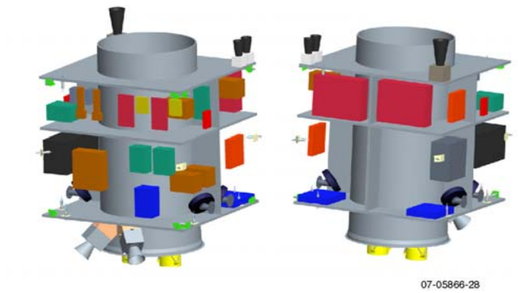

G. The star trackers' locations minimize contamination from sampling operations. The RF equipment has its own dedicated panel, as does the SEP propulsion system electronics, streamlining integration and test.

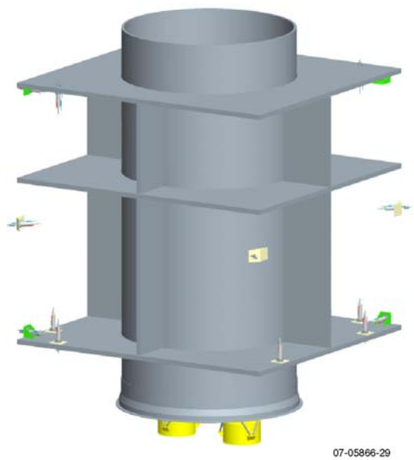

H. Direct load paths enable a 9% primary structure mass.

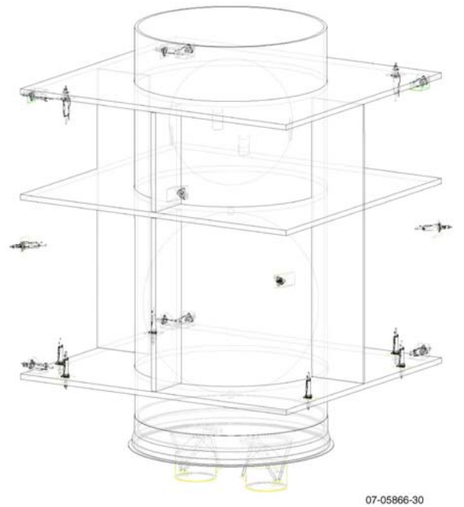

I. The propulsion system is highly integrated with the structure for mass efficiency. Tanks have a direct load path through the cylinder into the separation ring.

Foldout 4-3. SEP spacecraft layout.

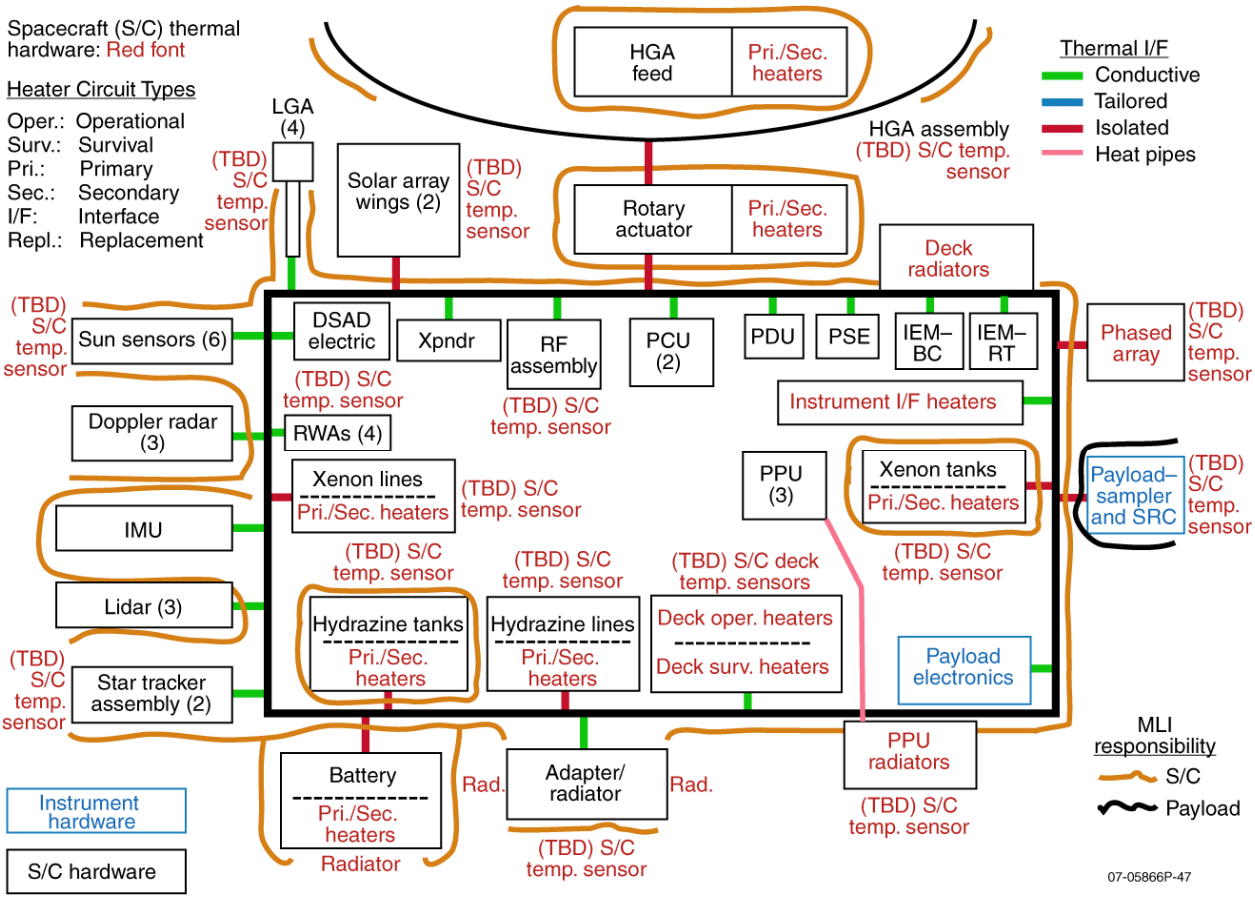

Figure 4.4.6-1. The thermal system uses waste heat to minimize heater power.

Component	Temperature limit (°C)
Spacecraft Electronics	–20 to +40
HGA/Phased Array	–90 to +90
Solar Arrays	–125 to +100
Instrument Interface	–20 to +40
Star Trackers	–20 to +60
Battery	+5 to +30
Propulsion Tanks	+10 to +50
SEP Propulsion Tanks	+25 to +35
PPUs	–20 to +50

07-05866P-48

Figure 4.4.6-2. The system is divided into thermal zones to group components with similar temperature requirements and to optimize heater performance.

The bus is required to survive in cruise mode from 1 AU to 5.5 AU. The 5.5 AU case is the cold case. The bus and SAS are required to operate at approximately 2 AU. This is the peak power condition and, therefore, the hot case for the bus; the hot case for the PPUs will be during

SEP engine firing with maximum thrust. The hot case drives the required radiator area of the bus to be 1.3 m^2, and the PPU radiator is an additional 2.0 m^2 for a total of 3.3 m^2. This radiator area and the minimum bus power lead to a required bus heater power of 200 W. This includes 115 W of propulsion heaters, 25 W of payload heaters, 40 W of battery heaters, and 20 W of star tracker heaters. No power is required for the bus heaters because of the louvers. In addition to the required bus heater power, an additional 92 W is needed for the PPU radiator when the PPUs are in nominal operation and 30 W is needed during standby operation. The PPU radiator area is sized for maximum power operation and the louvers only close during standby operation, which leads to the greater need for heater power in the nominal operation case.

The thermal control of the SAS and SRV is passive. The SRV is thermally isolated from the bus and the SAS is thermally isolated from the SRV. The contamination shroud surrounding the SAS will be deployed 2 days before sampling, which will allow the SAS and sample canisters to cool down. This allows sampling at the surface at −10°C or colder and maintains the samples inside the SRV below −10°C until reentry. During and after reentry, wax packs inside the payload volume of the SRV keep the samples below −10°C for 2 hours after landing in the given capsule environment.

A science goal was to preserve the sample at all times $\leq$−135°C. In order to reach the goal temperature of −135°C for the comet sample temperature, active cooling was considered. If the sample size is reduced to 10 cc, the best-case heat load during the mission will be 0.3 W, and during reentry it will be 0.6 W. For the worst case, the numbers jump to 1.4 W for the mission and 2.8 W during reentry. In order to provide this cooling, several options were considered including thermal electric coolers (TECs) and cryocoolers. In the worst case listed above a single cryocooler is not capable of providing all the cooling and, therefore, two would have to be installed. This would use the available space inside the capsule. A problem with either of these solutions is that they both need to reject heat. This is very difficult to accommodate in the current sampler and SRV design because everything needs to stay cool to reduce the parasitics on the sample. Also, it is difficult to get these cooling systems the power they need for the cooling, especially during reentry, when the SRV is powered by batteries only. The other problem with both solutions is that the sample is required to be kept below the goal temperature for 2 hours after reentry and landing. This would mean that either solution would have to be capable of surviving a 1500-*g* landing and still operate. Therefore, the −10°C requirement was focused on a best effort for keeping the sample cold during the various mission phases.

4.4.7 Avionics Subsystem

The avionics subsystem hardware provides C&DH, mass data storage, and intra-spacecraft communications and power interfaces. The key components are the integrated electronics module (IEM), power distribution unit (PDU), and remote input/output units (RIOs). The avionics subsystem is block redundant with two IEM units; a single, internally redundant PDU; and two separate RIO chains. A hardware fault protection module (FPM) is implemented in the redundant IEM to autonomously monitor main processor health and initiate a side changeover if a problem is detected.

The spacecraft will feature a SpaceWire (ESA ECSS-E50-12A compliant) communications network. A multi-point ring topology will be used to provide full cross-strapping capabilities between the avionics and spacecraft components. SpaceWire maturity and applicability for the CSSR spacecraft architecture will be evaluated during Phase A with a MIL-STD1553B bus remaining a viable alternative.

The CSSR IEM combines C&DH, mass data storage, and G&C interfaces into a single chassis. The IEM concept has been employed on all APL missions starting with TIMED and carried through RBSP. The IEM is MESSENGER-based featuring a four-card design. MESSENGER featured dual BAE RAD6000 single board computers (SBCs), which are replaced for CSSR by a single RAD750-class SBC, increasing performance and mitigating concerns over future RAD6000 component availability. A single interface card will provide data interfaces to non-SpaceWire G&C and H&MS components such as reaction wheels, Sun sensors, lidar, and radar. The solar array drive electronics and RIO chain will also interface to this card. This represents a consolidation of mission-specific interfaces within the IEM to reduce the customization of the PDU. Circuit-level heritage for the G&C interfaces is preserved with a common subsystem design team approach. The CSSR IEM will also have a 16-Gbit SSR and a custom DC-DC converter design (improving overall efficiency). The IEM will use SpaceWire for its internal communications bus. A 32-bit, 33-MHz PCI bus will be used as a SpaceWire replacement pending the outcome of a Phase A SpaceWire trade study.

The RIO units will handle various analog and discrete inputs to the avionics subsystem and are string redundant. The temperature remote input/output (TRIO) units will condition and digitize thermal subsystem temperature sensors, and voltage remote input/output (VRIO) units will sense the sample pressures as well as propulsion subsystem components (pressure transducer and latch valve position telltales), deployment indicators, and other miscellaneous telemetry points. The RIOs communicate on a daisy-chained bus with the IEM interface card.

The PDU provides switched, unswitched, and pulsed power to the spacecraft components. The PDU receives primary power from the PSE. The PDU box is a modular slice design. Each slice consists of a printed circuit board housed in a mechanical frame. The slices are electrically connected using internal stacking connectors for signals. A wiring harness external to the box is used for power connections. It is planned that the PDU will use identical slices being designed for the Living With a Star (LWS) RBSP mission with modifications to accommodate the SpaceWire bus. The PDU design contains a number of heritage circuits from the PDUs flown on the STEREO and MESSENGER spacecraft. Compared with those missions, the PDU mechanical design is simplified for improved manufacturability and is constructed similar to the New Horizons LORRI ASE assembly and other instrument avionics boxes that have flown.

The PDU includes power metal-oxide semiconductor field effect transistor (MOSFET) switches for the load power services. For hazardous functions, such as thrusters, deployment actuators, and RF transmitters, electromechanical relays are used to “arm” the safety-critical power busses. Additional power MOSFETs are used in series to provide a sufficient quantity of inhibits to meet the range safety requirements. Majority voting of separation signals is used to control one of the inhibits. Mechanical safe/arm plugs are employed during I&T. Individual load current monitors are provided for each switched and unswitched power service. These DC current monitors are galvanically isolated from the power circuits. Bus voltage and total load current are provided in telemetry and also to the spacecraft umbilical interface. Switched power services include a circuit breaker function implemented in the switch control circuit that makes use of the previously mentioned current monitors and power MOSFET switches. The circuit breakers have individual command-programmable current thresholds and trip times. Also, the circuit breakers can be individually disabled. To protect the main power bus, each load power service also has an upstream fuse. These fuses are type FM12A, which are of solid-body construction and have no cavity. These high-reliability fuses have significant spaceflight heritage and are rugged with respect to mechanical vibration and shock. The fuses are located on fuse boards, which plug di-

rectly into the PDU power switching slices. The fuse boards are enclosed by a single housing that is mechanically secured to the main PDU box. A fuse board can be removed and replaced after removing the fuse housing without having to disassemble the remainder of the PDU and without having to re-qualify the unit. Non-flight fuse boards are used during initial I&T. The non-flight fuse values are "un-derated," i.e., they have lower current ratings than the flight fuses. The flight fuses are installed prior to spacecraft environmental testing. The PDU includes low voltage sensing and autonomous load shedding. The PDU also features a power-on-reset circuit with an autonomous initialization sequence to ensure that loads are in an appropriate pre-defined power state following bus voltage recovery in the unlikely event of a bus undervoltage. To meet the EMC requirements, power and return paths are routed close together throughout the power electronics and are located on the same connectors. This also facilitates twisting of wire pairs in the spacecraft harness. To minimize EMI, bus filtering capacitance is provided within the PDU, and this supplements the filtering provided by the PSE.

4.4.8 Flight Software

The flight software is defined as the software that executes on the single spacecraft on-board computer, a RAD750-class processor. Instrument software is assumed to be embedded in payload components, is developed by the instrument science team for the selected instruments, and is not described in this section. The overall flight software architecture is based on Core Flight Executive (cFE) middleware and heritage software from the RBSP, MESSENGER, and New Horizons missions. An incremental build model is used to meet the varying I&T and operations needs in a timely fashion over the developmental life of the mission.

The flight software consists of four main elements: Boot, cFE, C&DH, and GN&C software. Boot is responsible for initializing the minimum set of hardware required to start the cFE and the C&DH and GN&C applications. cFE is a middleware layer that provides a level of abstraction over the processor hardware and a multi-tasking real-time operating system. cFE provides software messaging using Consultative Committee for Space Data Systems (CCSDS), table services, time services, file services, event and error reporting services, memory management, and various other operating system-level services. In the cFE architecture, C&DH and GN&C run as independent applications that communicate using the cFE.

Features of the C&DH software include real-time command processing and the ability to execute stored command sequences; autonomous control and fault protection and time management and distribution; management of the uplink and downlink; distribution of commands to instruments and collection of telemetry from instruments; management of the SSR; and support for managing memory objects and uploads of new code applications. The software manages the Flash-based SSR using a file system with science and engineering data stored on the SSR in file format. Uploads are managed in the form of files as well. File-based recording enables the flight software to make use of CFDP (Consultative Committee for Space Data Systems File Delivery Protocol) for transmitting data to Earth. This protocol optimizes downlink bandwidth by allowing retransmission of any file fragments previously lost to dropouts, without unnecessarily retransmitting an entire file. Both the onboard file system and CFDP capabilities are drawn from MESSENGER flight heritage.

C&DH provides autonomous control and fault protection for the spacecraft. This software is based on the MESSENGER, STEREO, and New Horizons autonomy engine. Autonomy rules will monitor the state of the spacecraft and trigger command macros to execute if an unsafe state is detected. The command macros will attempt to remedy the problem or will put the spacecraft in a Safe-Hold Mode described in Section 4.4.10. Simple problems, such as an over-current or

over-voltage condition for an instrument, or an automatic switchover to a redundant backup unit, can be made without transitioning to Safe-Hold. Other more complex failures, such as exceeding the pre-defined Sun angle during a maneuver, will require transitioning to this mode.

The GN&C software implements the spacecraft guidance, navigation, and control functions described in Section 4.4.9. Attitude control and attitude estimation algorithms are developed as Matlab models, which are used with automated code generation tools to produce C code that is integrated into the flight software application. The C&DH software is developed using the C language and is human-generated. Data-handling functions in the C&DH software encapsulate the autocoded GN&C algorithms and manage sensor and actuator inputs and outputs to and from those control algorithms.

4.4.9 Guidance, Navigation, and Control Subsystem

The GN&C subsystem contains sufficient functionality for mission success to support the following operating regimes:

1. Post-separation despin, solar array deployment, and Sun acquisition
2. Earth acquisition and stable platform for communications
3. Transfer orbit maneuvering including use of chemical and ion propulsion
4. Momentum control for minimization of propellant use during cruise
5. Comet rendezvous and proximity operations
6. Survey properties of comet, including surface mapping, gravitational field, dust effects on trajectory, comet spin axis and rate
7. Practice approach and takeoffs
8. Actual landing and takeoff from surface of comet
9. Departure from comet and transfer orbit maneuvering back toward Earth
10. Pointing and trajectory control for precise release of SRV

To operate in these varied regimes, the GN&C will require the following components and capabilities (see Fig. 4.4.9-1 for a subsystem block diagram):

Sensors

1. Inertial Measurement Unit (2) including accelerometers and gyros
2. Star tracker(s)
3. Sun sensors
4. Wide Angle Camera
5. Lidars
6. Doppler radars

Actuators

1. Fully coupled attitude control thrusters
2. Full thruster control in six independent directions
3. Quad Reaction Wheel Assembly
4. NEXT ion propulsion or chemical propulsion for trajectory correction maneuver (TCM)

Algorithms

1. Inertial attitude determination
2. Momentum management
3. Inertial and ephemeris based pointing
4. Terrain Relative Navigation with passive optics and lidar
5. Latitude/longitude/altitude pointing and trajectory targeting
6. Single and multi-axis thrust vector control

7. Position and velocity following trajectory guidance
8. Safe mode with emergency comet vicinity departure and sun pointing

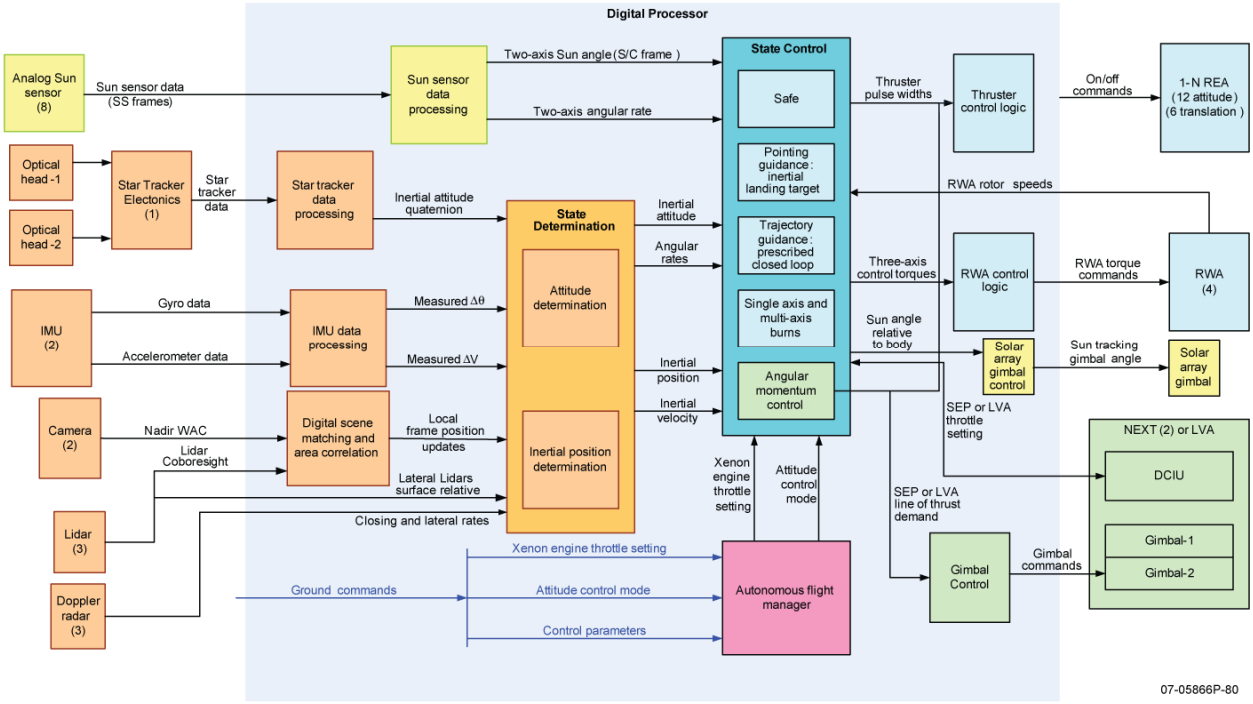

Figure 4.4.9-1. The GN&C subsystem uses simplified interfaces to effectively manage layers of information to ensure safe operation.

The GN&C subsystem is responsible for controlling the spacecraft upon separation from the launch vehicle upper stage, initially detumbling the spacecraft down to a three-axis controlled attitude and rate, slewing to a Sun orientation, and maintaining a Sun-pointing attitude as the solar arrays are deployed.

A handoff from thruster-based attitude control to reaction wheel control will allow conservation of propellant for the cruise phase of the mission. During cruise phase, the NEXT thrusters, mounted on gimbals, will steer the thrust vector inertially and maintain spacecraft momentum by steering torque vectors to counter any center-of-mass offsets. Based on legacy G&C subsystems, MESSENGER, New Horizons, and STEREO, the spacecraft will be navigated to the comet through ground-computed solutions of position and velocity.

The GN&C subsystem contains the H&MS for all functions related to proximal activities to the comet. All primary sensors and actuators used by GN&C are also used here, in addition to sensors used only during this phase of the mission. The WFV along with lidars (three total) and Doppler radars (three) are needed to assist with navigation down to the surface. The principal functions that shall be executed include navigating to approximately 100 km from the comet, mapping the comet's surface, and descending down to a Home State orbit of 1–5 km. Several landing attempts, including at least one practice run and a couple of repeat landings, shall be facilitated by the GN&C subsystem in order to collect the comet sample and ascend back to the Home State. Specific details of the landing sequence and comet operations are provided with the concept of operations in Section 4.5.3, including contingency handling and descent profiles.

4.4.10 Fault Protection

The CSSR fault protection process includes fault analysis, requirements development, requirements allocation to hardware, software, autonomy, or operations, and a rigorous spacecraft-level test program. Fault analysis involves the performance of failure mode effects analysis/fault tree analysis (FMEA/FTA), spacecraft modes development, and critical sequence analysis. Critical sequence analysis is a use case-based approach to identifying time-critical or Level 1 science-critical portions of a mission and determining how the spacecraft will accomplish these sequences even through faults. For CSSR, the critical sequences will be the cometary approach, descent and landing operations, sample acquisition, ascent operations, SRV separation, and descent through the Earth atmosphere. Each of these sequences will be analyzed in Phase A/B so that fault protection can be incorporated into the architecture design early. This process has already begun, as these critical sequences have yielded fault protection architecture features such as the fault protection monitor device. Born out of the time-critical nature of many of the critical sequences, the watcher is a hardware-only device that determines which processor is in control based on a select set of discrete signals. The fault protection monitor provides a simple and fast-acting solution that allows a hot-hot processor redundancy operation for critical sequences and a hot-cold operation for cruise periods.

Specific analysis was performed to determine the frequency and duration of ground contacts to effectively monitor the spacecraft during the use of the NEXT ion thruster. NASA typically requires continuous spacecraft monitoring during propulsive activity. Since this is not economically or technically feasible for the CSSR mission, the impact of anomalous events on active thrusting periods will be reduced with a robust concept of operations and fault protection strategy. Specific details are provided in the cruise portion of the concept of operations, Section 4.5.2.

The fault protection process will continue into requirements and requirements allocation as spacecraft functions fleshed out during fault analysis can be formally defined and then allocated into appropriate subsystems. The allocation process is a trade-off based on reliability versus flexibility. A fault protection function implemented in hardware will be inherently more reliable than one implemented in autonomy because of the nature of hardware and the fact that hardware will receive more testing over the life of the I&T program. However, the hardware, once implemented, is fixed, while autonomy can be manipulated up to and after launch. For the SEP mission, faults related to the main processor's safe operation of the NEXT system and the NEXT subsystem components will not result in a shutdown of the electric propulsion system. This fault protection strategy will increase the reliability of the spacecraft to achieve high thruster duty cycles. In addition, using a hardware command loss time, low-voltage battery sensors, and a hardware fault protection monitor will increase the reliability of CSSR's lowest level of safing.

Finally, the fault protection program will be completed with a rigorous test program. The test program will include multiple scenario-based tests similar to mission simulations conducted by the operations team except that, for each scenario, one or more faults will be injected. This testing is black-box and requirements-based so that the spacecraft performance in the presence of faults can be formally validated.

4.4.11 Assembly, Test, and Launch Operations

Assembly, Test, and Launch Operations (ATLO) are conducted in four phases: (1) spacecraft bus, SRV, and SAS individual I&T programs at the respective development institutions, (2) individual environmental test programs, (3) system I&T, and (4) field operations at Kennedy Space

Center/Cape Canaveral Air Force Station, culminating in the launch. Each phase is discussed below.

4.4.11.1 Integration and Testing

Space system I&T has the following objectives:

- Verify system-level performance
- Identify unexpected interactions among subsystem elements
- Identify failure modes from design weakness, material defects, and workmanship
- Operate components long enough to identify failures due to "infant mortality"
- Establish standard operating and contingency procedures for mission operations
- Verify spacecraft will operate properly through launch and in on-orbit environments

APL follows a methodical, hierarchical I&T approach design to verify requirements and uncover potential problems early, reducing risk during both system-level integration and flight operations. This I&T approach has been heritage on numerous planetary spacecraft. Testing starts at the breadboard level where all designs undergo interface compatibility testing prior to release for flight fabrication. This practice minimizes the number of interface problems encountered during system-level integration. Piece parts, components, and boards are environmentally tested at stress levels higher than those the system will encounter in test or operation. Imposing more stressful test levels at lower integration levels is a proven technique to find problems early and minimize problems at system-level integration. This I&T approach was successful on other APL spacecraft programs, including NEAR, TIMED, MESSENGER, STEREO, and New Horizons.

A proto-flight approach (qualification levels for flight duration) will be followed for CSSR spacecraft. Instrument and spacecraft components will be fully tested, both functionally and environmentally, before delivery for system integration. All components will be vibrated in three-axis at proto-flight levels. The design levels used will envelop all EELV environments. Results from the structure qualification testing will be used to correlate the coupled-loads analysis finite element model prior to integration.

The CSSR spacecraft is composed of three separate assemblies: the spacecraft, the SRV, and the SAS. Each assembly shall go through similar but separate I&T. These I&T efforts will be performed in parallel and, where appropriate, mass simulators will be incorporated in the absence of flight structures. Following completion of environmental testing, the assemblies will be transported to the launch site and finally assembled and system tested together.

The study assumes the spacecraft will be integrated in the APL Kershner Space Building. This spacecraft I&T facility maintains Class 100,000, 10,000, and 100 clean rooms. The spacecraft's payload suite is composed of an SRV and the SAS. Contamination control requirements shall be driven by the needs of the payload to protect against cross contamination of the comet sample. The spacecraft and payload suite shall be integrated in a Class 7 (10,000) clean-room environment with a surface cleanliness level of 500 A/2 in accordance with IEST-STD-CC1246D. The contacting surfaces of the drills and the interior sample container walls shall have a cleanliness level of 300 A/2. All housing facilities shall maintain the integrity of contamination control requirements of Class 7 from initial I&T through launch.

The Kershner building also houses a vibration test facility and thermal vacuum chambers in a variety of sizes. When possible, subsystem and instrument mechanical models, data simulators, and engineering models will be integrated early with spacecraft structural or electrical components to provide early mechanical and electrical interface verification. Integration of the spacecraft begins with the delivery of the flight-qualified primary structure, which already includes the

propulsion system. The spacecraft harness is installed and rung out to ensure that flight hardware can be integrated safely.

Pre-Integration Reviews are held for each spacecraft component and instrument. The integration team will review the results of the component or instrument testing program and present plans for mechanical and electrical integration with the spacecraft. During the integration program several special tests are conducted. These include RF compatibility, time system verification, special guidance and control, system self-compatibility, and jitter tests, as appropriate. Following integration of all of the spacecraft subsystems and instruments, the baseline comprehensive performance test (CPT) will be performed measuring all key performance parameters. The CPT follows APL's proven "test as you fly" approach with all command execution and telemetry evaluation performed at the Mission Operations Center (MOC). System-level test equipment provides power and stimulates all sensors throughout the I&T flow (Fig. 4.4.11.1-1).

The testbed provides a simulation environment for IEM hardware checkout, flight software development, flight software acceptance testing, autonomy testing and development, GN&C subsystem development and device checkout, spacecraft integration, and Mission Operations training and simulation. Following on MESSENGER, STEREO, New Horizons, and RBSP legacy, the testbed will be developed using the common TestBed ToolKit (TBTK).

The testbed simulates all spacecraft components connected to the IEM. This includes the transponders, the RF transfer switch, the uplink and downlink interface, the PDU and PSE, the star tracker/scanner, the height and motion sensors, the Sun sensors, the thruster and propulsion system interfaces, the TRIO temperature and VRIO voltage sensors, and the instrument interfaces. The testbed will include a truth model to simulate the environmental effects from solar pressure, gravity gradient torque and atmospheric drag, and structural vibrations, including boom vibrations and fuel tank slosh, required to verify the G&C subsystem.

4.4.11.2 Environmental Testing

The environmental test program exercises the spacecraft in the launch in-orbit environments. After a Pre-Environmental Review, the spacecraft vibration test will be performed with the shock/separation tests in the APL vibration test laboratory. The spacecraft will be in launch configuration for these tests. The spacecraft and necessary ground support equipment will then be shipped via air-ride van to the Goddard Space Flight Center (GSFC) acoustic test facility for the spacecraft acoustic test. Next are mass properties measurements (performed with the spacecraft tanks filled with stimulant). Finally, the thermal balance test and thermal vacuum cycling tests are conducted. During the thermal cycling tests, the DSN Compatibility Test Trailers are used for RF compatibility tests and mission operations end-to-end simulations. CPTs are run prior to the thermal vacuum tests, during the thermal cycling test, and after the thermal cycling test. In addition, deployment tests and mechanical alignments are completed before and verified after completion of the environmental program. Electromagnetic compatibility testing is performed to verify vehicle-to-vehicle and vehicle-to-launch vehicle compatibility.

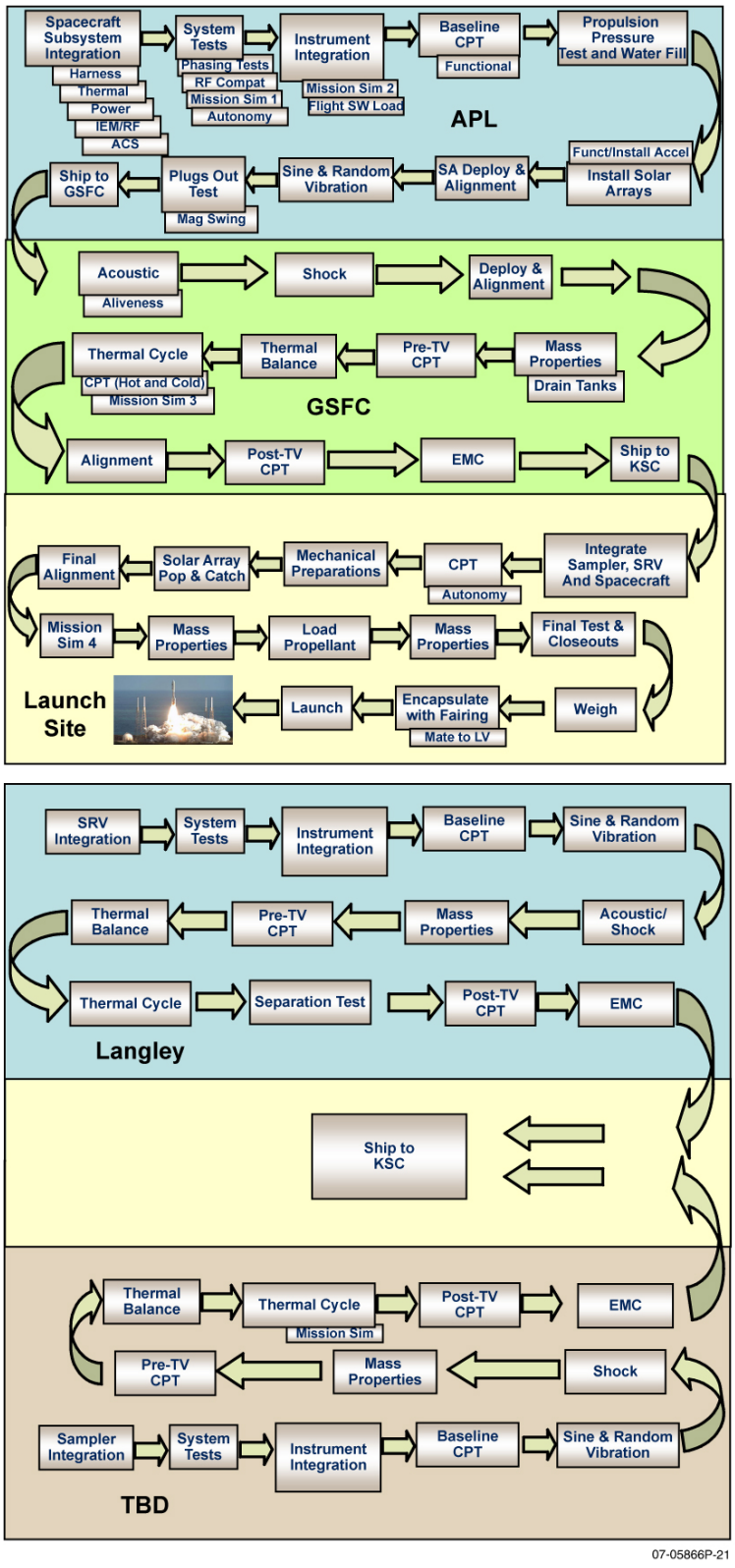

Figure 4.4.11.1-1. The CSSR I&T flow is based on past successful performance.

4.4.11.3 System Testing

The minimum set of system-level test events required for CSSR launch readiness is shown in Fig. 4.4.11.3-1. Although Phase D testing is more comprehensive at the subsystem level, these system tests are considered "incompressible," meaning that each is repeated until a fully successful result is achieved. The incompressible tests are designed to exercise all spacecraft systems, including full flight software and autonomy in the loop. Incompressible tests are also designed to fully exercise the operations team and the ground system, including the planning and sequencing system, MOC workstations and architecture, load-dump-compare tools, and near-real-time assessment tools. The DSN is typically not included since other forms of comprehensive testing with the DSN take place. Successful execution demonstrates spacecraft readiness, as well as the operations team's level of preparedness. Incompressible tests are executed with the final launch version of flight software and the autonomy suite, and a test would be repeated if there are any late changes to either of these. Only the latest configuration-controlled versions of the operational policies, processes, and scripts are used for these tests.

Mission Simulations and Fault Protection Scenarios
Launch plus first-day operations
Maneuvers
Maneuver abort
Safe mode demotion and recovery
Low state of charge safing and recovery
Autonomy tests
Comet orbit insertion
Orbit operation day
Comet descent operations
Comet landed operations
Comet liftoff operations
Spacecraft and SRV separation operations

Figure 4.4.11.3-1. The CSSR incompressible test suite demonstrates launch readiness.

The incompressible test list includes validation of the most critical aspects of the fault protection subsystem and its autonomous responses, especially those that result in major spacecraft reconfigurations, or fallback "safe" states. These demonstrate the system's ability to successfully maintain spacecraft health and safety through any single-fault scenario without immediate ground intervention. These tests also provide an opportunity for the operations team to validate and make launch-ready the required recovery procedures and documentation.

4.4.11.4 Field Operations

Following the Pre-Ship Review, the spacecraft, SRV, SAS, and ground support equipment will be shipped to the KSC launch processing facility. Initial electrical tests for the three assemblies will be performed. Following the electrical tests, the SRV and SAS will be assembled into the flight-configured suite and attached to the top of the spacecraft. A final CPT will be conducted. The operations team will be provided time for mission simulations and DSN testing that will use Mil-71 at KSC. Next, the final mechanical build will be initiated, including ordnance installation, flight blanket installation, and final spin balance. Once the spacecraft is moved to the launch pad and mounted on the launch vehicle, final preparations will be conducted. These include electrical system functional testing and launch rehearsals. The final steps prior to launch will be the launch readiness review and red tag item removals.

4.5 Concept of Operations

The CSSR mission's concept of operations is divided into several distinct operational phases as shown in Fig. 4.5-1.

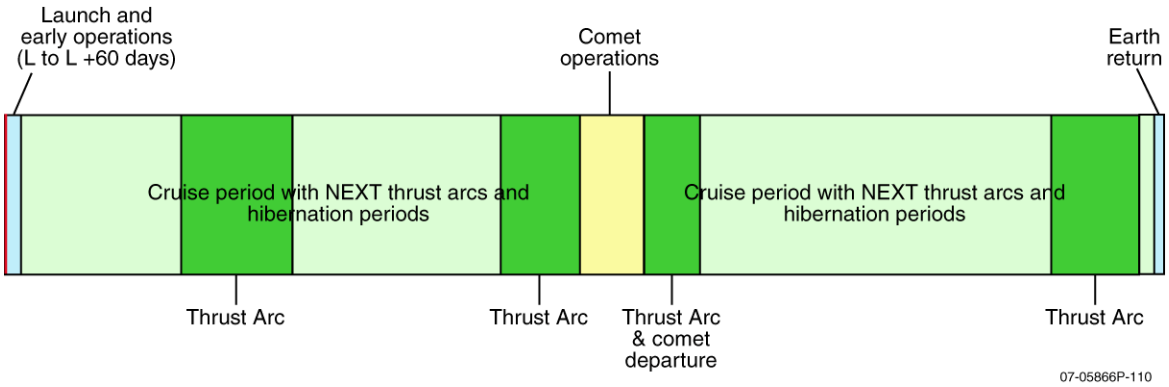

Figure 4.5-1. The SEP CSSR post-launch operations period contains several distinct phases of activity.

4.5.1 Launch and Early Operations

The mission starts with a 60-day early operations period initiated with launch on an Atlas 521 in 2015 or an Atlas 531 for the 2016 launch window. Following upper stage separation, the GN&C subsystem will perform its first task of measuring spin rate and firing thrusters to detumble the spacecraft down to a three-axis controlled attitude and rate. Upon completion of the spin down, the spacecraft will be slewed to a Sun orientation. Solar arrays will then be deployed as the attitude and rates are controlled to a Sun-pointing attitude to minimize torques on the deployment mechanisms. Early operations will consist of commissioning and checking out the spacecraft and payload to the best extent possible, including a series of NEXT engine tests. The DSN coverage during early operations will gradually step down from continuous coverage during the first week, to 8 hours of contact per day for 2 weeks, and ending at approximately 5 weeks with two 8-hour contacts per week. The baseline DSN schedule for the 2015 launch opportunity with a 2027 sample return is shown in Fig. 4.5.1-1, and the schedule for the backup opportunity is shown in Fig. 4.5.1-2.

Mission Phase	Period (days)	Days from Launch	DSN Contact
Early Operations (NEXT engine tests)	L to L+6 L+7 to L+20 L+21 to L+60	0–6 7–20 21–60	Continuous 8 h/d 2×8 h/wk
Coast	L+61 to TAstart–10	61–693	Beacon hibernation mode† One checkout every 6 months‡
Thrust Arc 1	TA1start–10 to TA1start TA1 (380 days) TA1end to TA1end+10	694–703 704–1084 1085–1094	Continuous to TA start 2×8 h/wk (90% duty cycle) Continuous after TA end
Coast	TA1end+10 to TA2start–10	1094–1870	Beacon hibernation mode One checkout every 6 months
Thrust Arc 2	TA2start–10 to TA2start TA2 (294 days) TA2end to TA2end+10	1871–1880 1881–2175 2176–2185	Continuous to TA start 2×8 h/wk (90% duty cycle) Continuous after TA end

Mission Phase	Period (days)	Days from Launch	DSN Contact
C-G Operations (P is perihelion in Nov. 2, 2021)	P–23 to P+118 3 Landings, P+118 to P+122 P+122 to Departure –10	2186–2325 2326–2330 2331–2437	3×8 h/wk (but each month, 1 wk 8 h/d & 2 d continuous) Continuous 3×8 h/wk less than 3 AU; 8 h/wk more than 3 AU from Sun
Thrust Arc 3 C-G Departure	TA3start–10 to TA3start TA3 (169 days) TA3end to TA3end+10	2438–2447 2448–2617 2618–2627	Continuous to TA start 2×8 h/wk (90% duty cycle) Continuous after TA end
Coast	TA3end+10 to TA4start–10	2628–4007	Beacon hibernation mode One checkout every 6 months
Thrust Arc 4	TA4start–10 to TA4start TA4 (307 days) TA4end to TA4end+10	4008–4016 4017–4324 4325–4334	Continuous to TA start 2×8 h/wk (90% duty cycle) Continuous after TA end
Coast Earth Return	R–73 to R–11 R–10 to R–5 R–4 to R	4335–4396 4397–4402 4403–4407	3×8 h/wk 8 h/d Continuous

† Beacon hibernation mode is 1× 1.5 h/wk (carrier only)
‡ Checkout is 20 d operations, 2× 8 h/wk, every 6 months

07-05866P-107

Figure 4.5.1-1. Baseline DSN schedule for CSSR 2015 launch minimizes costs while satisfying all mission requirements.

4.5.2 Cruise Operations

Upon completion of the specified commissioning activities, the spacecraft shall begin its first cruise phase, which leverages experiences documented on the Hyabusa, DAWN, DS-1, Genesis, and Stardust missions. The cruise phase can be further divided into coast periods and thrust periods. The cruise to C-G lasts for 2126 days, contains two NEXT thrust arcs of 380 days and 294 days, respectively, and transverses two "phasing orbits" around the Sun for the prime launch opportunity. The cruise from the comet back to Earth is 1960 days long and has two NEXT thrust arcs of 169 days and 307 days, respectively. Throughout cruise the spacecraft will be navigated through ground-computed solutions of position and velocity. The coast periods are characterized by placing the spacecraft into beacon hibernation mode, similar to that used by the New Horizons – Pluto mission, with full spacecraft checkouts no less than every 6 months. Thrust periods are characterized by using the NEXT thrusters at a 90% duty cycle to steer the thrust vector inertially. Thrust vectors will also maintain spacecraft momentum by steering torque vectors as needed to counter center-of-mass offsets as propellant depletes and any asymmetries resulting from solar radiation pressure acting on the solar arrays and spacecraft body. Thrust duration and directions will be uploaded from mission design solutions produced on the ground and uploaded through mission operations processes proven on previous deep-space missions including MESSENGER and NEW Horizons.

Mission Phase	Period (days)	Days from Launch	DSN Contact
Early Operations (NEXT engine tests)	L to L+6 L+7 to L+29	0–6 7–29	Continuous 8 h/d
Thrust Arc 1	TA1 (493 days) TA1end to TA1end+10	30–523 524–534	2×8 h/wk (90% duty cycle) Continuous after TA end
Coast	TA1end+10 to TA2start–10	535–1579	Beacon hibernation mode† One checkout every 6 months‡
Thrust Arc 2	TA2start–10 to TA2start TA2 (171 days) TA2end to TA2end+10	1580–1589 1590–1761 1762–1772	Continuous to TA start 2×8 h/wk (90% duty cycle) Continuous after TA end
C-G Operations (P is perihelion in Nov. 2, 2021)	P–86 to P+118 3 Landings, P+118 to P+122 P+122 to Departure –10	1773–1901 1902–1906 1907–2070	3×8 h/wk (but each month, 1 wk 8 h/d & 2 d continuous) Continuous 3×8 h/wk less than 3 AU; 8 h/wk more than 3 AU from Sun
Thrust Arc 3 C-G Departure	TA3start–10 to TA3start TA3 (171 days) TA3end to TA3end+10	2071–2080 2081–2252 2253–2263	Continuous to TA start 2×8 h/wk (90% duty cycle) Continuous after TA end
Coast	TA3end+10 to TA4start–10	2264–3637	Beacon hibernation mode One checkout every 6 months
Thrust Arc 4	TA4start–10 to TA4start TA4 (318 days) TA4end to TA4end+10	3638–3647 3648–3966 3967–3977	Continuous to TA start 2×8 h/wk (90% duty cycle) Continuous after TA end
Coast Earth Return	R–61 to R–11 R–10 to R–5 R–4 to R	3978–4027 4028–4035 4036–4039	3×8 h/wk 8 h/d Continuous

† Beacon hibernation mode is 1× 1.5 h/wk (carrier only)
‡ Checkout is 20 d operations, 2× 8 h/wk, every 6 months

07-05866P-108

Figure 4.5.1-2. Backup DSN schedule for CSSR 2016 launch achieves all mission objectives, including a 2027 sample return, without significant changes to the mission design and implementation.

The SEP mission requires a minimum of a 90% duty-on cycle of a NEXT ion thruster during the active thruster arc orbit periods, which can last for a year or more. Nominally, NASA requires operations teams to continuously monitor spacecraft when propulsive activity, is occurring. Since this is not economically or technically feasible for the CSSR mission, the impact of anomalous events on active thrusting periods will be reduced with a robust concept of operations and fault protection strategy. During active electric propulsion thrusting activity the ground will communicate with the spacecraft once every 3 days. Four of five of these contacts will be for a

short duration (<4 hours), and the spacecraft will only return a low-data-rate (<10 bps) health status signal similar to the New Horizons beacon telemetry. From this signal, ground personnel will be able to determine the overall health status of the spacecraft and its orbital position. If the health status signal is being reported as nominal, operators will continue with the nominal track schedule. If the health status signal is off-nominal, ground operators will schedule extra track time, stop thrusting operations, and establish a high data rate to determine the anomalous issue. One of every five communication contacts with the spacecraft will be a longer (8-hour), high-data-rate event during which active electric propulsion thrusting will not occur. During this time period, operators will play back the SSR containing detailed health and status housekeeping telemetry. From this, supporting engineers will assess the status of the spacecraft and analyze the performance of the NEXT propulsion system.

An analysis was performed to determine how the frequency of spacecraft ground contacts and the length between high-data-rate contacts affected the yearly total number of allowed anomalous events that shut down the electric propulsion system. The analysis accounted for the length of regularly scheduled non-thrusting periods for high-data-rate contacts (8 hours), the period of time between the ground observing the anomalous condition and fully recovering nominal thrusting operations (7 days), and the required thruster duty-on cycle (90%). It was found that the nominal CSSR concept of operations that downlinks housekeeping data once every 2 weeks and routinely maintains a health status signal contact once every 3 days allows 2.64 faults per year. As a reference, the last three of the missions APL built and currently operates (MESSENGER, New Horizons, and STEREO) have had an average of <1 anomaly per year that resulted in a loss of nominal operations. Furthermore, the typical recovery time for the anomalies is significantly less than the 7 days accounted for in the CSSR analysis.

4.5.3 Comet Operations

Comet operations begin approximately 4 weeks before reaching C-G's perihelion and last for 252 days. DSN coverage in this phase will typically be three 8-hour contacts per week, with continuous coverage during each of the landing sequences. During this phase, systems shall model the environment in the vicinity of the comet, including mapping the comet's surface from an altitude of approximately 100 km for several weeks. The NFV images will be processed on the ground to produce a digital elevation map (DEM) that will then be uploaded to the spacecraft. Further data collected will include characterization of the rotational period, the rotational axis, dust environment, and initial gravity field approximation. The shape model will be built from at least 600 images of the surface, taken at multiple phase and incidence angles, with sufficient accuracy to provide navigation within ±100 m of a chosen location on the surface. Once the comet and its surrounding environment have been characterized, landing location(s) will be selected. Two weeks of practice for "touch and goes" will be followed by 2 weeks for the actual sample run, aided by lidar and Doppler. There are built-in 4-week contingency periods at the end of both mapping and sampling for dealing with contingencies.

From 100-km altitude down to the surface, a series of GN&C functions will be used to facilitate the comet encounter. The spacecraft shall descend into a Home State orbit of 1–5 km using ground-based ΔV solutions and primary pointing based on the comet ephemeris. Instead of "turn and burn" thrust vector control, the thrust vector will be controlled in a multi-axis thrust vector pulse width modulation (PWM) to allow continuous pointing to the comet while maintaining roll control pointing of antennas toward Earth. The Home State orbit (Fig. FO 4-4B) lies in the Sun terminator plane of the comet. Further detailed studies of this environment (Fig. FO 4-4A) will be performed while orbiting to ensure that dust flux effects on the trajectory are understood.

Once a landing site has been chosen, at least one practice descent is planned before touchdown. Descent profile (Fig. FO 4-4C) continues from the Home State orbit at L−10,000 seconds with execution of a table-loaded trajectory that guidance will follow using a fuzzy logic control scheme. This provides a higher level of robustness to environmental disturbances during descent and keeps the spacecraft in the terminator plane for as long as possible. Prior to descent, the solar arrays are folded inward with solar cells facing outward for continuous power generation. This configuration will allow the arrays to avoid surface contact at touchdown.

From about 500-m altitude above the mean radius of the comet, the trajectory guidance is commanded to latitude/longitude/altitude targeting. A series of targeted "braking gates" will have been time-tagged and loaded earlier. This mode transitions the trajectory control from inertial to surface relative. Target way-points are chosen to "walk" the spacecraft down toward the final touchdown target in order to ensure that gravity forces are acting on spacecraft in the nadir face direction to avoid lateral disturbances in the trajectory. Timing of these maneuvers is designed to meet the requirement that during all phases of descent, on the surface, and on ascent, the Sun-comet-spacecraft angle is 90° ± 20° to keep Sun and comet geometry nearly orthogonal relative to the spacecraft to maintain continuous power positive and communications attitudes.

Braking gates are executed at 300, 100, and 50 m above the target surface radius at L – 7000, 5000, and 1000 seconds, respectively. At the 50-m point, the spacecraft will perform detailed imaging as needed to enhance DEM information on landing site and any navigation and science objectives. On a practice landing, this is where departure back to Home State will be executed using inertial trajectory targeting guidance.

During this stage of descent, the lidars and Doppler radars mounted to the nadir face and two lateral faces of the spacecraft will begin intersecting the surface (Fig. FO 4-4D). Nadir-facing lidar, radar, and WFV will be co-boresighted to within a tolerance of 0.01° to ensure no more than 1 m error from image boresight at 5 km distance from the surface. Laterally mounted lidars and radars will intersect the surface at an altitude of between 300 and 100 m. Pointing guidance will automatically switch to a surface normal alignment mode as trajectory guidance switches to nadir rate targeting and lateral rate nulling. The navigation will begin using these sensors as part of the extended Kalman filter algorithm. Also at this point, attitude control will begin to switch from thruster-based to reaction wheel control. Momentum will be continuously monitored and controlled and, if needed, preset to ensure adequate control during remaining landing sequence. Finally, all downward firing thrusters will be masked out to ensure that minimal contamination of sample area occurs.

During the entire descent profile from Home State orbit, the Terrain Recognition Navigation (TRN) algorithm will run at regular intervals of no greater than 10 seconds to regularly verify onboard navigation solutions. WFV images will be sent to the processor for correlation to DEM-derived images and position determination. The onboard navigation filter state vector solution from propagated orbit using accelerometers, gyros, and gravity model-based accelerations will be compared to position solutions from the TRN algorithm at each update interval. Should the errors between the two solutions differ by a predetermined amount, the descent will be aborted.

At the 10-m altitude at about L – 100 seconds, the trajectory guidance will be following rate commands to surface of 10 cm per second at contact and no more than several millimeters per second lateral rates. At contact, any attitude disturbance will be damped by reaction wheels and, if necessary, thrusters, to ensure attitude remains aligned with surface normal. All thrusters will then be masked out, and the controller will minimize torques on the body induced by reaction

wheels. Onboard state vector will be frozen in the comet body fixed International Astronomical Union (IAU) frame. Inertial propagation will be halted except to resolve the spacecraft position and velocity from the kinematic comet body motion back into the inertial frame. This, in combination with the quaternion updates from star trackers, will ensure a good knowledge state at takeoff from the surface.

Assuming touchdown at the beginning of the 40° Sun-comet-spacecraft angle window from 110° to 70°, and for a 12-hour comet rotation period, this provides about 1.5 hours of on-surface time, which exceeds the time needed on the surface. Upon completion of scientific objectives on the surface, a time-tagged latitude/longitude/altitude is executed, and all translation and rotational control thrusters are unmasked. At the appropriate time, the inertial propagation is enabled with the initial state from the kinematic propagation and control is subsequently enabled to lift off. Close timing between these two events will ensure integrity of the onboard state vector.

Surface departure geometry (Fig. FO 4-4E) has the spacecraft launching from the surface in as near normal to the surface orientation as possible to avoid any recontact. Surface-relative targeting keeps the spacecraft rotating with the comet out to the hover position of 300 m. At this point the solar arrays are commanded to redeploy to provide full Sun on arrays while continuing to maintain WFV target pointing to the surface (Fig. FO 4-4F), allowing continuous TRN monitoring of position relative to surface. Sun pointing with fully deployed arrays requires a spacecraft 90° roll slew to track right ascension of the Sun with gimbal as the spacecraft tracks Earth for communications. From this point, the Home State orbit is targeted and commanded with guidance.

Once back in the Home State orbit, CSSR can be commanded to perform additional landing sequences if necessary, can continue to conduct further observations of the comet and its nearby environment, or can be sent back to Earth by initiating the departure NEXT thruster arc and second cruise phase.

Contingencies have been considered that will require safing and time to take corrective actions. At any time during the descent, a condition leading to safe mode can lead to a safe state abort. The geometry (Fig. 4.5.3-2) to ensure that there is no contact with the surface with a loss of spacecraft and comet ephemeris knowledge requires reliance on sensors typically used for pointing Sun acquisition safe modes. With proximity to the comet in an unknown position relative to the spacecraft, a safe state condition has been developed where Sun orientation in the body frame is known from Sun sensors. Using IMU accelerometers and gyros, but no ephemeris, a ΔV is commanded by the safe state guidance toward the Sun vector using the multi-axis PWM while maintaining inertial attitude to ensure no comet contact with solar arrays. After a predetermined time period, an equal and opposite inertial ΔV is commanded autonomously to take translation out. At this point, the solar arrays are redeployed and 90° slew, similar to nominal post-landing scenario.

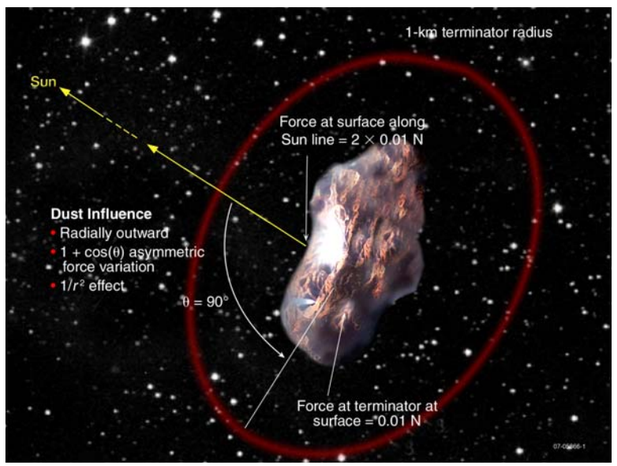

A. Comet vicinity environment modeling.

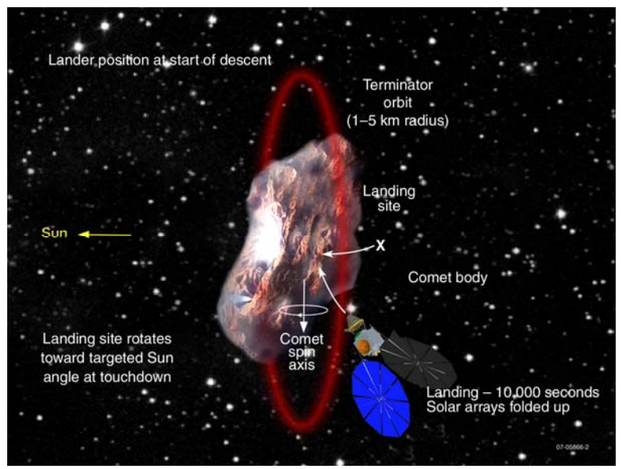

B. Descent geometry.

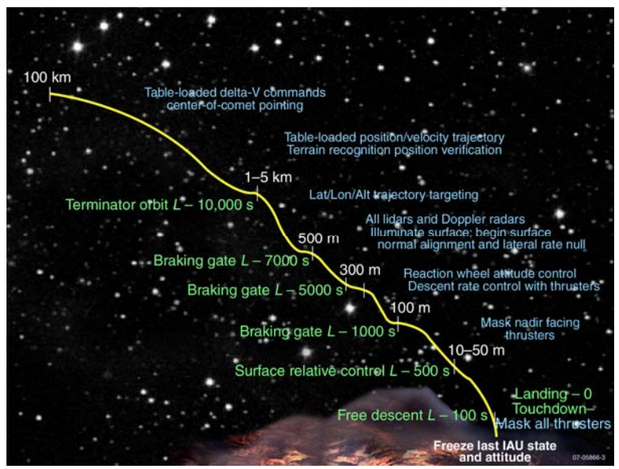

C. Nominal descent profile.

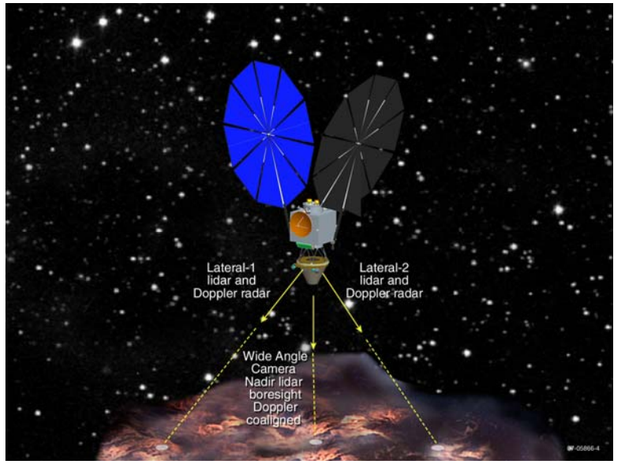

D. Height and motion system geometry. Combined range and range rate data used to compute current local surface normal and lateral translation rates.

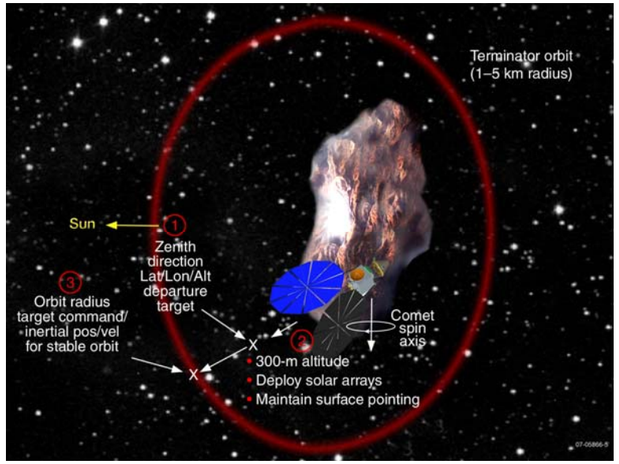

E. Surface departure geometry.

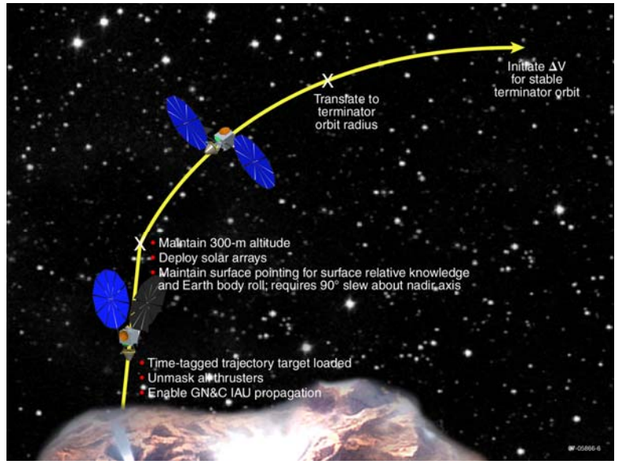

F. Ascent profile.

Foldout 4-4. CSSR proximity operations strategy.

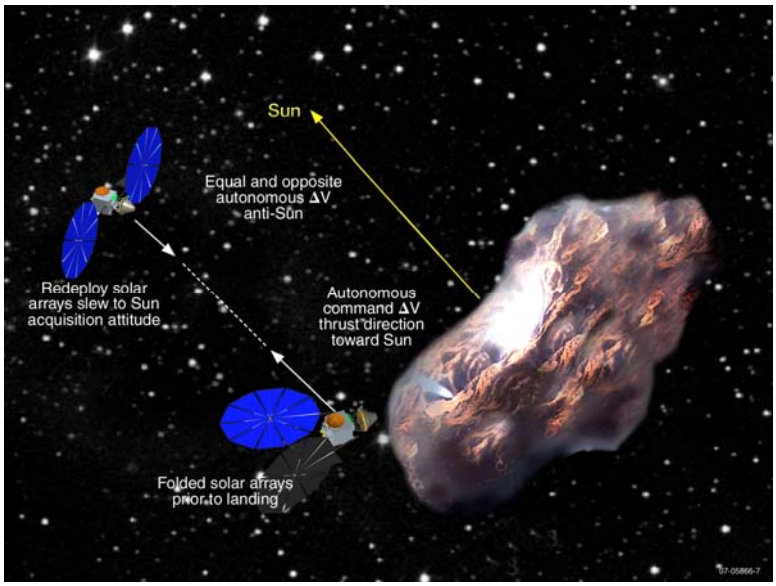

Figure 4.5.3-2. A pre-defined safe state provides for autonomous recovery in the event of a fault during proximity operations.

Abort conditions leading to Home State abort include but are not limited to conditions where the TRN position solutions do not agree with to the navigation solution. Nonconverging trajectory to navigation solutions as well as nonconverging targets can also lead to abort conditions. Lidar and radar invalid or out-of-tolerance signals can lead to abort. Loss of communications lock to Earth is yet another condition to abort to the Home State.

Starting at a 1-km radius Home State position, the nadir-facing lidar indicates an altitude profile as the spacecraft descends toward the landing site (Fig. 4.5.3-3). Figure 4.5.3-4 shows the trajectory displayed in the comet body fixed IAU frame. The final target was the landing site and was successfully attained. Final position error at touchdown is within 10 m of the targeted site.

During descent the angle between the Sun and the spacecraft as seen from the comet is no greater than 110° and no less than 70° (Fig. 4.5.3-5). This includes 5000 seconds on the surface, which far exceeds surface dwell time requirements. Note that at approximately 11,000 seconds, the spacecraft is attached to the comet and the angular rate is linear as the comet itself is rotating at a constant rate. At the start of the descent, targeting of a point off the surface but above the landing site results in a trajectory moving out of the terminator plane into the direction in which the comet is rotating from. As the landing site rotates toward the spacecraft, the targeting automatically begins to rate match with the comet rotation.

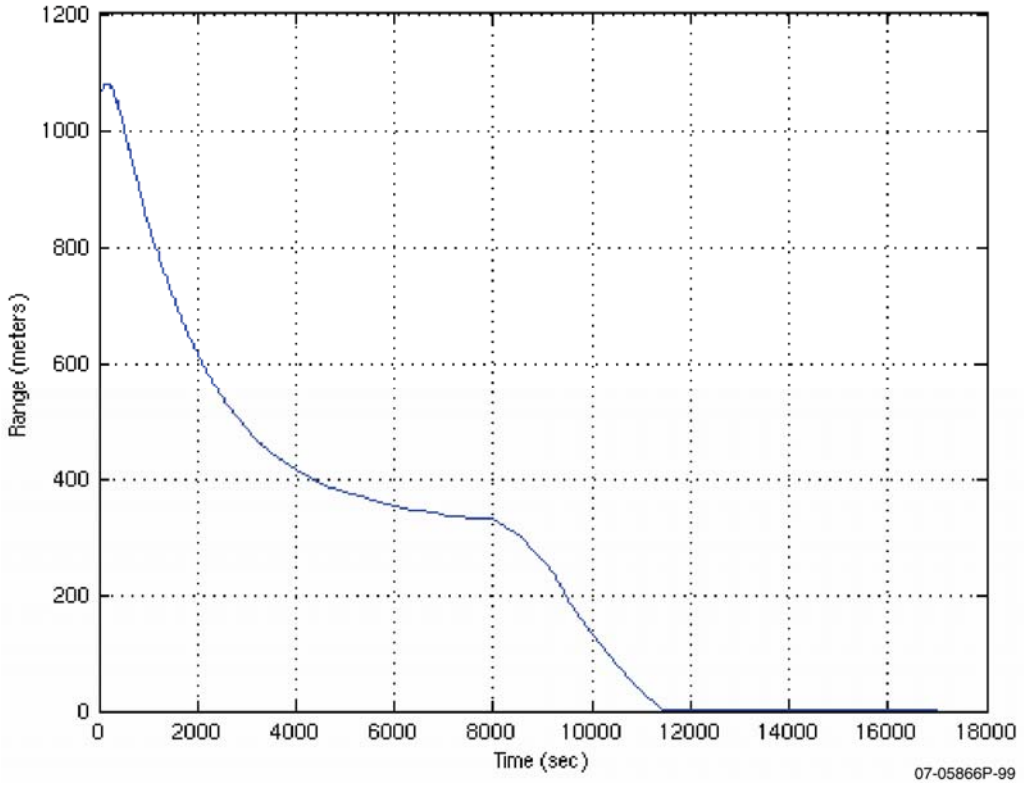

Figure 4.5.3-3. The nadir-facing lidar provides the altitude profile for control during descent.

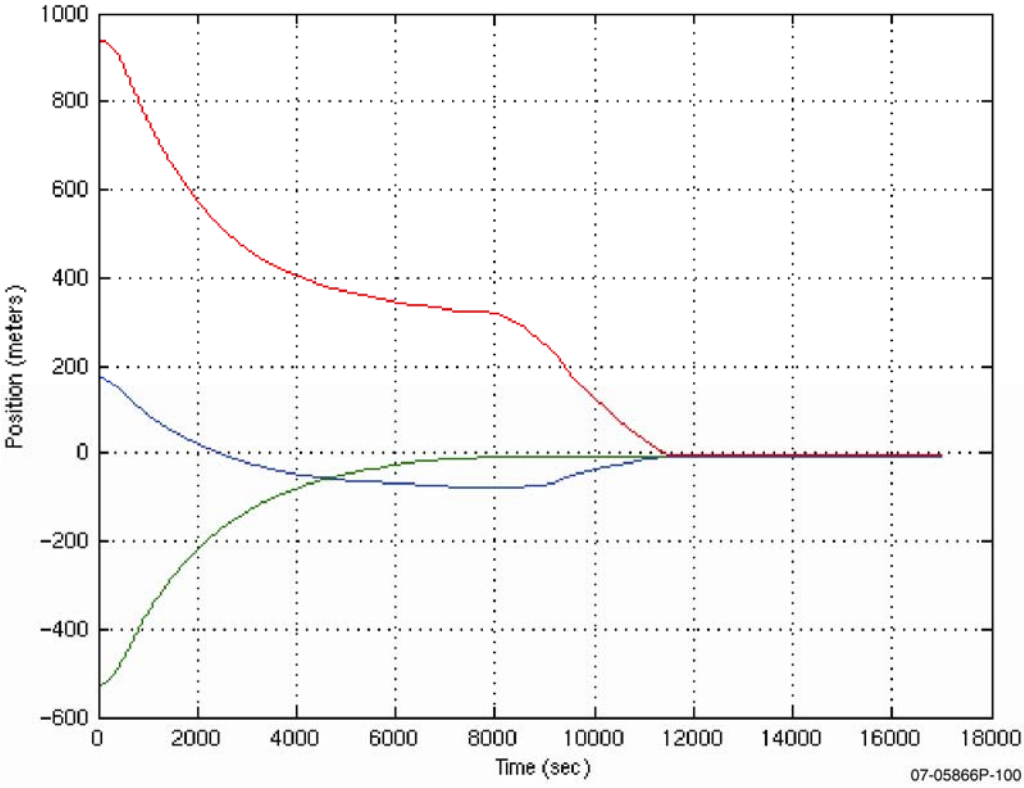

Figure 4.5.3-4. Simulations show that final position error of approximately 10 m (1-σ radial) is possible.

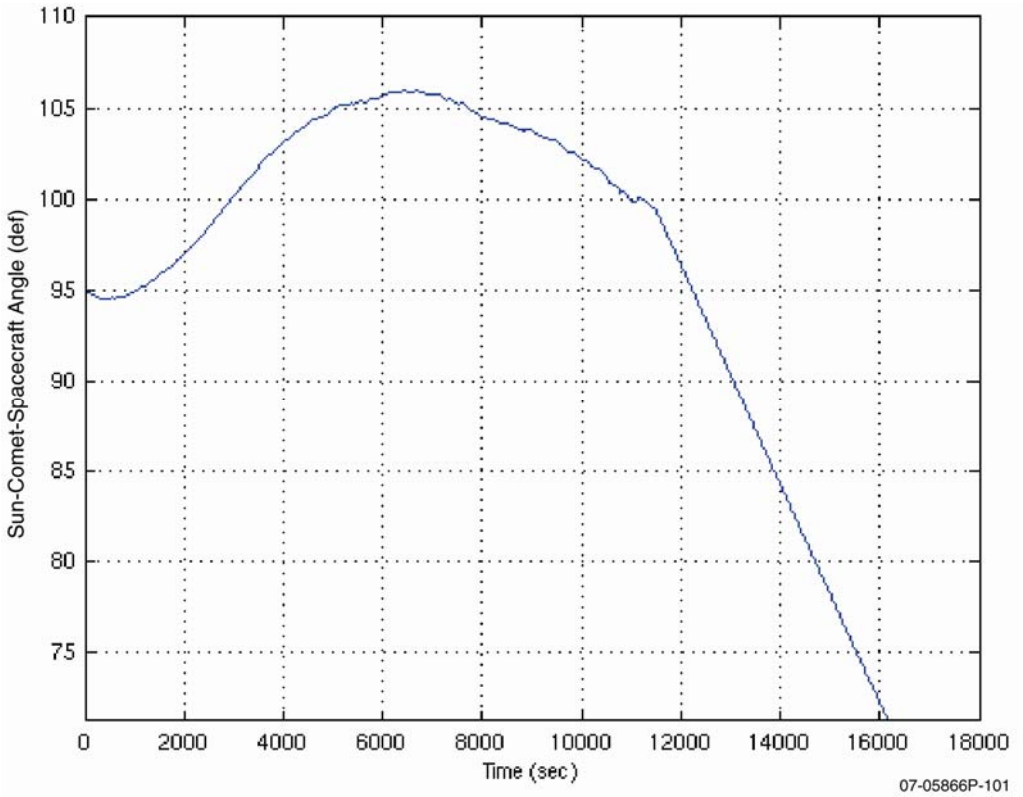

Figure 4.5.3-5. The angle between the Sun and the spacecraft shows that the descent profile can stay within 20° of the terminator.

4.5.4 Earth Return

The SEP mission will complete the second cruise phase and return the spacecraft containing the comet sample to Earth in 2027. Flight safety and ground recovery operations planning will begin about a year prior to the spacecraft return. Upon Earth arrival, the SRV shall be released from the main spacecraft, strategically planned to impact in the UTTR. This phase will leverage techniques proven by the Genesis and Stardust missions, and uses an SRV that is a scaled-down MSR EEV. For additional details on the SRV, refer to Section 4.2.3. Once on the ground, recovery teams will safe the SRV and arrange transport to Johnson Space Center.

Primary sample return entry, descent, and landing interfaces include United States Strategic Command for Earth targeting and return safety analysis; UTTR for airspace control and coordination; Dugway Proving Grounds for human and property risk analysis, geo-location, and recovery; and Johnson Space Center for long-term curation.

4.5.5 Mission Operations

The CSSR mission operations concept draws from spacecraft flight experience on the NEAR asteroid, the MESSENGER mission to Mercury, and the New Horizons – Pluto missions.

Mission operations for CSSR will be conducted from the MOC located at APL. A new multi-mission MOC is under development and will support the RBSP mission starting in 2009. Figure 4.5.5-1 depicts the primary elements that the MOC interfaces with, including the DSN, SOC, and Navigation. To ensure mission success, the mission management team complies with the Space

Mission Operations Standards (SMOS) PAS document. All pre- and post-flight activities and practices, at a minimum, will comply with standards defined for the following areas:

- Operations configuration management
- Spacecraft performance assessment and real-time monitoring
- Mission simulations and in-flight test practices
- Constraints, staff training, and certification
- Real-time operations, contingency planning, autonomy maintenance
- Formal reviews, documentation

Pre-launch, the mission operations team's primary responsibilities include the following:

- Support documentation development and reviews as outlined in the SMOS
- Development of operational and contingency procedures
- Command sequence development and testing
- Conduct simulations of critical activities
- Conduct operational readiness testing with DSN

Post-launch, primary responsibilities shift from development and testing to implementation focusing on:

- Subsystem and instrument checkout activities
- Simulation and execution of maneuvers, encounters, and data playback
- Spacecraft performance assessment and sequence optimization

The operations team consists of experienced spacecraft analysts, command sequencers, and flight controllers. Many of the team members support current and past APL space programs. This allows CSSR to draw on past experience, using people who are familiar with SMOS practices.

Staffing levels vary with phase of the mission, peaking during launch and comet encounters. APL supports multiple spacecraft operations, providing the ability to share resources and personnel, particularly among planetary missions with long cruise periods where quiescent operations do not require a complete, full-time team. The increase and reduction of staffing levels is done in a manner that has proven operationally sound and cost effective. In addition, the quiescent cruise periods will be used to plan the major events of upcoming, complex activities. Therefore, much of the comet encounter and sampling operations can be developed and pre-planned during cruise to comet C-G, using techniques used on New Horizons to maximize personnel knowledge and experience to create baselines of all of the CSSR critical events. Specific encounter details will then be identified and sequenced during the normal planning window within the comet operations phase. In a similar manner, the Earth rendezvous can be pre-planned during the cruise period following comet departure, with specifics completed within the normal planning cycle in the Earth return phase.

A standard process is used to validate all spacecraft command sequences. Heritage command sequencing and validation tools (SEQGEN/StateSim) verify command loads, ensuring all flight constraints are maintained during execution. For critical sequences, the hardware simulator is used to verify the command load, and results are analyzed to ensure sequence accuracy, prior to uplink.

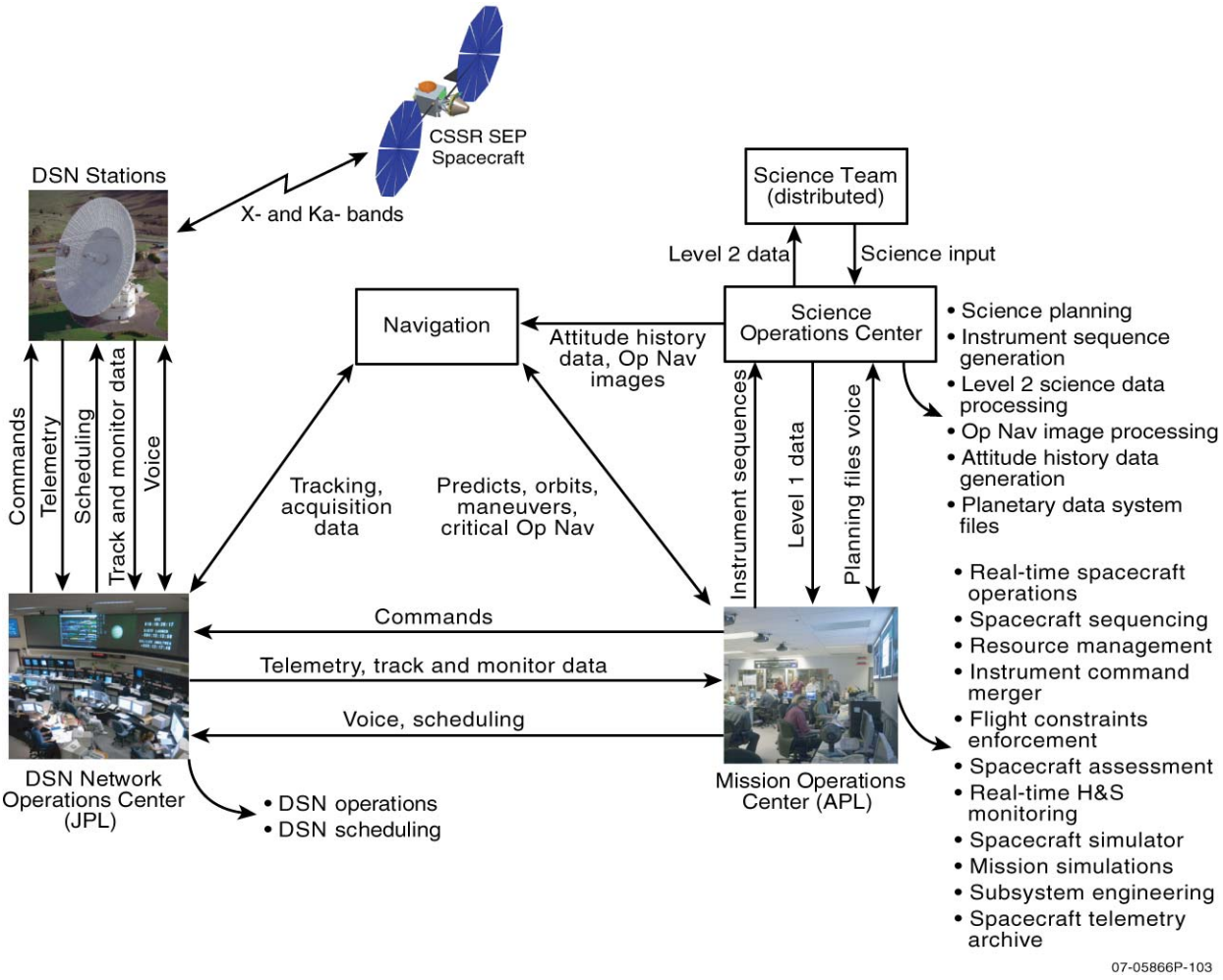

Figure 4.5.5-1. CSSR mission operations has simple functional interfaces.

4.6 Planetary Protection

As defined by NASA Procedural Requirements 8020.12C: Planetary Protection Provisions for Robotic Extraterrestrial Missions, Section A.1, the Comet Sample Return mission is classified as Class V, Unrestricted Earth Return. As such, planetary protection requirements are limited to Documentation for Outbound Phase and Certification of Unrestricted Earth Return prior to the end of Phase A. Since both mission design options are direct trajectories to the comet and return to Earth, not requiring another body flyby, the outbound phase is classified as Category II. Documentation requirements are thus release of a Planetary Protection Plan outlining intended or potential impact targets, brief Pre- and Post-Launch Planetary Protection Reports detailing any appropriate impact avoidance strategies, and an End-of-Mission Report providing the final actual disposition of launched hardware and impact location.

With the classification of Unrestricted Earth Return, the only protective measures needed are for the scientific integrity of the analysis of the returned comet samples. This need falls within the contamination control approach to ensure no forward contamination of the samples taken at the comet, no contamination via the SRV, and no Earth contamination of the samples during the

recovery and analysis process. This represents a critical requirement for contamination control and has been factored into the conceptual design of the mission hardware and operations and the planning for integration and test and the launch campaign.

4.7 Major Open Issues and Trades

A key trade in ion propulsion system sizing is in varying the solar array (input power) size and the number of operating thrusters. As the mission and science objectives are defined in detail, this trade can be performed to balance the mission performance and cost. The 1+1 system selected for this study is the minimum cost NEXT system. Adding a thruster string to a 2+1 system, in which two thrusters may operate simultaneously for high-power phases of the mission, can gain payload performance with increased cost of the propulsion system. Array size can then be tailored to further balance performance and cost. A trade study should be considered in distributing the DCIU functionality between the spacecraft and ion propulsion system. Further, functionality within the ion propulsion system can be allocated to the PPU, possibly eliminating the DCIU entirely. This would require further development of the PPU.

The SAS concept presented here is one of many options. If the uncertainty in surface properties can be reduced, the SAS may be simplified. Also, other design options may be considered depending on the risk tolerance and science priorities (e.g., "sticky" pads to pick up surface material). The SRV trade (MSR type vs. Stardust type) needs additional work with a detailed thermal analysis. If the existing Stardust, Genesis, or Hyabusa designs can be shown to satisfy requirements, a cost and risk savings may be realized. Further detailed analysis should be performed on the Height and Motion System. NEAR landed on Eros inertially; therefore, if the active sensor suite and TRN can be eliminated, a considerable cost savings could be achieved.

4.8 Technology Needs

The CSSR mission requires some system developments that are new in NASA space missions and do not have a history of development and qualification within the space community. A set of technology development tasks are recommended during the formulation phase of a CSSR mission. The technology development plans for the components considered below TRL 6 are detailed below. Costs are itemized separately. The four primary systems of concern are (1) the SAS, (2) the SRV, (3) the NEXT ion-propulsion engine and its ancillary equipment, and (4) the H&MS.

4.8.1 SAS Development

There are two concerns with the CSSR sample acquisition system. First, it must perform a number of separate individual mechanical operations that are all in series with one another. It must engage its sample gathering mechanism with the comet, collect the sample, transport the sample to the sample-holding canister cells in the SRV, seal the sample cells, seal the SRV door, and ensure that it does not interfere with the release of the SRV from the spacecraft at the time of reentry to Earth. The second concern is the large range of uncertainty in the physical nature of the surface of the comet. The estimates range from a loose, unconsolidated material with a consistency of powder, to a hard surface of solid ice. The sample mechanism must deal with these two extremes or anything in between, including a mix of ice and rock, and still reliably return a minimum amount of the sample. Because of the limited development time in the mission schedule, both of these concerns can best be alleviated by a technology maturation and risk reduction project that starts early in Phase A. This work will increase the system maturity to a level sufficient to pass review at the time of confirmation (i.e., bring the system to a TRL of 6 or better).

And, it will reduce the overall developmental risks to ensure that a fully qualified sample acquisition system is ready for the CSSR integration and test phase.

A focused effort over the first 23 months of the program will demonstrate that the sample acquisition devices (the drills) can collect samples over the range of materials, temperatures, and dynamic loads that the system might experience during operation at the comet. The specific milestones are the construction of prototype sampling drills with candidate materials, coatings, and lubricants. These drills would be subjected to a variety of tests with simulated comet surface materials over the full range of expected environmental conditions at the comet. The timeline and milestones for these efforts are shown in Section 4.10.2.

The second effort will construct a prototype sampling mechanism, including the sample drills, prototype SRV interior layout with sample holding cells, and the SRV cover. The tests of this assembly will demonstrate that the samples from the drills can reliably be transferred to the sample cells in the SRV, the cells can be sealed, and the SRV cover assembly locked in place. These tests must also be done in the appropriate environment expected at the sampling site.

4.8.2 SRV Development

The sample return vehicle design is based on the MSR EEV, but it must accommodate the mission-specific requirements to receive the samples and the additional requirement for thermal control. The thermal design must keep the samples cold throughout the cruise phase of the return as well as reentry and landing. It must also collect volatiles that may evolve from the sample during the return to Earth. These development risks can also be significantly reduced by an early technology maturation project.

Risk reduction activities during Phase A will concentrate on both the basic design of the SRV and on its interior that must accommodate and protect the samples. The risks associated with the overall design of the SRV and its thermal protection system will be resolved during Phase A. The design will be refined and the appropriate thermal protection materials will be selected for the re-entry conditions of this mission. Analyses will also determine if a drop test will be needed as part of the Phase B activities or if the drop tests performed for the Mars Sample Return technology development program are sufficient. Any interface issues between the spacecraft, sampler, and SRV will also be resolved during Phase A.

4.8.3 NEXT Propulsion System Development

The NASA GRC and its industrial partners have been developing the NEXT engine and some of the ancillary devices required to produce a complete propulsion system. However, some of these components remain to be developed, and some of the current designs still contain significant challenges in areas such as thermal design. The NEXT program is planning to resolve these remaining issues. The status of the NEXT propulsion system is described in Section 4.4.2, but it is listed here to make it clear that that development needs to continue to ensure that the NEXT system will be ready for this mission.

4.8.4 H&MS Development

The CSSR spacecraft can use its inertial guidance sensors and algorithms to orbit and approach the comet with high accuracy. However, the actual sampling interval requires precise control of the height and relative motion of the spacecraft at the comet surface. A number of individual components exist and have demonstrated the performance levels required for this portion of the mission. However, an integrated system of algorithms, sensors, actuators, and controls has not been demonstrated through the full simulated sampling activity. Confidence in this functionality cannot be gained by testing this system piecemeal, and a fully integrated test is needed.

Since these tests can be complex to set up and run, an early technology maturation activity will be important to reduce the overall mission risk.

4.9 Risks

A risk analysis of the CSSR mission has been performed by the study team. The top risks to be managed for successful execution of a CSSR mission (the project in the terminology of the risk assessment) are given below along with recommended plans for their mitigation. Programmatic risks are discussed further in Section 6.0.

The top risks and mitigation strategies are summarized in Fig. 4.9-1. Figure 4.9-2 provides a overview of these top risks in the standard 5×5 risk matrix format. The definitions of the risk consequences and likelihoods are given in Fig. 4.9-3.

The primary theme of the technical risks for a CSSR mission during this assessment is technology maturity. This was recognized by the National Academy decadal survey, but some significant progress in the basic technologies and our knowledge about the comet environment (see Section 2) has occurred since 2002. These advancements, combined with a vigorous Phase A/B risk reduction program, are capable of reducing the technical risks to very manageable levels.

Programmatic and schedule risk (also shown in Fig. 4.9.1) are focused on identifying and managing cost risk, including cost risk associated with on-going funded technology development of other programs that this study assumes would be completed in time for use on a CSSR mission. The remaining cost and schedule risks identified are very typical of any new project.

Risk	Description	Cf		Lf		R	Mitigation
T1	If the project cannot demonstrate that the sampler system can operate with low risk at the comet by confirmation, the project cannot proceed.	High	5	Moderate	3	15	A robust risk reduction program as described in Section 4.8 of this study is designed to provide the necessary demonstration by confirmation.
T2	If the sampling technique heats the sample above −10°C, important science data would be lost.	High	4	Moderate	3	12	The sample acquisition system risk reduction program will demonstrate that a sample can be collected over the range of potential sample material strengths while experiencing the dynamic forces of the spacecraft and sample acquisition mechanism without experiencing temperature excursions above −10°C. This will be demonstrated before the confirmation review.
T3	If the sample experiences temperature excursions during recovery in excess of −10°C, important science data would be lost.	High	4	Low	2	8	The project will monitor the thermal design progress to ensure that sufficient resources are available to ensure temperature margins sufficient to keep the sample below −10°C.
T4	The possibility of failures of critical components due to the duration of the flight mission.	High	4	Low	2	8	Redundancy of critical elements has been included in the baseline design. Additional analysis will be performed in Phase A to determine if additional redundancies are

Risk	Description	Cf		Lf		R	Mitigation
							appropriate.
T5	If the CEV wing development should not raise the maturity of the design to TRL 6 or above prior to the CSSR confirmation, the project would be required to apply resources for a demonstration test.	Moderate	3	Low	2	6	The project will monitor the CEV progress and determine if a CSSR-funded test would be required. The determination would be made at the time of the concept review to determine the impact on reserves.
T6	If the NeXT life capability is not demonstrated by 2010, the 1+1 design would require modification to a 1+1+1 option at the cost of mass margin.	Moderate	3	Low	2	6	The project will closely coordinate with Glen Research Center on the status of the NeXT life test and make the necessary changes to the configuration prior to PDR.
P1	If resource growth exceeds the reserves due to mission complexity, cost would exceed the cost cap.	Moderate	3	High	4	12	The CSSR mission requirements are demanding and result in a modestly complex mission design. The project management will assess the resources needed at each milestone to determine if reserves are sufficient and make recommendations to NASA on project descopes should it be determined that the resources are not sufficient.
P2	If risk reduction Phase A cost is too high, the funding profile cannot be achieved for a competitive proposal without an independent risk reduction program.	Moderate	3	High	4	12	Work with NASA to size the Phase A funding to meet the minimum acceptable risk reduction effort in Phase A.
P3	If the CSSR SRV design requirements should exceed the Mars SRV design envelope, additional resources could be required to complete the development.	Low	3	Low	3	9	The project plans a risk reduction program as described in Section 4.8 to identify any changes and incorporate them into the CSSR design sufficiently early to keep the technical and programmatic resources to minimize the impact on project reserves.
P4	If sufficient heritage system components are no longer available, the redesign costs will exceed the amount budgeted in the cost estimate.	Low	2	Low	2	4	The project would review the parts status in Phase A to determine the risk which is time dependent. Early (Phase B) purchase of parts for heritage designs will mitigate the risk. Assessment of cost growth due to the necessity of using new parts can be made well before project confirmation.

Risk	Description	Cf		Lf		R	Mitigation
P5	If NASA does not agree that the CSSR is a Category V (Unrestricted Earth Return) per NPR8020.12C, the mission could not be executed within the cost cap.	High	4	Very Low	1	4	Using the arguments made by the National Academy of Sciences, prepare the requisite application for Category V in Phase A and get agreement by NASA prior to PDR.
P6	If NASA does not continue to support the JSC curation facility, a new facility would have to be developed on project funds.	High	4	Very Low	1	4	Although the curation facility is outside the control of the project, NASA's stated intent is to maintain the facility. The project would maintain the visibility of the need for the facility within NASA to assure its continued support.
S1	If the propulsion tank material is not ordered early enough, shortages of titanium may delay the fabrication and delivery of the propulsion system, requiring a more expensive attachment design to maintain the overall schedule.	Low	2	Low	2	4	The project plan includes funds to support the procurement of the tank material at least 18 months before the required fabrication date.

07-05866P-121

Figure 4.9.1. Mission risks and mitigation strategies.

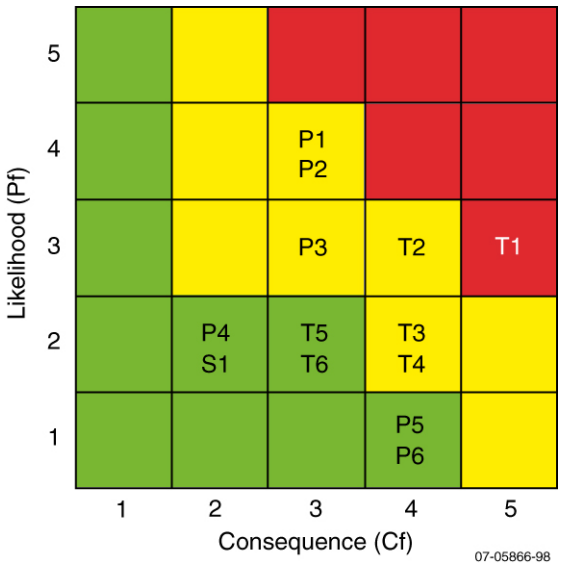

Figure 4.9-2. CSSR risk matrix.

Ranking		Likelihood		Consequence		
		Programmatic	Technical	Cost	Schedule	Technical
1	Very low	<10% chance of occurrence	0.1%–2% chance of occurrence	<$5M	<0.5 month slip	Loss of margin
2	Low	10%–25% chance of occurrence	2%–15% chance of occurrence	$5M–$10M	0.5–1 month slip	Reduced functionality, but minimum requirements still met
3	Moderate	25%–50% chance of occurrence	15%–25% chance of occurrence	$10M–$50M	1–2 months slip	Loss of redundancy or functionality that impacts ability to meet performance requirements
4	High	50%–75% chance of occurrence	25%–50% chance of occurrence	$50M–$100M	2–6 months slip	Loss of functionality; inability to meet full science
5	Very high	<75% chance of occurrence	>50% chance of occurrence	>$100M	>6 months slip	Inability to meet minimum science

07-05866P-97

Figure 4.9-3. Definitions of likelihood and consequence.

4.10 Mission Schedules

A CSSR mission schedule is highly dependent on target options and mission design.

- For the study target options, a 5-year development cycle (Phases A–D) is programmatic options for either the Solar Electric Propulsion or Ballistic mission if pre-Phase A activities are concluded prior to GFY 2010.
- The development cycle is well within the ability of the community to execute if there are no gaps between the phases as sometimes occurs between Phase A and Phase B.
- A Phase A/B risk reduction program is recommended to bring certain critical technologies to an acceptable level of risk prior to confirmation.

The CSSR Mission schedule is driven by launch dates as determined by the celestial mechanics of the desired targets and the available launch service options. For the ballistic mission option, the launch window opens on December 22, 2014; for the SEP mission option, it opens on October 27, 2015. The study team has organized the tasks to execute these missions on a schedule sufficiently aggressive to reduce technical risk by mission confirmation and make efficient use of resources to best control costs while leaving sufficient time to keep schedule risk low. Both missions can be developed in a 5-year period with the initiation of Phase A adjusted for the particular launch date. Figures 4.10-1 and 4.10-2 give the mission time line by phase for the two options. The structure of the development phase is the same for either option. Both schedules result in a proto-flight observatory being delivered in time for the opening of the launch window with 4 months of schedule reserve for the critical path with additional reserve for the comet sampler, which has greater development risk. The Mission Operation and Data Analysis phases have the same structure but differ in the total time of execution because of the differences in the two mission designs.

Phase A Concept Study	Phase B Formulation	07-056150 Development	Phase E MO&DA
12/1/2009 To 8/31/10 (9 months)	9/1/2010 to 10/31/2011 (14 months)	11/1/2011 to 1/31/2015 (39 months)	2/1/2015 to 10/31/2028 (165 months)

07-05866P-49

Figure 4.10-1. Baseline schedule summary: Ballistic mission option.

Phase A Concept Study	Phase B Formulation	Phase C/D Development	Phase E MO&DA
10/1/2010 to 6/30/2011 (9 months)	7/1/2011 to 8/31/2012 (14 months)	9/1/2012 to 11/30/2015 (39 months)	12/1/2015 to 11/30/2028 (156 months)

07-05866P-50

Figure 4.10-2. Baseline schedule summary: Solar electric propulsion mission option.

The key decision points for both mission options are given in Fig. 4.10-3. The development schedule implied by these dates is slightly longer than the New Horizons mission (which had a Phase A that began 4 months less than 5 years with a short hiatus between the completion of Phase A and the beginning of Phase B). Delaying the implementation of a mission after January 2010 for the ballistic option or October 2010 for the SEP option will incur significant risk (should NASA choose to implement a CSSR mission in the epoch of this study at a slightly later date). The Preliminary Design Review (PDR), Non-Advocate Review (NAR), and confirmation follows the typical order, but their timing is dependent on the sampler risk reduction program completion (23 months after initiation of Phase A) as described in Section 4.8. The sampler risk reduction program is designed to demonstrate the ability of the sampler to operate over the range of comet conditions identified by the Science Definition Team (SDT) and over the range of environmental conditions imposed by the mission design, and to meet the TRL criteria at confirmation of NPR 7120.5D.

KDPs	Ballistic Mission	SEP Option
Phase A begins	Jan-10	Oct-10
Concept Review	Aug-10	Jun-11
PDR	May-11	Mar-12
NAR	Jul-11	May-12
Confirmation	Nov-11	Aug-12
CDR	Apr-12	Feb-13
Launch	Dec-14	Oct-15

07-05866P-82

Figure 4.10-3. Key decision point dates for a CSSR mission.

4.10.1 Observatory Schedule

A top-level development phase schedule is given in Fig. 4.10.1-1. This schedule (at the level of detail shown) is the same for either mission option. The mission development plan is to design, fabricate, and test the three observatory elements (spacecraft, sampler, and SRV) separately and integrate them at the launch site. This approach is motivated by the general principle

of discovering any system weakness in test at the earliest practicable time. Thus the risk of delaying the testing of the other two elements should the third experience a problem in earlier testing is reduced. In addition, this approach reduces the number of environmental tests in series.

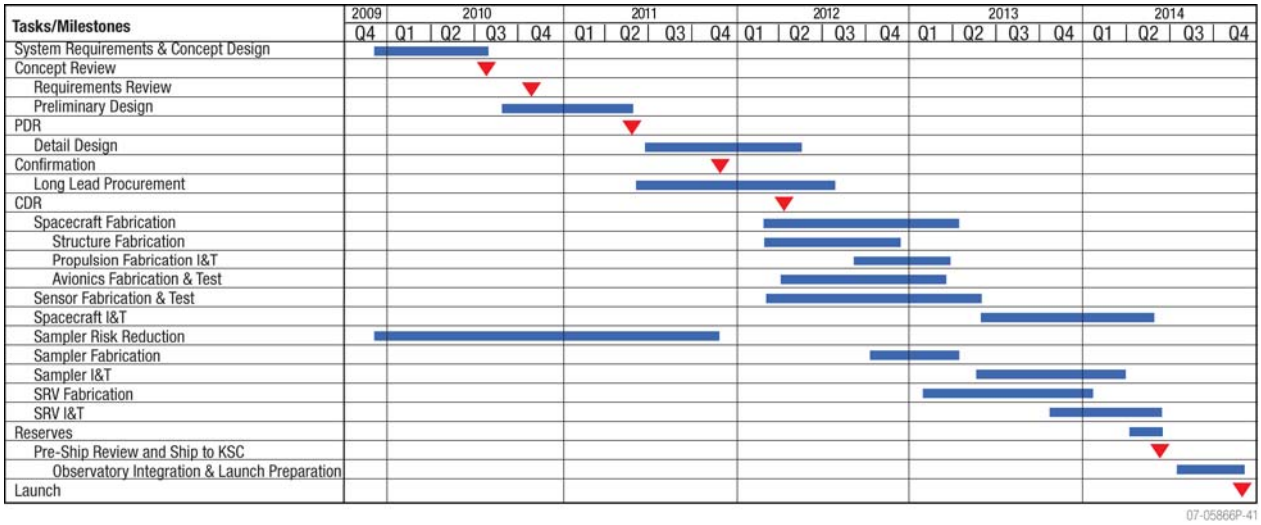

Figure 4.10.1-1. Phase A/D schedule.

The development phase critical path includes the spacecraft structure and propulsion design fabrication and test as well as the integration and test activity. The 9-month Phase A is more than adequate for mission concept and requirement development with resulting requirements revisions from the concept review incorporated early in Phase B. The structure design and interfaces are developed through PDR to a level of confidence such that the structure fabrication task can begin prior to mission CDR but after confirmation. This sequence is typical of proto-flight missions and incurs small technical risk while significantly reducing schedule risk. The propulsion system integration would be performed by the propulsion system vendor during a 3-month period. For the SEP system, the hydrazine and SEP propulsion system elements are assumed to be provided by the same vendor. The integrated structure and propulsion system would be tested as a system prior to the start of a 12-month spacecraft integration and environment test (I&T) program. A 12-month I&T schedule, although modestly aggressive, is not without numerous precedents, and the most serious risk (the delay in instrument delivery) is mitigated because the most complex element of the payload complement is not in series with the spacecraft critical path until after delivery to the launch site.

4.10.2 Sampler Schedule

The sampler system requires initial work to increase the system maturity to a level sufficient to pass review at the time of confirmation (i.e., bring the system to a TRL of 6 or better). This requires demonstration that the sample acquisition devices (the drills) can collect material over the range of materials, temperatures, and dynamic loads the system might experience during operation at the comet. A risk reduction program is envisioned to accomplish this task. Although the workflow has been organized to minimize the sampler development on the critical path, a focused effort over the first 23 months of the program can result in reducing this programmatic risk in time for the confirmation given in Fig. 4.10-3.

The sampler schedule shown in Fig. 4.10.2-2 identifies tasks associated with risk reduction program (as described in Section 4.8), the development of an engineering model, and the fabrication, assembly, and test of the flight system prior to delivery to the observatory at the launch site. The science team will continue the work of the SDT in supporting the development of appropriate stimulant materials in the correct environment. The schedule is based on the extension of already existing test chambers to develop the adequate test environment. The most critical tests would be concluded during the first 12 months of the mission development (Phase A and continuing into the first 3 months of Phase B). Additional testing of other elements of the mechanism to demonstrate that the sampler system can deposit the collected sample in the SRV canister will conclude the risk reduction phase prior to confirmation.

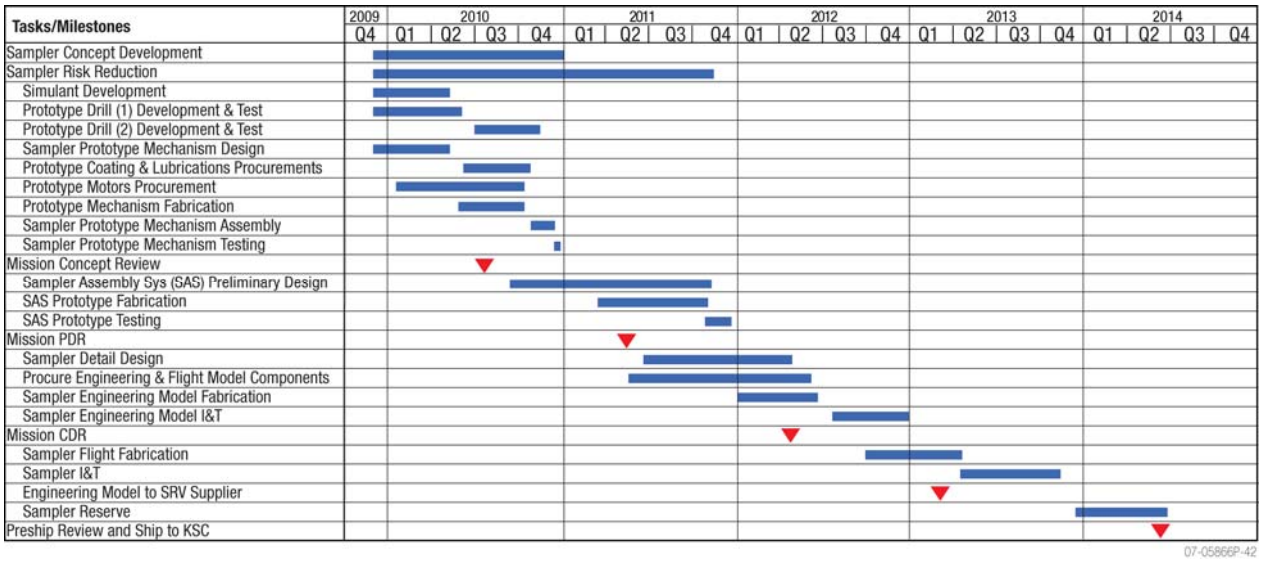

Figure 4.10.2-2. Sampler Phase A/D schedule.

Flight system elements will be procured in Phase B and used to fabricate both an engineering model and a flight model sampler system. The engineering model will provide a pathfinder for the flight unit environmental test program and be used to verify the interface with the SRV during SRV environmental testing. The flight unit will be completed on a schedule that includes an additional 8 months of reserve prior to delivery.

4.10.3 Sample Return Vehicle Schedule

The SRV development focuses on preliminary design and risk reduction tasks in Phases A and B with a nominal fabrication and test schedule in Phase C/D that does not pose a threat to the overall critical path. Also planned for Phases A and B is the purchase of long lead items, particularly the procurement of the materials needed to develop and build the necessary models for use in the risk reduction tests. Ballistic range and wind tunnel testing will be performed early in Phase B. Analysis during Phase A will determine if a drop test will be performed as part of the Phase B risk reduction (funding is included for this outcome) or if the drop tests performed for the Mars Sample Return technology development program are sufficient. An emphasis will be placed on resolving any interface issues between the spacecraft, sampler, and SRV in Phase A, which will allow the detail design to be completed sufficiently early for fabrication of the flight unit to begin some 10 months after the mission CDR. The I&T activity will include a thermal

vacuum test with the engineering model of the sampler that can be delivered to the SRV team months before it is needed to perform the test.

4.10.4 Mission Operations and Data Analysis Schedule

As shown in the schedule summaries of Figs. 4.10.1-1 and 4.10.1-2, the Mission Operations and Data Analysis (MO&DA) duration differs by 9 months for the two different mission options. These differences are associated with slightly different times to reach and return from the comet. The MO&DA schedule for the SEP mission is divided into eight phases associated with distinct activities as shown in the schedule of Fig. 4.10.4-1. Seven of these phases represent various flight activities that require significantly different levels of support. The operations during early checkout and the cruises to and from the comet are very similar to activities experienced by missions like New Horizons and Dawn. The 6-month period prior to arrival at the comet will be used to prepare for comet operations, and the increased monitoring will be used to prepare for operations in the vicinity of the comet. The science team will support the operations team during the observation period (just prior to and during the comet operations period). The science data collected during the period at the comet will be processed by the Science Operations Center, and the data will be delivered to the Planetary Data system during the preparation for the return home (cruise 2).

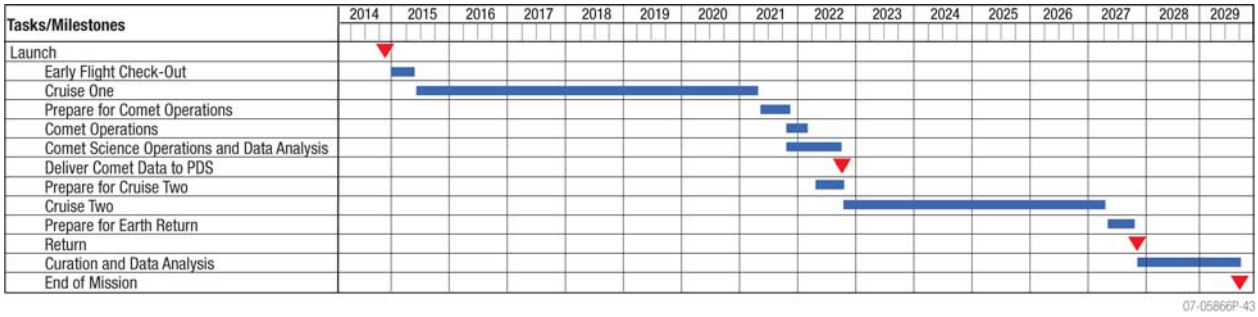

Figure 4.10.4-1. CSSR mission Phase E.

The initial planning for the return will occur during Phases A–D. Safety analysis, begun during the development phases to the point of ensuring a safe return, will continue during Phase E to ensure that skills required during the reentry are at the proper level during the final return phase. The SRV capsule will be retrieved and returned to Johnson Space Center for analysis. The final phase of the mission will result in inventory of the return sample and its initial analysis. The study envisions that the majority of the sample will be left intact at the curation facility for future analysis. The mission will officially end after the initial sample analysis and sample inventory are delivered to the Planetary Data System and the sample is officially transferred to a custodian under NASA direction.

4.11 Cost

Meeting the CSSR cost cap with the SEP mission design will be challenging because of the mission's technical complexity and duration.

- The estimated cost of the SEP mission is right at the CSSR cost cap in Fiscal Year 2007 dollars of $820 million.
- The bottom-up SEP mission cost estimate is comparable to a parametrically derived estimate based on the NAFCOM spacecraft cost model.

Detailed, bottom-up estimates of the Phases A–E costs were prepared for the SEP mission design by senior APL functional supervisors and lead engineers with the support of technical experts from Langley Research Center (LaRC), Johnson Space Center (JSC), Glenn Research Center (GRC), and AeroJet.

The total estimated cost of the SEP mission, $820 million in Fiscal Year 2007 dollars including unallocated cost reserves, is right at the $820 million CSSR cost cap. The mission cost, not including $5 million for Education & Public Outreach, is $676 million. Cost reserves and technology development account for the remaining $140 million, or 17%, of the total cost.

The SEP cost estimate with reserves is about 10% higher than the New Horizons funding requirement of $730M. The SEP mission's higher cost is reasonable given the relatively greater complexity of its mission and the fact that the New Horizons requirement excludes DSN charges.

5. ALTERNATE MISSION IMPLEMENTATION

The CSSR mission implementation minimizes risk while satisfying all baseline science objectives.

- The CSSR ballistic trajectory, conventional propulsion design reduces technical development risk by using only flight-proven technologies in the propulsion subsystem.
- Single spacecraft architecture reduces cost risk compared to multiple platform missions.
- MSR-style SRV provides technology advancements for future missions.
- Flexible sampling system facilitates return from a wide range of surface properties.
- Robust descope methodology provides programmatic flexibility.

Comet Surface Sample Return (CSSR) provides a bulk sample return using simple interfaces and flight-proven designs wherever possible. CSSR is developed with proven processes incorporating lessons learned from many past missions. Section 5 describes the ballistic trajectory conventional propulsion design. For those system elements that are the same as the SEP design, the reader is referred to the appropriate part of Section 4.

5.1 Mission Architecture Overview

CSSR science objectives drive the need for a complex mission design and spacecraft. To this end, a single spacecraft architecture using conventional propulsion has been defined incorporating a Mars Sample Return (MSR)-style sample return vehicle (SRV) and a drill-based sample acquisition system (SAS) to provide a robust mission with low development risk and risk mitigation options.

5.1.1 Draft Level I and Additional Driving Requirements

See Section 4.1.1.

5.2 Science Investigation

5.2.1 Science Instruments

See Section 4.2.1.

5.2.2 Sample Acquisition System

See Section 4.2.2.

5.2.3 Sample Return Vehicle

See Section 4.2.3.

5.3 Mission Design and Navigation

Key driving requirements for the mission design and navigation, flowed down from or in addition to those in Section 4.2.2, include the following:

- Prime and backup launch opportunities spaced as far as possible (>3 months)
- Launch on Atlas V
- Launch period at least 20 days
- Trip time minimized (>10 years preferred)

The selection of assessable comets for the ballistic mission design was described in Section 3. Trajectories to comets 67P/Churyumov-Gerasimenko (C-G) and 46P/Wirtanen (Wirtanen) were found to have the best overall performance in two 20-day launch windows. The first, adopted as the CSSR ballistic mission baseline, extends from December 22, 2014, to January 10,

2015, with C-G as the target. If for any reason that launch window cannot be met, there is a backup window from May 5 to 24, 2015, with Wirtanen the target.

5.3.1 Churyumov-Gerasimenko Baseline Launch Window

The baseline trajectory to C-G (Fig. FO5-1A) launches from the Eastern Test Range (ETR) on an Atlas 541. The first heliocentric orbit following injection by the Atlas 2nd stage is a ΔVEGA (ΔV-Earth Gravity Assist) orbit lasting just under 2 years. Near aphelion, 13 months after launch, the first deterministic ΔV maneuver, Deep Space Maneuver 1 (DSM-1) amounting to 649 m/s, is performed at a solar distance of 2.2 Astronomical Units (AU). Following the Earth gravity assist at an altitude of 300 km in early November 2016, the spacecraft enters a much larger orbit with a second ΔV maneuver, DSM-2, amounting to 774 m/s (on the first launch day) also near aphelion at a solar distance of 4.6 AU in late September 2019. Just before perihelion of this orbit, on October 1, 2021, the spacecraft reaches comet C-G and performs a 613-m/s ΔV maneuver (less later in the window) to rendezvous with the comet. This is 32 days before perihelion so the comet's activity can be observed through perihelion at a safe distance before proximity operations, described in Section 4, commence a few months after perihelion, by which time the comet's activity would decrease enough to safely descend to the comet surface. Proximity operations are completed in 6 months, well before the comet reaches a solar distance of 3.0 AU on August 1, 2022. After that, the spacecraft backs away from the comet to a safe distance. Over 2 years after arrival, on November 10, 2023, the spacecraft departs from the vicinity of the comet with a 751-m/s ΔV maneuver at a solar distance of 5.1 AU. On October 30, 2027, the spacecraft returns to Earth with a V_∞ of 10.1 km/s. The operations to capture the SRV in the Earth's atmosphere are described in Section 4. The solar and Earth distances over the course of the mission are shown in Fig. FO5-1B, while the basic angles are illustrated in Fig. FO5-1C.

Figure 5.3.1-1 gives information about the major events for the first day of the launch window (E.G.A. = Earth gravity assist [Earth swingby]). The Sun and Earth distances, and the trajectory perihelia and aphelia, are in AU, while all angles are in degrees. In this table, the phase angle is the angle that the Sun makes with the body's heliocentric velocity vector, or the ΔV vector in the case of maneuvers, called "space burns." The "Earth Angle" is like the phase angle, but for the Earth rather than the Sun. The "Earth Ph. A.," or Earth phase angle, is the Sun-Probe-Earth angle. The period of the orbit is in days. The pass distance is in planetary (equatorial) radii, while ΔV values are in m/s. The launch ΔV (1st line) is the ΔV that the launch vehicle upper stage gives the spacecraft at injection into the heliocentric orbit from the launch parking orbit, whose altitude is 185 km.

Event	Date			V_∞ (km/s)	Earth Dist.	Sun Dist.	Phase Angle	Earth Angle	Earth Ph.A.	Solar Elong.	Period	Inc.	Peri-helion	Aphe-lion	Pass Dist.	ΔV
	Year	Month	Day													
Launch	2014	Dec	22.8	5.15	0.000	0.984	283.0									4373.5
DSM-1	2016	Jan	31.7		3.115	2.197	88.5	96.4	7.9	17.8	735.6	0.0	0.98	2.21		649.2
E.G.A.	2016	Nov	8.5	9.49	0.000	0.991	158.1				697.4	0.0	0.87	2.21	1.05	0.0
DSM-2	2019	Sep	28.5		5.141	4.649	92.2	102.1	10.2	55.6	1771.7	5.0	0.98	4.75		774.2
Arrive C-G	2021	Oct	1.5	0.61	0.498	1.273	75.8	121.1	46.8	111.9	1887.3	3.7	1.21	4.77		609.6
Depart C-G	2023	Nov	10.9	0.75	6.108	5.129	76.2	178.5	105.3	7.8						751.5
Return	2027	Oct	30.4	10.07	0.000	0.993	117.3				2178.2	4.0	0.97	5.60		0.0

07-05866P-65

Figure 5.3.1-1. The C-G ballistic mission design minimizes the number of critical events necessary to reach the target and then return.

5.3.2 Launch

An optimum due-east launch from the ETR is possible for all days of the launch window. Liftoff will be just after 18h UT (1 PM EST). During the parking orbit coast phase, 20 minutes after launch, the second stage/spacecraft combination enters the Earth's shadow off the western coast of Africa. Fifteen minutes later, over southern Africa, the second stage fires, boosting the spacecraft to a C_3 orbital energy up to 26.6 km^2/s^2. Forty-four minutes after launch, high over the southern Indian Ocean, the spacecraft exits the Earth's shadow, enabling the solar panels to power the spacecraft. There is no shadow during the rest of the mission except when the SRC returns to Earth on the night side. The ground track is shown in Fig. FO5-1D, and a view showing the trajectory passing through the Earth's shadow is in Fig. FO5-1E.

5.3.3 Baseline Launch Window

Figure 5.3.3-1 lists launch C_3 and deterministic ΔV values for each day of the launch window. Both the highest C_3, 26.6 km^2/s^2, and highest total deterministic post-launch ΔV, 2785 m/s, occur on the first day of the window, December 22, 2014. The C_3 would be higher for a launch on the 21st day, January 11, 2015, so that and later dates are excluded. Data in Fig. 5.3.1-1 are given daily at the start and end of the window, needed to select the dates of the window, but only every other day in the middle of the window.

Date, 2014/2015	C_3 (km^2/s^2)	Total ΔV (m/s)	DSM-1 (m/s)	DSM-2 (m/s)	C-G Rendezvous ΔV (m/s)	C-G Depart ΔV (m/s)
Dec. 21*	26.794	2785.2	649	771.8	612.9	751.5
Dec. 22	26.56	2784.5	649.2	774.2	609.6	751.5
Dec. 23	26.35	2783.9	649.3	777	606.1	751.5
Dec. 24	26.164	2783.2	649.2	780	602.5	751.5
Dec. 26	25.863	2782.1	648.6	787.1	594.9	751.5
Dec. 28	25.656	2781.0	647.3	795.7	586.5	751.5
Dec. 30	25.543	2779.9	645.4	805.8	577.2	751.5
Jan. 1	25.521	2779.0	642.8	817.8	566.9	751.5
Jan. 3	25.588	2778.3	639.6	831.9	555.3	751.5
Jan. 5	25.744	2777.7	635.7	848.4	542.1	751.5
Jan. 7	25.985	2777.6	631.2	867.8	527.1	751.5
Jan. 9	26.307	2777.8	626	890.5	509.8	751.5
Jan. 10	26.498	2778.1	623.2	903.3	500.1	751.5
Jan. 11*	26.708	2778.6	620.2	917.3	489.6	751.5

* Date excluded from the planned 20-day launch window.

07-05866P-66

Figure 5.3.3-1. The baseline launch window provides a 20-day opportunity for a mission to C-G.

5.3.4 ΔV Budget

From the launch window in Section 5.3.1, we see that the highest total post-launch deterministic ΔV is 2785 m/s. But propellant will be used for other purposes, and enough must be supplied for a full mission ΔV budget, as detailed in Fig. 5.3.4-1. The heliocentric cruise navigation includes all trajectory correction maneuvers (TCMs) during the heliocentric cruise phases. The first TCMs correct launch injection errors. A 3σ value for an Atlas launch from a Titan mission study was 30 m/s for a C_3 of 15 km^2/s^2. Scaling this to our maximum of 26.6 gives 53 m/s; we will round that to 50 m/s, assuming the extra 3 m/s can be considered margin, or in the noise of

our scaling. TCMs needed to clean up errors in the deterministic maneuvers are considered to be 1.5% of the maneuvers. The similar bi-propellant accelerometer-controlled DSMs for both the NEAR and MESSENGER missions have been accurate to under 1% so this should be conservative; anything more would be part of the margin; 1.5% of 2785 m/s is 42 m/s. TCMs are also needed to target the B-planes of planetary flybys and target body arrivals due mainly to orbit determination errors. For these, the experience with NEAR and MESSENGER is a little less than 4 m/s per event. For CSSR, there is one Earth swingby, an arrival at C-G, and return to the Earth, or three events for a total of 12 m/s. So, the total cruise navigation ΔV is 50 + 42 + 12 = 104 m/s, the number specified in Fig. 5.3.4-1. Comet proximity operations are based mainly on NEAR's experience; see Section 4, which shows that these should amount to 58 m/s (including margin). Experience with other three-axis stabilized heliocentric missions, including NEAR, MESSENGER, and STEREO, show that, for the CSSR spacecraft mass, 1 kg of hydrazine per year can be expected to be used for attitude control and momentum management; for the almost 13-year duration, 13 kg is allocated, equivalent to ~24 m/s of ΔV.

ΔV	Purpose
2785	Maximum total post-launch deterministic ΔV
104	Heliocentric cruise navigation
50	Comet proximity operations
24	Attitude control
2963	Subtotal
3407	Total including 15% margin

07-05866P-67

Figure 5.3.4-1. The baseline ΔV budget provides 15% margin for the worst-case estimate.

5.3.5 Wirtanen Backup Launch Window

If for any reason the C-G baseline is missed, there is another opportunity 5 months later with slightly better performance (lower launch C_3 and lower total post-launch ΔV) allowing the same architecture to be used for both windows. The backup trajectory to Wirtanen also launches from the ETR on an Atlas 541. The trajectory has no deterministic DSMs; rather, it uses two swingbys of Venus and one of the Earth to reduce the launch C_3 to reach the comet. This trajectory is a variant of the WASP study trajectory [Block & Singer 2007] but has significantly better performance than WASP because the stay time at Wirtanen is not constrained by using another orbit to get back to Earth (that is, returning in 2028 rather than in 2023). This is necessary since, in order to keep 6 months of proximity operations at the comet within 3 AU of the Sun, the shorter WASP trajectory cannot be used because the solar distances while at the comet are too great. The backup trajectory to Wirtanen is shown in Fig. FO5-1F, and the event information, similar to that for C-G in Fig. 5.3.1-1, is given in Fig. 5.3.5-1. Fig. 5.3.5-1 is like Fig. 5.3.1-1 except that, if just a planet's name is given, the event is a swingby of that planet. The solar and Earth distances over the course of the mission are shown in Fig. FO5-1G, while the basic angles are illustrated in Fig. FO5-1H.

Event	Date			Excss Speed	Earth Dist.	Sun Dist.	Phase Angle	Earth Angle	Earth Ph.A.	Solar Elong.	Period	Inc.	Peri-helion	Aphe-lion	Pass Dist.	ΔV
	Year	Month	Day													
Launch	2015	May	5.362	4.56	0.000	1.008	114.0									4134.0
Venus	2015	Aug	27.130	8.53	0.306	0.728	169.6	26.7	153.4	18.8	268.339	3.8	0.61	1.02	1.68	0.0
Venus	2016	Dec	28.298	8.51	0.797	0.723	41.2	121.7	80.5	46.5	456.831	3.4	0.69	1.63	1.05	0.0
Earth	2019	Jan	20.908	14.64	0.000	0.984	7.5				705.454	1.9	0.72	2.38	1.21	0.0
Arrive Wir.	2020	Apr	20.291	1.56	3.246	4.163	108.4	109.7	6.4	152.4	1777.641	6.6	0.85	4.89		1560.2
Depart Wir.	2024	Oct	24.581	0.81	3.044	2.135	69.3	170.9	119.0	19.8						814.8
Return	2028	Dec	13.280	11.06	0.000	0.984	75.9				1665.670	11.8	0.98	4.52		0.0

07-05866P-68

Figure 5.3.5-1. The Wirtanen ballistic mission design uses planetary flybys to lower the required mission ΔV.

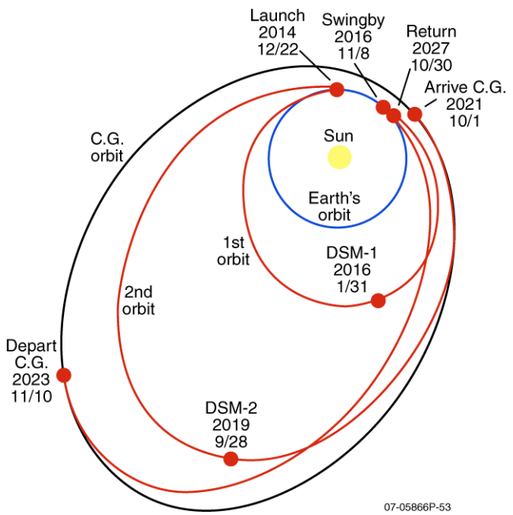

A. Ecliptic-plane plot of CSSR trajectory to/from comet C-G, 1st day of launch window.

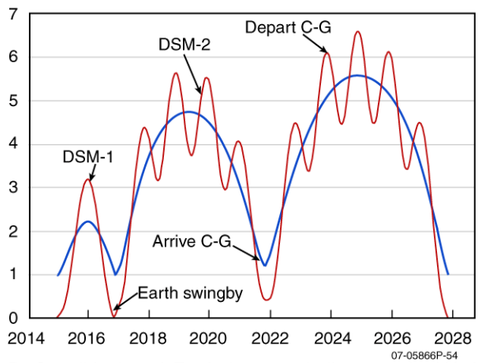

B. Sun (blue) and Earth (magenta) distances in AU during the mission.

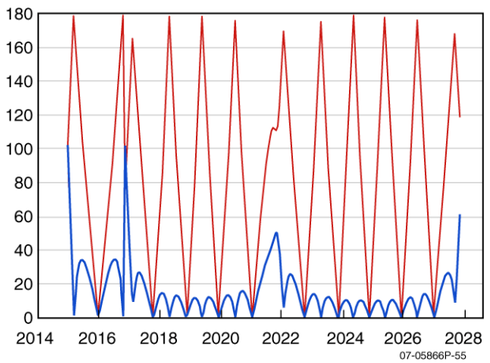

C. Phase (Sun-Probe-Earth, blue) and solar elongation (Sun-Earth-Probe, magenta) angles, in degrees, during the mission.

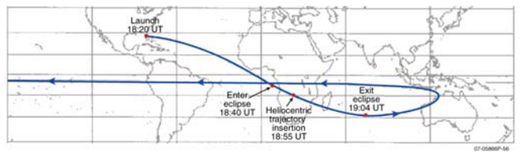

D. Ground track and major launch events for launch on January 1, 2015.

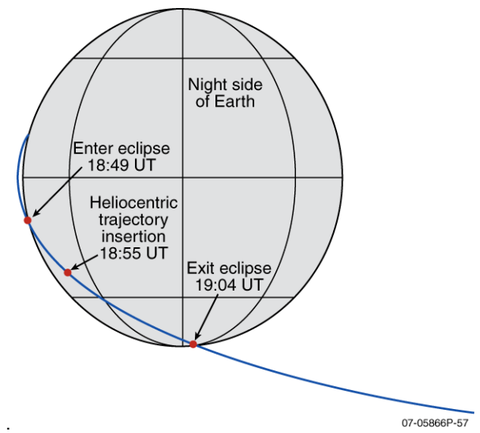

.

E. View of trajectory looking toward the Sun (launch on January 1, 2015).

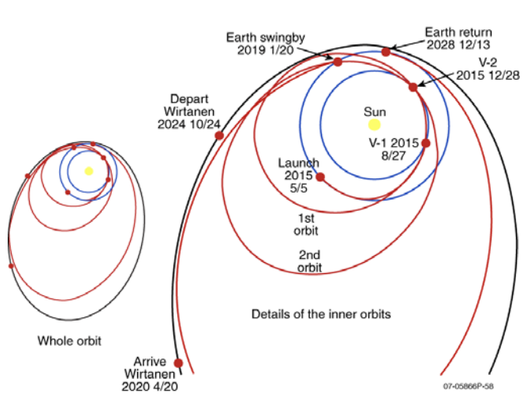

F. Ecliptic-plane plot of CSSR trajectory to/from comet Wirtanen, 1st day of launch window. V-1 and V-2 are Venus gravity assists (swingbys).

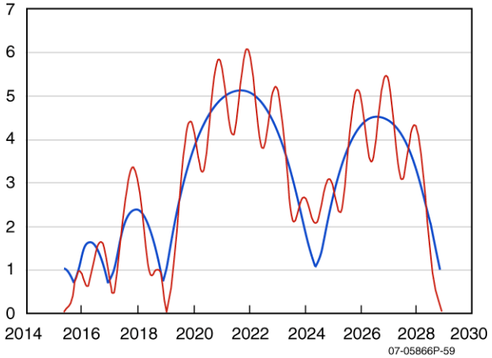

G. Sun (blue) and Earth (magenta) distances in AU during the mission.

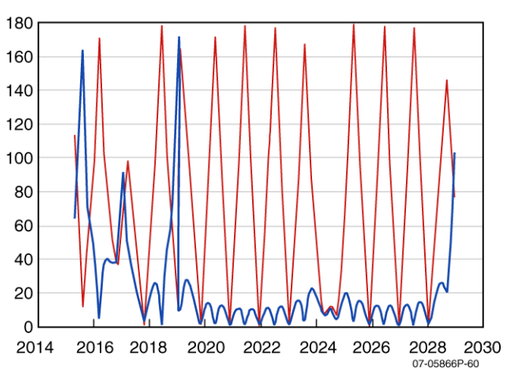

H. Phase (Sun-Probe-Earth, blue) and solar elongation (Sun-Earth-Probe, magenta) angles, in degrees, during the mission.

Foldout 5-1. Ballistic mission design.

5.3.6 Backup Launch Window

Figure 5.3.6-1 lists launch C_3 and deterministic ΔV values for each day of the launch window. The highest C_3, 21.0 km^2/s^2, occurs on the first day of the window, while the highest total deterministic post-launch ΔV, 2407 m/s, occurs on the last day. Data in Fig. 5.3.6-1 are given daily at the start and end of the window, needed to select the dates of the window, but only every 4^{th} day in the middle of the window. A separate ΔV budget has not been prepared, but the almost year-longer increase in attitude control, as well as costs for more planetary swingbys, will be more than offset by the over 350 m/s less total post-launch ΔV than the baseline.

Launch Date May 2015	C_3 (km^2/s^2)	Total ΔV (m/s)	Wirtanen Rendezvous ΔV (m/s)	Wirtanen Depart. ΔV (m/s)
4*	21.037	2385.4	1570.6	814.8
5	20.791	2375.0	1560.2	814.8
6	20.551	2365.5	1550.7	814.8
10	19.661	2337.5	1522.7	814.8
14	18.897	2326.8	1512	814.8
18	18.282	2336.8	1522	814.8
22	17.846	2374.0	1559.2	814.8
23	17.77	2389.0	1574.2	814.8
24	17.707	2406.9	1592.1	814.8

* Date excluded from the planned 20-day launch window.

07-05866P-69

Figure 5.3.6-1. The backup launch window provides a 20-day opportunity for a mission to Wirtanen with >15% ΔV margin over the worst-case estimate.

5.4 Flight System Design and Development

Discussion of the flight system design and development approach, including the use of new versus existing hardware and software and fault tolerance, is included within the following sections. The manufacturer and flight heritage information provided assumes that the vehicle is being built today. This information is representative, and it is expected that a project will leverage additional advancements and flight heritage that occur between now and project start.

The technology readiness level (TRL) for each component is estimated based on current technology. All components are considered TRL>6 except for the SAS, SRV, and the height and motion subsystem (H&MS), as there are no additional exotic requirements and existing representative heritage components for each subsystem. For any component considered TRL<6, technology development required to bring the level to TRL 6 by Preliminary Design Review (PDR) is described in Section 4.8. The technology costs are included in the total project cost where applicable.

5.4.1 Flight System Overview

Key features and benefits of the flight system are listed in Fig. 5.4.1-1. The spacecraft design heavily leverages heritage from previous and current APL missions: MESSENGER, STEREO, New Horizons, and Radio-Belt Sensor Probes (RBSP). Design flexibility allows commonality on the avionics, telecommunications, and guidance, navigation, and control (GN&C) subsystems between the ballistic architecture presented here and the low-thrust architecture presented in the

previous section. The ballistic mission chemical propulsion subsystem is a pressure-regulated dual-mode system that provides delta-V and attitude control capability during all phases of the mission. The mechanical spacecraft designs for both the ballistic and low-thrust missions are simple and efficient, with a center cylinder as the primary load-bearing structure that interfaces directly with the launch vehicle. Lessons learned from previous missions are incorporated to simplify development, integration and testing (I&T), and flight operations. The design is compatible with all evolved expendable launch vehicles (EELVs). However, the Atlas 541 is baselined for the chemical propulsion design and the Atlas 521 is baselined for solar electric propulsion (SEP) design to reduce the cost risk of the mission. The mass and power budgets are shown in Fig. 5.4.1-2.

Feature	Benefit
70-m Equivalent Ka DSN Capability During Orbit and Critical Events Only	Reduces onboard requirements (HGA size, power); reduces DSN time to satisfy requirements; 34-m baseline for cruise reduces mission cost
Front/Back Phased Array Antennas	Facilitates higher bandwidth communications during electric propulsion thrusting and proximity operations; eliminates the need for an antenna gimbal
Ballistic-type SRV	Eliminates the need for a parachute and spin table; feeds forward into MSR program
UltraFlex Solar Arrays	Reduced S/C launch mass; leverages NASA exploration investment
Height and Motion System	Provides improved accuracy for sampling site; ensures S/C velocities are nulled during proximity operations simplifying sampling scenario and eliminating the need to land; autonomous abort capability reduces mission risk
Sample Acquisition System	Active drills facilitate sampling over a wide range of surface properties; allows “touch and go” sampling, eliminating the need to land; single mechanism used to acquire and to store the sample
Chemical Propulsion System	Heritage design; lower mission operations cost

07-05866P-78

Figure 5.4.1-1. The CSSR architecture features provide multiple benefits.

Subsystem	CBE Mass (kg)
Payload	127
Avionics and Power	227
Telecommunications	38
GN&C	52
Thermal	54
Propulsion	159
Structure	309
Harness	27
Total Dry Mass	993
Propellant & Pressurant	2602
Total Wet Mass	3595
Max Launch Mass	3920 (3892 design)
Dry Mass Margin	30%

07-05866P-95a

Subsystem	Cruise Power (W)	Orbit Power (W)	Sampling Power (W)
Payload	1	21	13
Avionics and Power	71	71	65
Telecommunications	68	187	68
GN&C	85	85	121
Thermal	156	169	169
Propulsion	3	3	3
Harness	6	8	7
Total Power	389	544	446
Margin	34%	Max range cruise is worst-case	

07-05866P-95b

Figure 5.4.1-2. The CSSR mass and power budgets demonstrate significant margin that meet APL design requirements.

5.4.2 Propulsion Subsystem

The CSSR propulsion subsystem is a pressure-regulated, dual-mode system that provides delta-V, attitude control, momentum management, and landing/liftoff capability. Pressure-regulated systems of this size and type have significant flight history. All components, including commercial off-the-shelf (COTS) propellant and pressurant tanks, have extensive flight heritage. The system is built around the Intelsat-9-heritage Aerojet HiPAT 400 N engine: a proven, highly reliable, bipropellant apogee engine with a wide operating range. CSSR also incorporates 22 monopropellant thrusters with substantial flight heritage: four 20 N Aerojet MR-106E steering thrusters and 18 Aerojet 1 N MR-103G ACS thrusters. The dual-mode system, shown in Fig. 5.4.3-1, will be procured as a complete system from a subcontractor.

Several flight-proven options exist for each component of the propulsion system; therefore, the tanks, as well as all other heritage items, will not require qualification testing. There will be one ETS-8-heritage hydrazine tank, one TEMPO-heritage oxidizer tank, and three identical Lockheed Martin A2100-heritage pressurant tanks. Different propellant management devices (PMDs) will be developed for inside the propellant tanks. The baseline propellant load for CSSR is 1110 kg of hydrazine and 858 kg of oxidizer. For a 2968-kg launch wet mass, this provides 3407 m/s of ΔV. The remaining components used to monitor and control the flow of propellant—latch valves, filters, orifices, check valves, pyro valves, pressure regulators, and pressure and temperature transducers—will be selected from a large catalogue of components with substantial flight heritage on APL and other spacecraft.

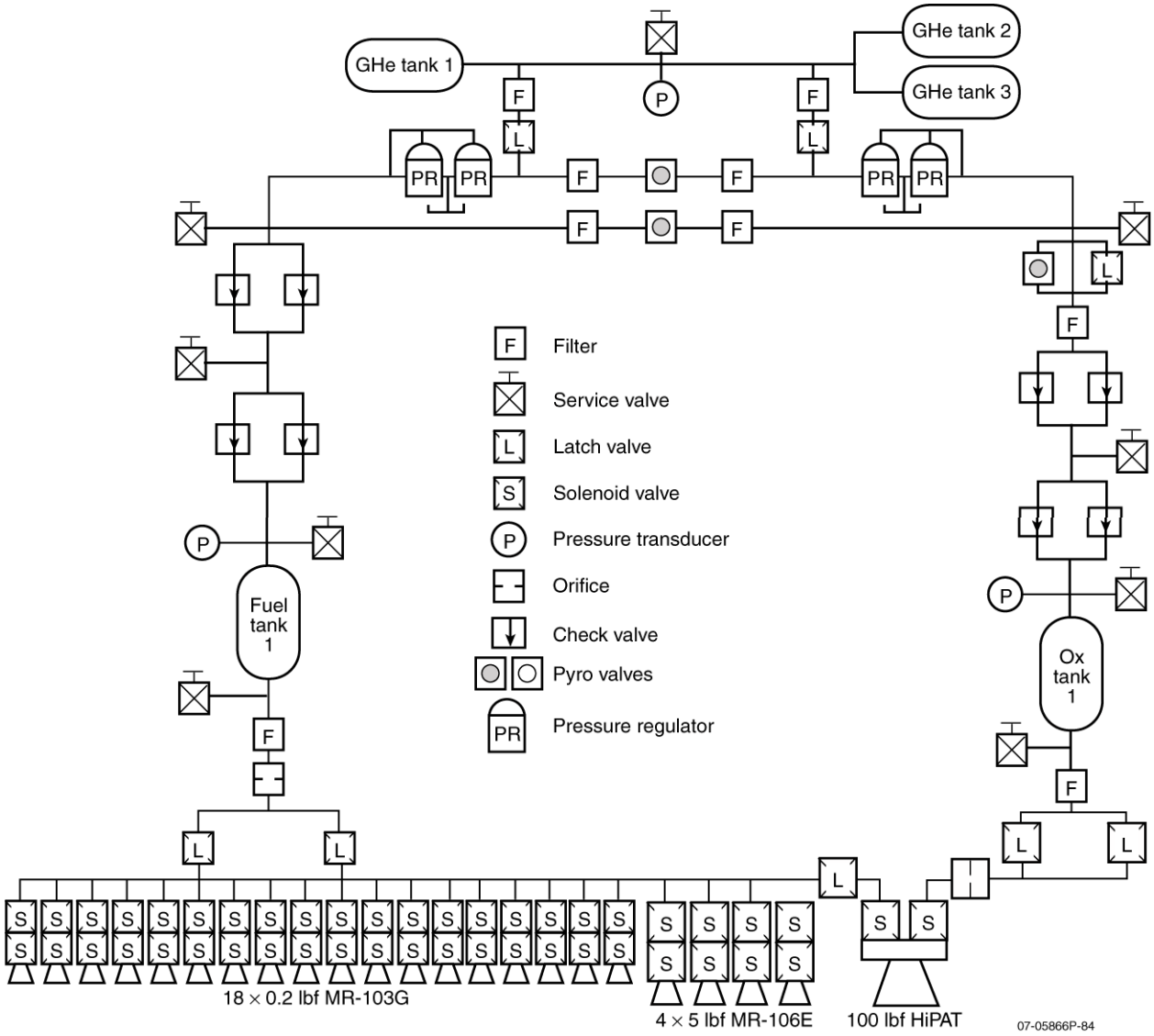

Figure 5.4.3-1. The ballistic mission CSSR propulsion subsystem schematic depicts a heritage dual-mode system.

5.4.3 Communications Subsystem

See Section 4.4.3.

5.4.4 Power Subsystem

The power subsystem uses peak power tracking electronics with photovoltaic solar array wings for electrical power generation and a lithium-ion battery for energy storage. Power electronics are contained within the power system electronics (PSE) box and two solar array junction boxes (SAJBs). The spacecraft block diagram in Section 4 includes a simplified diagram of the power subsystem.

The power bus voltage is unregulated and is specified to operate within the range of 22 V to 35 V. The peak power tracking electronics, with flight heritage from the MESSENGER and STEREO spacecraft, isolates the battery-dominated bus voltage from the solar array voltage and maximizes solar array output over the widely varying operating conditions.

The power subsystem is designed to provide at least 400 W of load power to support cruise between near-Earth and 5.6 AU distance from the Sun. For orbit operations at the comet, 660 W can be supported indefinitely at a Sun distance of up to 4.2 AU. The battery supports the load during times when solar array power may not be available (e.g., launch and comet descent) and when the load exceeds solar array output, such as during comet sampling, when up to 900 W can be supported.

The power subsystem is single-fault tolerant. Full redundancy is provided for power electronics control circuits and command/telemetry paths. Subsystem sizing is such that the loss of a battery cell or several solar cells would not degrade mission performance. Also, the mission requirements would still be met even with a failure of one of the multiple, parallel power converter modules.

The PSE performs solar array peak power tracking, battery charge control and cell balancing, and bus overvoltage protection. The PSE contains nine peak power tracker (PPT) modules, two PPT controller slices, two command/telemetry interface slices, one filter slice, and two slices associated with battery interfaces including cell balancing. The PSE provides primary power to the power distribution unit (PDU) and has a serial digital command/telemetry interface with the integrated electronics module (IEM). Each PPT module is a pulse-width-modulated buck-topology dc/dc converter using current mode control.

The PPT and controller circuits have heritage from the STEREO and MESSENGER spacecraft. The peak power tracking algorithm, proven on those missions, is contained within the IEM main processor. The other slices are planned to be similar or identical to those for the RBSP spacecraft, presently in detailed design.

The two SAJBs feed power to the PSE PPT modules. Included in the SAJBs are solar array string isolation diodes and solar array current sensors. The SAJB design is similar to that flown on MESSENGER and STEREO.

The solar array (S/A) consists of two wings, each with 10 flexible blankets (gores) that deploy to form a disk-shaped structure. The ATK UltraFlex S/A wing design has been baselined due to its low mass, high strength, high stiffness, and compact stowage volume. This design has spaceflight heritage on the Mars Phoenix Lander. A larger S/A wing design, similar to the size needed for CSSR, is under development for NASA's Orion crew exploration vehicle. Each wing is independently articulated in two axes to maintain Sun pointing. Triple-junction, GaAs-based solar cells are used on the S/A. It is planned that standard-production, spaceflight-qualified cells will be screened for low-intensity, low-temperature (LILT) performance, similar to the approach used by the Dawn and Juno missions. For CSSR, the total S/A blanket area on both wings is approximately 50 m^2.

Although improved solar cells with increased efficiency are expected in the near future, the power analysis conservatively assumes a 28% minimum average efficiency (beginning of life, standard test conditions), as such spaceflight quality production-run cells are currently available and have been qualified and flown. While the spacecraft performance will benefit from further improvements in solar cell efficiency, it is recognized that newly developed cells will need to be characterized and qualified for the LILT conditions. Such a test program is planned early in the program in addition to the LILT screening during the flight production.

The solar cell LILT performance was estimated out to 5.6 AU using data from the Dawn cell characterization testing (out to 3 AU) and performance predictions for the Juno solar array (to 5.5 AU). The estimates consider uncertainties related to cell yield, screening versus operating conditions, and effects of sorting cells into strings.

Power analysis was performed taking into account the solar cell LILT operating conditions, solar array optical, assembly, and wiring losses, and degradation due to ultraviolet radiation, charged particle radiation, micrometeoroid impacts, and thermal cycling fatigue. Other power system losses that are modeled include S/A string isolation diodes, dc/dc power conversion efficiency, peak-power tracking accuracy, load power service components, power subsystem wiring, and spacecraft wiring harness.

The battery has a nameplate capacity of 50 Ah and contains eight spaceflight-qualified lithium-ion cells in series. Advantages of lithium-ion cells are their high energy density, good cycle life, non-magnetic materials, and successful spaceflight heritage. The battery design is planned to be identical to the battery assembly being developed for RBSP. Battery cell balancing and bypass control circuits are included within the PSE.

The battery capacity is driven by maximum discharge rate during peak loads and the power during comet descent, where it is conservatively assumed that there is no solar array power available during that time due to solar array off-pointing to minimize mechanical loads. The maximum battery depth of discharge is expected to be no more than 55%.

5.4.5 Structural/Mechanical Subsystems

The CSSR structure design is simple and efficient (Foldout 5-2). The primary load path is a 119-cm aluminum honeycomb, aluminum facesheet composite center cylinder, which interfaces with the launch vehicle using its attached separation ring. The two large propulsion tanks and the interface structure for the sampler and the sample return vehicle are mounted directly to the cylinder. On the lower part of the cylinder, two bulkhead panels, spaced 180° apart, run down the cylinder between top and bottom equipment section decks. Equipment is then mounted to two panels that close out the prismatic rectangular structure along with two light close-out panels. On the upper part of the cylinder, two panels that are parallel to the top and bottom decks are separated by four gussets. The top-most panel is used for accommodating ACS thrusters, the IR imager, the two panchromatic imagers, and the phased array antenna. The cylinder is 330 cm tall, and the avionics box structure is 130 cm tall, 148 cm wide, and 188 cm deep. Attaching the highest mass components (tanks, SAS, SRV) directly to the cylinder and reacting the loads from the equipment and solar arrays directly into the cylinder enables a structure that is 8% of the launch mass. The honeycomb cylinder is a common element among domestic geosynchronous communication satellites, and the box structure is very similar to the flight-proven STEREO structure.

The only mechanisms on the bus are associated with the S/As. The S/A selected for the study implementation consists of two ATK-built UltraFlex wings, very similar to the wing in development for the Crew Exploration Vehicle (CEV). Each of the S/A wings is pointed by a two-axis gimbal. The two-axis gimbals allow efficient energy collection and off-pointing the arrays, which minimizes loads on the array during sampling operations and minimizes sampling-induced contamination on the arrays. During launch, the lower array tie-downs mount through the equipment panels into the bulkheads, which react load to the center cylinder. The upper array tie-downs mount to the top deck of the structure, which reacts load back to the center cylinder.

A. The spacecraft can be stowed in the smallest Atlas V 5-m fairing.

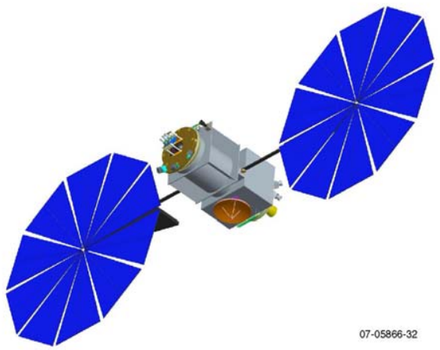

B. Two-axis gimbals allow complete freedom in pointing the UltraFlex arrays.

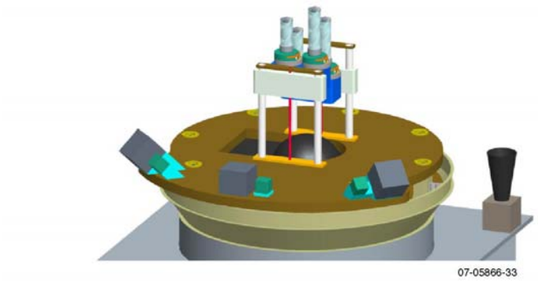

C. The SAS, shown in pre-sampling configuration, is thermally isolated from the bus. Its placement protects the bus from contamination during sampling operations.

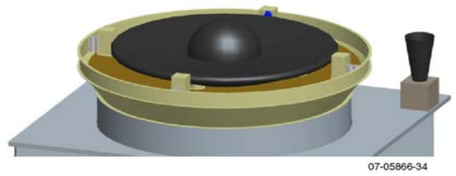

D. The SAS support panel separates from the spacecraft, reducing mass for the cruise back to Earth. Jettisoning the panel allows a near-complete field of view to cold space for the SRV, preserving the sample.

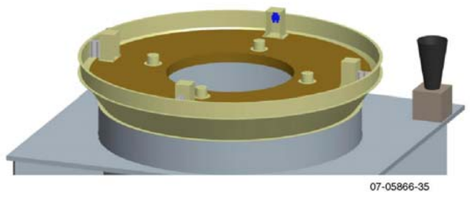

E. The SRV deploys with a simple pyrotechnic actuator and separation spring system.

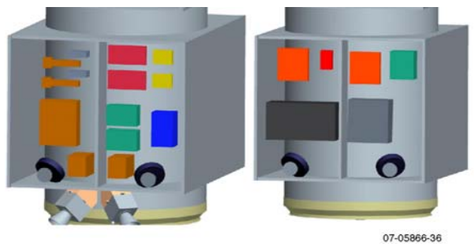

F. The star tracker locations minimize contamination from sampling operations.

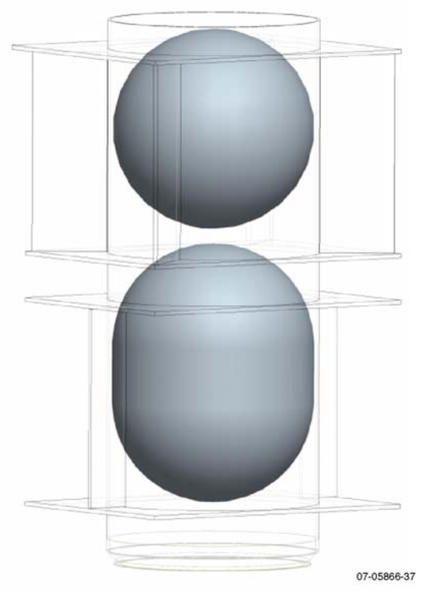

G. Direct load paths enable an 8% primary structure mass. Weld-seam flexure skirt tank interfaces efficiently transfer load into the center cylinder.

Foldout 5-2. Ballistic mission spacecraft layout.

The study implementation takes advantage of the CEV wing development. The CEV array size is similar and the load requirements (3 g, each axis when deployed) envelop those for CSSR during sampling (0.15 g at spacecraft center of gravity [CG]). The UltraFlex wings boast reduced mass (~50% of conventional arrays). They lower spacecraft inertia because of their circular shape, which puts the CG of the wings closer to the spacecraft. The industry-best mass per watt contributes significantly to spacecraft mass reduction on this deep space mission. The lower mass and inertias contribute significantly to the stability of the spacecraft during proximity operations because they minimize CG shifts when off-pointed.

During launch, the SAS and SRV are protected from contamination by a shroud, which is separated by pyrotechnic actuators and separation springs. The panel that accommodates the sampler and the panel that restrains the SRV are attached to a rigid spacer, which is mechanically isolated from the spacecraft using shock mounts. The rigid spacer ensures co-alignment between the sampler and SRV during sampling and sample stowage operations. The shock mounts limit the loads into the sampler and acceleration seen by spacecraft appendages. Following sampling operations, the panel that accommodates the sampler and the height and motion sensing equipment is jettisoned from the spacecraft by pyrotechnic actuators and separation springs. Prior to reentry operations, the spacecraft is spun to 2 rpm, and the sample return vehicle is jettisoned from the spacecraft by pyrotechnic actuators and separation springs. The pyrotechnic actuators, incorporated into hold-down and release mechanisms have heritage to various APL spacecraft (TIMED, MESSENGER, and STEREO).

5.4.6 Thermal Control Subsystem

The CSSR ballistic thermal control subsystem provides a low-risk design approach using passive thermal control including heat pipes and multi-layer insulation (MLI). Waste heat from electronics will be distributed throughout the MLI-covered structure, greatly reducing the need for heater power. All electronics are directly coupled to the structure. Heat dissipated by electronics is spread throughout the structure by conduction and thermal radiation. The propulsion components are isolated from the bus and controlled with heaters. High-power electronics like the SSPAs and TWTs will be placed on a heat pipe radiator panel in order to reduce the required radiator area and heater power. The bus consists of seven thermal zones that are independently controlled. The temperature of each zone is shown in Fig. 5.4.7-1. Figure 5.4.7-2 shows the block diagram of the thermal control system.

Component	Temperature limit (°C)
Spacecraft Electronics	–20 to +40
HGA/Phased Array	–90 to +90
Solar Arrays	–125 to +100
Instrument Interface	–20 to +40
Star Trackers	–20 to +60
Battery	+5 to +30

07-05866P-46

Figure 5.4.7-1. The thermal system uses waste heat to minimize heater power.

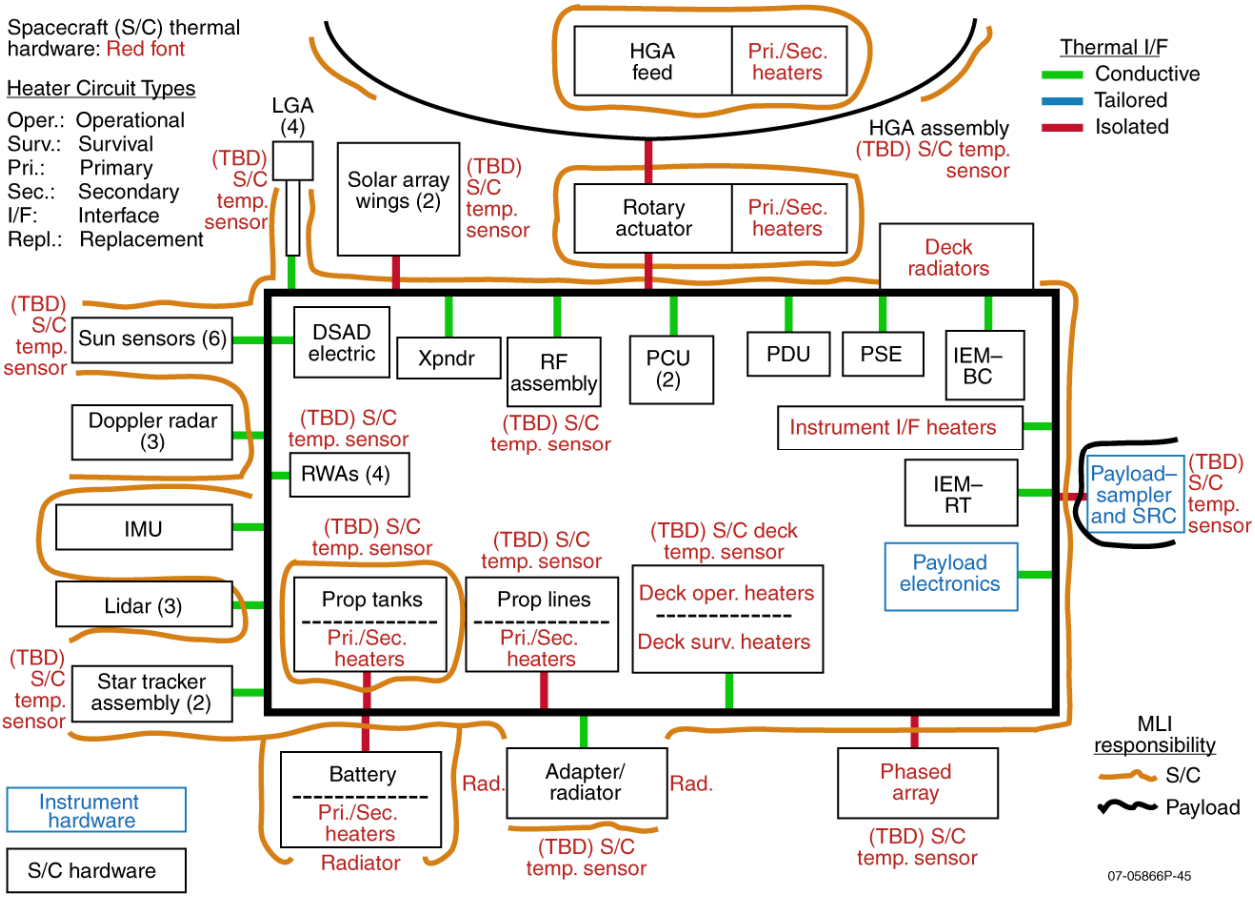

Figure 5.4.7-2. The system is divided into thermal zones to group components with similar temperature requirements and to optimize heater performance.

The bus is required to survive in cruise mode from 1 AU to 5.6 AU. The 5.6-AU case is the cold case. The bus and sampler are required to operate at approximately 2 AU. This is the peak power condition and therefore the hot case. The hot case drives the required radiator area of the bus to be 1.3 m^2. This radiator area and the minimum bus power lead to a required heater power of 236 W. This includes 152 W of propulsion heaters, W of payload heaters, 16 W of battery heaters, 20 W of star tracker heaters, and the remainder in bus heaters.

The thermal control of the sampler and SRV is all passive. The SRV is thermally isolated from the bus and the sampler is thermally isolated from the SRV. The contamination shroud surrounding the sampler will be deployed 2 days before sampling, which will allow the sampler and sample canisters to cool down. This allows sampling at the surface at –10°C or colder and maintains the samples inside the SRV below –10°C until reentry. During and after reentry, wax packs inside the payload volume of the SRV keep the samples below –10°C for 2 hours after landing in the given capsule environment.

5.4.7 Avionics Subsystem

See Section 4.4.7.

5.4.8 Flight Software

See Section 4.4.8.

5.4.9 Guidance, Navigation, and Control Subsystem

See Section 4.4.9.

5.4.10 Fault Protection

See Section 4.4.10.

5.4.11 Assembly, Test, and Launch Operations

See Section 4.4.11.

5.5 Concept of Operations

The concept of operations for the ballistic CSSR mission is similar to that presented for the SEP mission in Section 4.5. The primary delta is the use of a ballistic trajectory in place of the NEXT engine that will alter execution of the cruise phases and the timing between phase boundaries. Figure 5.5-1 shows the post-launch phases of the ballistic version of the CSSR mission:

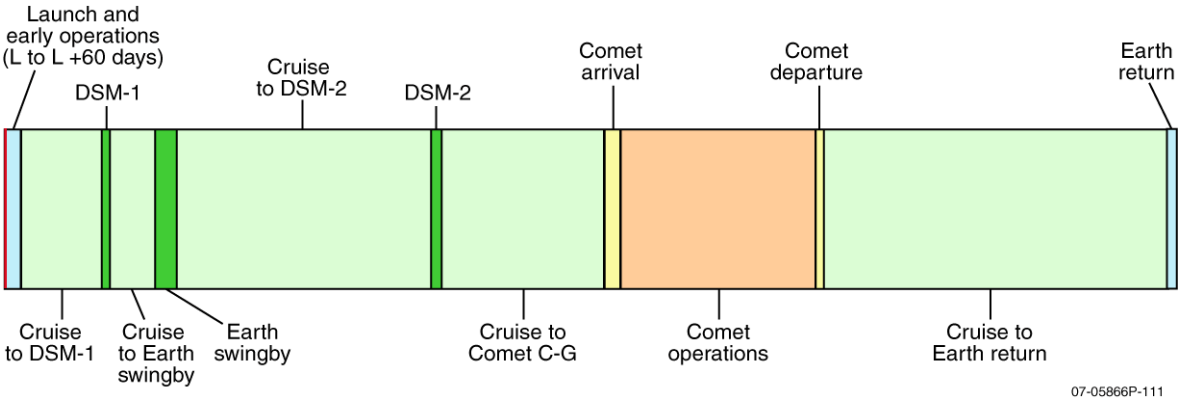

Figure 5.5-1. The ballistic CSSR post-launch operations period contains several distinct phases of activity, with traditional ΔV events and extended time at the comet.

This section only considers deviations in the concept of operations for this alternate approach, while deltas to the spacecraft's technical design are covered earlier. The descope of the NEXT engine means that the necessary ΔV changes must be enacted using the traditional methods of key propulsive events and the addition of an Earth swingby.

The principal operational activities during the launch and 60-day early operations phase will consist of the same commissioning and checkout events as the SEP mission, except that the NEXT engine testing shall be eliminated.

The cruise phases for the ballistic trajectory shall use beacon hibernation mode with full spacecraft checkouts no less than every 6 months. In place of the NEXT engine thrust arcs, the ballistic mission necessitates two DSMs and an Earth swingby gravity assist maneuver en route to comet C-G. The DSN schedule for a ballistic trajectory for the 2014/2015 launch is shown in Fig. 5.5-2 and for the 2016 backup launch window and mission to comet Wirtanen in Fig. 5.5-3.

Mission Phase	Period (days)	Days from Launch	DSN Contact
Early Operations	L to L+6 L+7 to L+20 L+21 to L+60	0–6 7–20 21–60	Continuous 8 h/d 2×8 h/wk
Cruise to DSM1	L+61 to DSM1−11	61–394	Beacon hibernation mode† One checkout every 6 months‡
DSM1	DSM1−10 to DSM1−1 DSM1−1 to DSM1+1 DSM1+1 to DSM1+30	395–404 404–406 406–435	2×8 h/wk Continuous 2x8 h/wk
Cruise to Earth Swingby	DSM1+31 to E−61	436–626	Beacon hibernation mode One checkout every 6 months
Earth Swingby	E−60 to E−11 E−10 to E−2 E−2 to E+2 E+2 to E+40	627–676 677–685 685–689 689–727	3×8 h/wk 8 h/d Continuous 3×8 h/wk
Cruise to DSM2	E+41 to DSM2−11	728–1730	Beacon hibernation mode One checkout every 6 months
DSM2	DSM2−10 to DSM2−1 DSM2−1 to DSM2+1 DSM2+1 to DSM2+30	1731–1740 1740–1742 1742–1771	2×8 h/wk Continuous 2x8 h/wk
Cruise to C-G	DSM2+31 to C-G−61	1772–2414	Beacon hibernation mode One checkout every 6 months
C-G Arrival	A−60 to A−21 A−20 to A−8 A−7 to A	2415–2454 2455–2467 2468–2475	3×8 h/wk 8 h/d Continuous
C-G Operations	A to A+10 A+11 to A+180 3 Landings, L−2 to L+2 A+181 to Departure −5	2475–2485 2486–2655 3–4 d periods TBD between 2595 & 2655 2656–3240	Continuous 3x8 h/wk (but each month, 1 wk 8 h/d & 2 d continuous) Continuous 3x8 h/wk less than 3 AU; 8h/wk more than 3 AU from Sun
C-G Departure	D−5d to D−1d D−1d to D+1d D+1d to D+30d	3240–3244 3244–3246 3246–3275	8h/d Continuous 3x8 h/wk
Cruise to Earth Return	D+31 to R–61	3276–4634	Beacon hibernation mode One checkout every 6 months
Earth Return	R–60 to R–11 R–10 to R–5 R–4 to R+2 R+2 to R+20	4635–4684 4685–4690 4691–4697 4697–4715	3×8 h/wk 8 h/d Continuous 3×8 h/wk

† Beacon hibernation mode is 1×1.5 h/wk (carrier only). 07-05866P−104

‡ Checkout is 20 d operations, 2×8 h/wk, every 6 months.

Figure 5.5-2. DSN schedule for CSSR 2014/2015 launch and mission to comet C-G achieves all mission objectives, including a 2027 sample return, using a ballistic trajectory.

Mission Phase	Period (days)	DSN Contact
Early Operations	L to L+6 L+7 to L+20 L+21 to L+60	Continuous 8 h/d 2×8 h/wk
Cruise to Venus1	L+61 to V1–60	Beacon hibernation mode† One checkout every 12 months‡
Venus and Earth Swingbys	E–60 to E–11 E–10 to E–2 E–2 to E+2 E+2 to E+40	3×8 h/w 8 h/d Continuous 3×8 h/w
Cruises Between Swingbys	E+40 to E–60	Beacon hibernation mode One checkout every 12 months
Cruise to Wirtanen	E+41 to C-G–61	Beacon hibernation mode One checkout every 12 months
Wirtanen Arrival	A–60 to A–21 A–20 to A–8 A–7 to A	3x8 h/wk 8 h/d Continuous
Wirtanen Operations (P is perihelion in 2018)	A to A+3 A+4 to A+16 A+16 to P–120 P–120 to P+120 3 Landings, L–2 to L+2 P+120 to Departure –5	Continuous 3x8 h/wk (but each month, 1 wk 8 h/d & 2 d continuous) 1x4 h/wk (but each month, 1 wk 3x8 h/d) 3x8 h/wk (but each month, 1 wk 8 h/d & 3 d continuous) Continuous 3x8 h/wk
Wirtanen Departure	D–5d to D–1d D–1d to D+1d D+1d to D+30d	8 h/d Continuous 3x8 h/wk
Cruise to Earth Return	D+31 to R–61	Beacon hibernation mode One checkout every 12 months
Earth Return	R–60 to R–11 R–10 to R–5 R–4 to R+2 R+2 to R+20	3×8 h/wk 8 h/d Continuous 3x8 h/wk

† Beacon hibernation mode is 1× 1.5 h/wk (carrier only) 07-05866P-105

‡ Checkout is 20 d operations, 2× 8 h/wk, every 12 months

Figure 5.5-3. Backup DSN Schedule for CSSR 2015 launch and mission to comet Wirtanen achieves all mission objectives, including a 2028 sample return, without significant changes to the mission design and implementation.

In addition, propulsive activities will be required to settle into orbit at the comet, and again to initiate the departure for return to Earth. These operations will be considered part of the comet arrival and departure phases shown above, but will consist of proven activities performed on previous APL missions and will leverage experiences and lessons learned from the NEAR, Stardust, and Deep Impact missions.

The activities and operations planned at the comet remain unchanged in either goal or design from those describe for the SEP mission in Section 4.5.3. Once the spacecraft is in orbit around the comet, the operational events of studying the local environment, mapping the surface, and developing the DEM shall take place starting at an altitude of approximately 100 km. The spacecraft will then settle into the Home State orbit position. Landing sites will be identified,

practice landing attempts performed, followed by the designated sample collection "touch-and-go" landing. Multiple attempts will be possible, and the abort mechanisms back to the Home State shall remain unchanged and available to the mission. In fact, the ballistic alternative offers greater time at the comet for science activities although this additional time may be unnecessary and comes with other costs such as increased mission weight. Once science activities at the comet are complete, the spacecraft shall depart and return to Earth.

The ballistic mission will complete a post-comet cruise phase and return the spacecraft containing the comet sample to Earth in 2027. A final delta from the SEP mission is that the ballistic CSSR spacecraft will need to manage its arrival velocity to ensure that the SRV can be jettisoned in a manner that its structural and thermal design can safely deliver the comet sample to the Utah Test and Training Range (UTTR), assuming that no major redesign of the SRV has occurred for this alternate approach.

5.6 Planetary Protection

See Section 4.6.

5.7 Major Open Issues and Trades

See Section 4.7.

5.8 Technology Needs

See Section 4.8.

5.9 Technical Risk Assessment

See Section 4.9. Note that risk T6 of Figure 4.9.1 does not exist for a ballistic conventional propulsion mission.

5.10 Schedule

See Section 4.10.

5.11 Cost

Meeting the CSSR cost cap with the ballistic mission design will be challenging because of the mission's technical complexity and duration.

- The estimated cost of the ballistic mission is within 3% of the CSSR cost cap in Fiscal Year 2007 dollars of $820 million.
- The bottom-up ballistic mission cost estimate is comparable to a parametrically derived estimate based on the NAFCOM spacecraft cost model.

As with the SEP mission, detailed, bottom-up estimates of the Phases A–E costs were prepared for the ballistic mission design. To do so, senior APL functional supervisors and lead engineers were provided with the mission technical description and schedule summarized in Section 4, mission ground rules and assumptions, and a level-3 work breakdown structure (WBS) for Phases A–E and asked to estimate the materials, labor resources, and skill mix required to complete each WBS element. The APL estimators were supported by technical experts from Langley Research Center (LaRC) and Johnson Space Center (JSC) with estimates of the SRV and sample curation center, respectively. Prices for launch vehicles and services and DSN services were derived from study guidelines.

The estimated cost of the ballistic mission, $801 million ($801M) in Fiscal Year 2007 dollars, including unallocated cost reserves, is $19M less than both the $820M CSSR cost cap and the SEP mission's estimated cost. The non-reserves cost, including Education and Public Outreach, is $672M. Cost reserves account for $129M, or 16%, of the total cost. The ballistic cost

estimate with reserves is nearly 10% higher than the New Horizons funding requirement of $730M. The ballistic mission's higher cost is reasonable given that the relatively greater complexity of its mission and the fact that the New Horizons requirement excludes DSN charges.

6. SUMMARY

A Comet Surface Sample Return (CSSR) mission is technically feasible but programmatic risks remain.

- Knowledge gained during the past 5 years on the nature of comet surfaces and sample return technologies have reduced a CSSR technical risk.
- Comet targets of scientific interest can be accessed by missions launched in the 2014–2016 time frame.
- A mission within the cost cap of $820M (in FY2007$) is achievable with moderate cost risk.

The Comet Surface Sample Return mission study has identified mission options for returning a comet sample to Earth by the year 2027. The Science Definition Team (SDT) has identified a set of top-level requirements (focused on returning to Earth a sample of surface material of at least 500 cc) that provided a focus for the mission definition by the engineering team. Two mission options were identified: a mission design using solar electric propulsion (SEP) technology and the second (ballistic mission design) using more conventional propulsion technologies. The technical challenges of the mission include accessing a comet from Earth, collecting the sample, and returning the sample to Earth while keeping the sample at a sufficiently cold temperature (–10°C) to preclude aqueous alteration. Both the knowledge of comet surfaces and the technologies to meet these challenges have been significantly advanced in the past 5 years. Although the technical challenges have been significantly reduced and a focused goal consistent with a mid-class mission identified, the mission complexity and duration of the flight to reach a comet and return a sample raises the missions cost risk when measured against a $820M cost cap in 2007 constant dollars.

6.1 Science Value of a Focused CSSR Mission

The study SDT has confirmed the value of a CSSR mission as documented by the National Academy of Sciences Decadal Survey of solar system science ("New Frontiers in the Solar System," 2003). Further, their review of the current state of knowledge as advanced by recent NASA missions (Deep Space 1, 2001; Stardust, 2006; Deep Impact, 2006) has provided better understanding of the nature of comet surfaces. This understanding has led to the consensus that these comet surfaces are likely to be very porous with low surface strengths. These surface characteristics ease the challenge of collecting a surface sample. However, there remains sufficient uncertainty in surface variations that the selected mission should sample a comet that has been identified to have properties similar to those now known to exist and the spacecraft should be robust enough in design to allow more than one sample attempt. The mission options developed by the study meet both of these criteria as the comet selected for sampling (67P/Churyumov-Gerasimenko [C-G]) will be well characterized by the Rosetta mission in 2014. The ballistic mission backup target (46P/Wirtanen) has slightly higher risk in this regard. As described in Sections 4 and 5, the spacecraft concepts developed for this study have sufficient resources for multiple sampling attempts and the actual acquisition and storage of two separate samples within the sample return vehicle (SRV).

A risk recognized early in the study was the potential of developing a long list of science goals that would require a payload of many instruments, thus increasing the complexity and cost of the mission. The SDT reviewed the options and value of different measurement and sampling requirements and agreed that a clear focus on a simple objective of returning a sizeable sample of comet material was sufficiently compelling to justify the mission alone. The remaining requirements included in the floor science (Group 1) and baseline (Group 2) are associated with maintaining the acquired sample without significant alteration through its return to the curation

facility at Johnson Space Center and understanding the geologic context of the sample at the comet. The principal derived requirement is to maintain the sample temperature below -10^{o}C at all times. This focus on a few critical science requirements ensures that resources are focused on sample collection and not dissipated in achieving secondary objectives.

6.2 Mission Options and Programmatic Risk

As described in Sections 4 and 5, the mission design requirements for comet rendezvous and subsequent return to Earth are challenging. Both mission options have a number of similar risks as defined in Sections 4.9 and 5.9. The differences in risk are associated with the robustness of the mission design and cost. As described in Section 3, a significant number of potential targets were considered early in the study with only a few being viable in terms of available (for a mid-size mission) launch energy and post-launch ΔV. Further, there are only a few launch windows available in the time frame of late 2014 (GFY2015) through 2016. A ballistic mission design that falls within the cost cap is available to launch to C-G with a launch window opening in late December 2014, but the backup would require a change of target (to Wirtanen) with a launch in May 2015. The SEP mission is more robust as there are two launch window options to C-G with a year between the dates. However, the SEP mission cost is at the stated cost cap for this study.

Significant advancement of the technologies required to execute a CSSR mission have taken place in the past few years. This includes demonstration of SEP, demonstration of SRV technology (Stardust, Genesis), and risk reduction work on the next generation of sample return technology (the Mars sample return vehicle). Further, the demonstration of the feasibility of landing on a small body by the NEAR mission and the development work by ESA on the Rosetta mission provide a solid foundation for collecting and returning a sample from a similar small body.

With this foundation in place, the technology risk level is sufficiently low to begin mission formulation and preliminary design, but additional work is required to reduce the remaining risks associated with the sampling system and the SRV to a level acceptable for implementation. This risk is described in Section 4.9 and is a common risk to both a ballistic and SEP option. The technology risk reduction program described in Section 4.8 describes a plan to reduce these risks to acceptable levels at the time of mission confirmation.

Other programmatic risks are quite normal for a planetary mission at this stage of formulation. They include risk associated with not receiving approval as a Class V, Unrestricted Earth Return; lifetime issues associated with a greater than 10-year flight time before the science floor requirements can be met; and schedule issues resulting from the time to acquire long lead parts and materials. All of these risks can be managed with appropriate attention. The planetary protection issue will need early attention, but the history of comet impacts on the Earth and the position taken by the National Academy of Sciences should provide a solid basis for getting Class V approval.

6.3 Cost Risk and Funding Requirements

The principal risk associated with the CSSR mission is the risk of exceeding the cost cap. Advances since 2002 have reduced much of the technology risk, but the mission remains both complex and of a significantly long duration. These two factors result in costs at the cost cap and significant risk of growing beyond the cost cap even for the minimum cost mission.

The primary cost drivers for the mission are the cost of the on-board propulsion system, the power system, and the duration of mission operations. Other mission complexity that drives cost is associated with the guidance and navigation system for operations at the comet and the implementation of sample capture and return requirements. Although the science instruments have

been minimized and are not cost drivers, the instrumentation required to safely navigate at the comet add to the overall payload costs.

As described in Section 4.11 the cost of the SEP mission is $820M, which includes 30% reserves for Phases A–D and 15% reserves on Phase E. (No reserves are included for the launch service costs.) This results in an actual estimated cost, based on a bottom-up process, of $686M. The cost of the ballistic mission is $801M with a pre-reserve cost estimate of $677M. The differences in the three major cost drivers (propulsion, power, and mission operations) account for nearly all the difference in the two mission options.

Note that the New Horizons funding requirements in FY07$ is $730M (this funding level does not include Deep Space Network costs). Though there are specific differences in the development plans between the two missions (e.g., the Radioisotope Thermoelectric Generator power system for New Horizons with its associated cost versus the cost implied by the complexities for a CSSR discussed above), the overall complexity and duration of the two are in the same class. Thus the cost risk of the CSSR mission with the stated reserves should be considered moderate.

6.4 Conclusions

A focused CSSR mission is achievable within the cost cap of $820M. Such a focused mission would result in a significant advancement in the science of primitive bodies and our understanding of the origins of the solar system. A slight increase in the cost cap would provide sufficient margin to broaden the options and lower overall risk.

7. REFERENCES

Section 2

A'Hearn, M. F., et al. (1995). The ensemble properties of comets: Results from narrowband photometry of 85 comets, 1976–1992. *Icarus*, **118**, 223–270.

Basilevsky, A. T., and Keller, H. U. (2007). Craters, smooth terrains, flows, and layering on the comet nuclei. *Sol. Sys. Res*., **41**, 109–117.

Belton, M. J. S., et al. (2003). *New Frontiers in the Solar System*, National Academies Press, Washington, DC.

Bockelée-Morvan, D., et al. (2004). The Composition of Cometary Volatiles. In *Comets II*, ed. M. C. Festou, H. U. Keller, and H. A. Weaver, Univ. of Arizona Press, Tucson, AZ.

Britt, D. T., et al. (2004). The morphology and surface processes of Comet 19P/Borrelly. *Icarus,* **167**, 45–53.

Brown P., et al. (2000). The fall, recovery, orbit, and composition of the Tagish Lake meteorite: A new type of carbonaceous chondrite. *Science,* **290**, 320–325.

Brownlee, D. E., et al. (2006). Surface of Young Jupiter Family Comet 81P/Wild 2: View from the Stardust Spacecraft. *Science,* **304**, 1764–1969.

Chyba, C. F., and C. Sagan (1992). Endogenous production, exogenous delivery, and impact-shock synthesis of organic molecules: an inventory for the origins of life. *Nature,* **355**, 125.

Cody G. D., et al. (2007). Placing Comet 81p/Wild 2 Organic Particles Into Context With Chondritic Organic Solids. *Lunar And Planetary Science XXXVIII,* Abstract 2286.

Delsemme, A. H. (1992). Cometary origin of carbon and water on the terrestrial planets. *Adv. in Space Res*., **12**, 5.

Dones, L., et al. (2004). Oort Cloud Formation and Dynamics. In *Comets II*, ed. M. C. Festou, H. U. Keller, and H. A. Weaver, Univ. of Arizona Press, Tucson, AZ, pp. 153–174.

Duncan, M., et al. (2004). Dynamical Evolution of Ecliptic Comets. In *Comets II*, ed. M. C. Festou, H. U. Keller, and H. A. Weaver, Univ. of Arizona Press, Tucson, AZ, pp. 193–204.

Ehrenfreund, P., et al. (2004). From Interstellar Material to Comet Particles and Molecules. In *Comets II*, ed. M. C. Festou, H. U. Keller, and H. A. Weaver, Univ. of Arizona Press, Tucson, AZ, pp. 115–133.

Feaga, L. M., et al. 2007). Asymmetries in the distribution of H_2O and CO_2 in the inner coma of Comet 9P/Tempel 1 as observed by Deep Impact, *Icarus*, **190**, 345–356.

Fujiwara, A., et al. (2006). The rubble-pile asteroid Itokawa as observed by Hayabusa. *Science,* **312**, 1330–1334.

Keller, H. U., et al. (1986). First Halley Multicolour Camera Imaging Results from Giotto. *Nature,* **321**, 320–326.

Lamy, P. L., et al. (2004). The Sizes, Shapes, Albedos, and Colors of Cometary Nuclei. In *Comets II*, ed. M. C. Festou, H. U. Keller, and H. A. Weaver, Univ. of Arizona Press, Tucson, AZ, pp. 223–264.

Lisse, C. M., et al. (2006). Spitzer Spectral Observations of the Deep Impact Ejecta. *Science*, **313**, 635–640.

Lisse, C. M., et al. (2007). Comparison of the Composition of the Tempel 1 Ejecta to the Dust in Comet C/Hale-Bopp 1995 O1 and YSO HD100546. *Icarus*, **187**, 69–86.

Merk, R., and Prialnik, D. (2006). Combined modeling of thermal evolution and accretion of trans-neptunian objects—Occurrence of high temperatures and liquid water. *Icarus*, **183**, 283–295.

Owen, T. C., and Bar-Nun, A. (2001). Contributions of Icy Planetesimals to the Earth's Early Atmosphere. *Origins of Life and Evolution of the Biosphere*, **31,** 435–458.

Prialnik, D., et al. (2004). Modeling the Structure and Activity of Comet Nuclei. In *Comets II*, ed. M. C. Festou, H. U. Keller, and H. A. Weaver, Univ. of Arizona Press, Tucson, AZ, pp. 359–387.

Reinhard, R. (1986). The Giotto Encounter with Comet Halley. *Nature*, **321**, 313–318.

Robert, F. (2001). The Origin of Water on Earth. *Science*, **314**, 1056–1058.

Sandford S. A., et al. (2006). Organics Captured from Comet Wild 2 by the Stardust Spacecraft. *Science*, **314**, 1720–1724.

Soderblom, L. A., et al. (2002). Observations of Comet 19P/Borrelly by the Miniature Integrated Camera and Spectrometer aboard Deep Space 1. *Science*, **296**, 1087–1091.

Solar System Exploration Roadmap. (2006). NASA HQ publication.

Stern, S. A. (2003). The evolution of comets in the Oort cloud and Kuiper belt. *Nature*, **424**, 639–642.

Veverka, J., et al. (2001). Imaging of small-scale features on 433 Eros from NEAR: Evidence for a complex regolith. *Science* **292**, 484–488.

Zolensky M. E., et al. (2006). Mineralogy and Petrology of Comet Wild 2 Nucleus Samples. *Science*, **314**, 1735–1739.

Section 4

Herman, D., G. Soulas, and M. Patterson (2007). NEXT Long-Duration Test after 11,570 h and 237 kg of Xenon Processed. In *30th Int. Electric Propulsion Conf*., 17–20 Sep 2007, Florence, Italy, IEPC-2007-033.

Van Noord, J. (2007). Lifetime Assessment of the NEXT Ion Thruster. In *43rd AIAA/ASME/*SAE/*ASEE Joint Propulsion Conf. and Exhibit*, 8–11 July 2007, Cincinnati, OH, AIAA-2007-5274.

Section 4.2.1

Cheng, A. F., H. A. Weaver, S. J. Conard, M. F. Morgan, O. Barnouin-Jha, J. D. Boldt, K. A. Cooper, E. H. Darlington, M. P. Grey, J. R. Hayes, K. E. Kosakowski, T. Magee, E. Rossano, D. Sampath, C. Schlemm, and H. W. Taylor (Aug 2007). Long-Range Reconnaissance Imager on New Horizons. *Space Sci. Rev*., **21**.

Section 4.2.3

Mitcheltree, R., S. Hughes, R. Dillman, and J. Teter (2001). An Earth Entry Vehicle for Returning Samples from Mars. In *2nd Int. Symp. on Atmospheric Reentry Vehicles and Systems*, 26–29 Mar 2001, Arcachon, France, AAAF paper ARVS-102.

Section 4.3

Benson, S. W., J. P. Riehl, and S. R. Oleson (2007). NEXT Ion Propulsion System Configurations and Performance for Saturn System Exploration. In *43rd AIAA/ASME/SAE/ASEE Joint Propulsion Conf. & Exhibit*, 8–11 Jul 2007, Cincinnati, OH, AIAA-2007-5230.

Fiebrich, H., J. E. Haines, and F. Tonicello (2004). Power System Design of the Rosetta Spacecraft. In *2nd Int. Energy Conversion Engineering Conf*., 16–19 Aug 2004, Providence, RI. Paper AIAA 2004-5535.

Sims, J. A. (2000). Trajectories to Comets Using Solar Electric Propulsion. AAS/AIAA Space Flight Mechanics Meeting, Clearwater, FL, Jan 2000. AAS Paper 00-134.

Section 4.4

Driesman, A., S. Hynes, and G. Cancro (Fall 2007). The STEREO Observatory. *Space Sci. Rev*., **128**(1).

Fountain, G., SSR paper (NH Spacecraft)

Leary, J. C., R. F. Conde, G. Dakermanji, C. J. Ercol, K. Fielhauer, D. G. Grant, T. J. Hartka, T. A. Hill, S. E. Jaskulek, M. A. Mirantes, L. E. Mosher, M. V. Paul, C. E. Person, D. F. Persons, E. H. Rodberg, D. K. Srinivasan, R. M. Vaughan (all at JHU/APL), and S. R. Wiley (Aerojet) (2007). The MESSENGER spacecraft. *Space Sc. Rev*., **131**, 187–217.

Section 5.3

Block, K. M., and S. M. Singer (2007). Wirtanen Surface Sampler Probe. http://www.lpi.usra.edu/opag/nov_2007_meeting/presentations/wssp.pdf

8. ACRONYMS AND ABBREVIATIONS

ACS	Attitude Control System
ADC	attitude determination and control
ATLO	Assembly, Test, and Launch Operations
AU	Astronomical Unit
BOL	beginning of life
C_3	launch energy
CCD	charge coupled device
CC&DH	command, control, and data handling
CCSDS	Consultative Committee for Space Data Systems
C&DH	command and data handling
CDR	Concept Design Review
CEV	Crew Exploration Vehicle
CFD	computational fluid dynamics
CFDP	Consultative Committee for Space Data Systems File Delivery Protocol
cFE	Core Flight Executive
CG	center of gravity
C-G	Churyumov-Gerasimenko
CGS	Common Ground Software
CMOS	complementary metal oxide semiconductor
COTS	commercial off-the-shelf
CPT	comprehensive performance test
CSCI	computer software configuration item
CSSR	Comet Surface Sample Return
D/A	digital-to-analog
DCIU	digital control interface unit
DEM	digital elevation map
D/H	deuterium to hydrogen
DI	Deep Impact
ΔDOR	Delta-Differential One-way Range

DPU	Data Processing Unit
DS-1	Deep Space One
DSM	Deep Space Maneuver
DSN	Deep Space Network
DSS	Digital Sun Sensor
EELV	evolved expendable launch vehicle
EEV	Earth Entry Vehicle
EM	Engineering Model
EMI/EMC	electromagnetic interference/electromagnetic capability
ESD	electrostatic discharge
ETR	Eastern Test Range
FMEA/FTA	failure mode effects analysis/fault tree analysis
FOV	field of view
FPM	fault protection module
FPU	focal plane units
GEMS	glass with embedded metal and sulfide
GSFC	Goddard Space Flight Center
GN&C	guidance, navigation, and control
GRC	John H. Glenn Research Center
HGA	high gain antenna
H&MS	height and motion subsystem
HPA	high-pressure assembly low-pressure assembly
IAU	International Astronomical Union
IDP	interplanetary dust particle
IEM	integrated electronics module
I/F	interface
IMU	Inertial Measurement Unit
IOM	insoluble organic matter
IRC	infrared camera
ISM	interstellar medium
ISPT	In-Space Propulsion Technology
I&T	integration and testing

JFC	Jupiter Family Comet
JPL	Jet Propulsion Laboratory
JSC	Johnson Space Center
KDP	key decision point
KSC	Kennedy Space Center
LaRC	Langley Research Center
Lat/Lon/Alt	latitude/longitude/altitude
LED	light emitting diode
LGA	low gain antenna
LILT	low-intensity, low-temperature
LORRI	Long-Range Reconnaissance Imager
LPA	low-pressure assembly
LRC	Langley Research Center
LWS	Living With a Star
MEMS	microelectromechanical system
MGA	medium gain antenna
MLI	multi-layer insulation
MOC	Mission Operations Center
MO&DA	Mission Operations and Data Analysis [use this one]
MODA	Mission Operations and Data Analysis
MOSFET	metal-oxide semiconductor field effect transistor
MP	main processor
MRO	Mars Reconnaissance Orbiter
MSR	Mars Sample Return
NAC	Narrow Angle Camera
NAFCOM	NASA-Air Force Cost Model
NAR	Non-Advocate Review
NEXT	NASA's Evolutionary Xenon Thruster
NICM	NASA Instrument Cost Model
NF	New Frontiers
NFV	narrow field visible
NPA	non-principal axis

NRC	National Research Council
NSTAR	NASA Solar Electric Propulsion Technology Application Readiness
PDR	Preliminary Design Review
PDS	Planetary Data System
PDU	power distribution unit
PFCV	Proportional Flow Control Valve
PM	Prototype Model
PMD	propellant management device
PPT	peak power tracker
PPU	power processing unit
PSE	power system electronics
PTP	Programmable Telemetry Processor
PWM	pulse width modulation
RBSP	Radio-Belt Sensor Probes
RIO	remote input/output
RTG	Radioisotope Thermoelectric Generator
S/A	solar array
SAS	sample acquisition system
SAJB	solar array junction box
SBC	single board computer
SDT	Science Definition Team
SEM	scanning electron microscopy
SEP	solar electric propulsion
SMC	sample monitoring camera
SMOW	standard mean ocean water
SOC	Science Operations Center
SRC	Sample Return Capsule
SRV	sample return vehicle
SSPA	solid-state power amplifier
SSR	solid-state recorder
STOL	System Test and Operations Language
TBTK	TestBed ToolKit

T&C	telemetry and command
TCM	trajectory correction maneuver
TEC	thermal electric cooler
TEM	transmission electron microscopy
TLM	telemetry
TRIO	temperature remote input and output
TRL	technology readiness level
TRN	Terrain Recognition Navigation
TPS	thermal protection system
TWTA	traveling wave tube amplifier
UTTR	Utah Test and Training Range
ΔVEGA	ΔV-Earth Gravity Assist
VLBI	Very Long Baseline Interferometry
VRIO	voltage remote input and output
WAC	Wide Angle Camera
WBS	work breakdown structure
WFV	wide field visible
XANES	X-ray Absorption Near Edge Structure